

Inaugural-Dissertation zur Erlangung der Doktorwürde
der Tierärztlichen Fakultät
der Ludwig-Maximilians-Universität München

**Murine tumor models for the in vivo evaluation of natural compounds and
their derivatives as new cancer therapeutics**

von

Melanie Ulrich

aus Kelheim

München 2016

Aus dem Veterinärwissenschaftlichen Department der Tierärztlichen Fakultät
der Ludwig-Maximilians-Universität München

Lehrstuhl für molekulare Tierzucht und Biotechnologie

Arbeit angefertigt unter der Leitung von Univ.-Prof. Dr. Eckhard Wolf

Angefertigt an:

Fakultät für Chemie und Pharmazie, Lehrstuhl für Pharmazeutische Biologie
der Ludwig-Maximilians-Universität München

Mentorin: Univ.-Prof. Dr. Angelika Vollmar

Gedruckt mit Genehmigung der Tierärztlichen Fakultät
der Ludwig-Maximilians-Universität München

Dekan: Univ.-Prof. Dr. Joachim Braun
Berichterstatter: Univ.-Prof. Dr. Eckhard Wolf
Korreferent/en: Univ.-Prof. Dr. Johannes Hirschberger

Tag der Promotion: 16. Juli 2016

to my grandmothers

Table of contents

I. Introduction.....	1
1. Investigated experimental anti-cancer drugs	3
1.1. Natural compounds	3
1.1.1. Archazolid A	4
1.1.2. Tetrandrine	5
1.1.3. Soraphen A	6
1.2. Synthetic compounds	7
1.2.1. PS89	7
1.2.2. Roscovitine and its analogue LGR 2674.....	8
1.2.3. Dinaciclib	9
2. Compounds used for combinatorial treatment	10
2.1. Nutlin-3a.....	10
2.2. Simvastatin	11
2.3. Sorafenib	12
3. The role of Cdk5 in cancer development	13
4. Murine tumor models in cancer research	14
5. Aim of the thesis	15
II. Materials and Methods	17
1. Materials	17
1.1. Compounds.....	17
1.2. Cell culture	17
1.3. In vivo experiments	18
1.4. Laboratory mouse strains	19
1.4.1. C57BL/6	19
1.4.2. BALB/c	19
1.4.3. BALB/c nu/nu	19
1.4.4. Scid.....	19
1.4.5. Nod Scid	20
1.4.6. NSG (Nod Scid Gamma).....	20

1.4.7. Housing	20
1.5. Instruments	20
1.6. Software	21
2. Methods	21
2.1. Cell culture	21
2.2. In vivo experiments	22
2.2.1. In vivo imaging system (IVIS®).....	22
2.2.2. Preliminary dose finding experiments.....	23
2.2.2.1. Simvastatin	23
2.2.2.2. LGR 2674	23
2.2.2.3. Archazolid A and nutlin-3a	23
2.2.2.4. PS89	24
2.2.2.5. Soraphen A	24
2.2.3. Murine models concerning pharmacokinetics.....	24
2.2.3.1. Archazolid A	24
2.2.3.2. Roscovitine.....	25
2.2.4. Murine tumor models for tumor growth evaluation.....	25
2.2.4.1. Effect of archazolid A treatment on murine breast cancer shown in an allograft tumor model.....	26
2.2.4.2. Combinatorial effect of simvastatin and archazolid A on HCC tumors evaluated in a xenograft tumor model.....	26
2.2.4.3. Effects of combinatorial treatment of nutlin-3a and archazolid A on glioblastoma tumors using a xenograft model	26
2.2.4.4. Effect of LGR 2674 on HCC tumors using a xenograft setup	27
2.2.4.5. Evaluation of the effect of PS89 in combination with sorafenib on HCC tumors using a xenograft model	27
2.2.4.6. Effect of soraphen A on HCC tumors shown in a xenograft tumor model	27
2.2.5. Murine tumor experiments concerning tumor dissemination	28
2.2.5.1. Searching for a murine tumor model within a leukemia project... 28	
2.2.5.2. Effect of tetrandrine on tumor dissemination evaluated in three different murine experiments	28
2.2.5.3. Effect of soraphen A on tumor dissemination shown in an allograft tumor model.....	29
2.2.6. The influence of Cdk5 in cancer processes evaluated in murine tumor experiments	29

2.2.6.1. Effect of Cdk5 knock-down in cells in combination with sorafenib treatment on HCC tumors evaluated in a Scid mouse model.....	29
2.2.6.2. Using Cdk5 knock-out mice and roscovitine treatment to evaluate their effects on melanoma cells	30
2.2.6.3. Limiting dilution experiment with T24 cells.....	30
2.2.6.4. Limiting dilution experiment with 4T1-luc cells	31
2.3. Statistical analysis	31
III. Results.....	32
1. Preliminary dose finding experiments in murine models.....	32
1.1. Simvastatin	33
1.2. LGR 2674.....	33
1.3. Archazolid A and nutlin-3a	34
1.4. PS89	36
1.5. Soraphen A.....	37
2. Murine experiments for pharmacokinetic studies	38
2.1. Archazolid A distribution.....	38
2.2. Roscovitine distribution	39
3. Murine tumor models to evaluate the reduction of tumor growth through various compounds	40
3.1. Evaluation of the effect of archazolid A treatment on murine breast cancer in an allograft tumor experiment.....	41
3.2. Examination of combinatorial effects of simvastatin and archazolid A on HCC using a xenograft model.....	42
3.3. Effects of combinatorial treatment of nutlin-3a and archazolid A on glioblastomas shown in a xenograft tumor model.....	44
3.4. Effect of LGR 2674 on HCC tumors evaluated in a xenograft model.....	45
3.5. Effect of PS89 in combination with sorafenib on HCC tumors shown in a xenograft model.....	47
3.6. Use of a xenograft tumor model to evaluate the effect of soraphen A on HCC tumors	48
4. Murine tumor models to evaluate tumor dissemination.....	49
4.1. Evaluation of suitable mouse models for a leukemia project.....	50
4.2. Murine tumor models to evaluate the effect of tetrandrine on tumor dissemination	52

4.3. Using an allograft tumor model to evaluate the effect of sorafenib A on tumor dissemination.....	56
5. Murine tumor experiments to show the influences of Cdk5 on tumor development	58
5.1. Evaluation of the effect of a Cdk5 knock-down in Huh7 cells in combination with sorafenib treatment in a xenograft model.....	58
5.2. Effect of an inducible endothelial Cdk5 knock-out in mice in combination with roscovitine on melanoma tumors	60
5.3. Limiting dilution experiment with T24 cells.....	62
5.4. Limiting dilution experiment with 4T1-luc cells	64
IV. Discussion	69
1. Murine models for preliminary dose finding experiments.....	69
2. Murine experiments to evaluate the pharmacokinetics of archazolid A and roscovitine	71
3. Murine tumor models to evaluate the reduction of tumor growth through various compounds	72
3.1. Murine tumor models to evaluate the efficacy of archazolid A	73
3.2. In vivo experiment to evaluate the anti-cancer potential of LGR 2674	74
3.3. Evaluation of PS89 as anti-cancer agent in a xenograft tumor model	75
3.4. Murine tumor model to evaluate the efficacy of sorafenib A.....	76
4. In vivo evaluation of new approaches to reduce tumor dissemination	76
4.1. Establishment of a murine leukemia model	77
4.2. In vivo evaluation of the inhibition of tumor cell dissemination by tetrandrine and sorafenib A.....	78
5. In vivo evaluation of the involvement of Cdk5 in cancer processes	79
5.1. Efficacy of Cdk5 knock-down in Huh7 cells and endothelial Cdk5 knock-out in mice	80
5.2. Evaluation of the effect of Cdk5 inhibition in murine limiting dilution experiments	80
V. Summary	82
VI. Zusammenfassung	84

VII. References	87
VIII. Appendix.....	98
1. Abbreviations.....	98
2. Publications.....	101
IX. Acknowledgements	102

I. Introduction

Cancer is a major health problem worldwide, its occurrence is increasing because of risk factors such as smoking, overweight, physical inactivity, growth and aging of the population and changing reproductive patterns associated with urbanization and economic development. In 2012, 14.1 million new cancer cases and 8.2 million deaths occurred worldwide [1]. All in all, the most common cancers occurring per year, are lung (1.82 million), breast (1.67 million) and colorectal cancer (1.36 million) while the most common causes of death were lung cancer (1.6 million), liver cancer (745.000) and stomach cancer (723.000). According to estimates, over 20 million new cancer cases are expected annually as early as 2025 [2]. Among females breast cancer is the most frequently diagnosed type of cancer while lung cancer is the leading type diagnosed in males. By trend, people in developing countries display a lower survival rate than people in developed countries because of a combination of late stage diagnosis and limited access to timely and standard treatment. The application of existing cancer control knowledge, implementing programs for tobacco control, vaccination (e.g. for liver and cervical cancers), early detection and treatment, as well as public health campaigns promoting an active and healthy lifestyle contribute to the fight against cancer [3]. The classical therapeutic strategies are surgery, radiotherapy and chemotherapy. Especially chemotherapy is affiliated with a variety of wearing side effects because the used drugs do not specifically affect cancer cells, but all cells with a fast division rate, e.g. cells of the skin, the mucosa and the blood and hair roots. This is the reason why patients suffer from, among other side effects, skin problems, gastrointestinal pain and hair loss. The solution for such problems is that cancer therapy has to become more target-oriented.

The term cancer itself is used for a large group of diseases that are able to batter almost any part of the body. One decisive characteristic is an uncontrolled cell division and so the rapid creation of abnormal cells that grow beyond their usual boundaries [4]. Normally, the body forms as many cells as needed because old and damaged cells die and have to be replaced by new ones. In cancer processes, this regular mechanism does not work properly, so old or damaged cells are able to survive and unneeded new cells are produced. The initiation of cancer is marked by a carcinogenic influence on a normal cell, it is due to either environmental factors such as tobacco, obesity, infections, radiation or it is due to inherited genetics [5]. The genetic changes that contribute to cancer tend to affect three main types of genes, namely proto-oncogenes, tumor suppressor genes, and DNA repair genes [6]. Many cancers are represented through solid tumors while others, e.g. blood cancer as leukemia, do not form a solid growth. Cancerous tumors are malignant, which means they can spread into or invade nearby tissues. Some of the cells of the growing tumor also use the blood or lymph system to reach parts of the body, distant to the original tumor, and form new tumors there. This is a characteristic benign tumors normally do not show. The difference between cancer cells and normal cells is the less specialisation of tumor cells, they do not mature into very distinct cell types with clear functions, so they are able to divide without stopping. In addition, cancer cells are

able to ignore signals that normally tell cells to stop dividing or to begin a process known as programmed cell death or apoptosis, which the body uses to get rid of unneeded cells [6]. According to recent publications, tumor initiating cells, so-called cancer stem cells (CSCs), possibly play an important role in tumor formation. They constitute a small minority of neoplastic cells within a tumor, have strong self-renewing properties and are defined by their ability to seed new tumors, which is why they are called tumor initiating cells [7]. They are associated with the formation of metastases and promotion of resistances against anti-cancer therapy [8]. In addition to this, there exists a mechanism called epithelial-mesenchymal transition (EMT) which is a highly conserved cellular process that transforms epithelial cells into mesenchymal cells. EMT is involved in normal embryogenesis and tissue repair, but it also contributes to tumor progression, including tumor metastasis, therapy resistance and disease recurrence. The link between EMT and CSCs might be the relevance of an EMT for the acquisition and maintenance of stem cell-like characteristics [9].

In 2000, Hanahan and Weinberg defined six hallmarks of cancer, including sustained proliferative signaling, evading growth suppressors, resistance against cell death, enabling replicative immortality, inducing angiogenesis and activating invasion and metastasis. These biological capabilities are acquired during cancer development and form the perfect strategies to outlast all efforts of the body to fight cancer and to create the best environment for development [10]. In 2011, these scientists enlarged their list of hallmarks with the deregulation of cellular energetics, the avoidance of immune destruction, tumor promoting inflammation and genome instability and mutation as additional capabilities of cancer for its development. In Figure 1, an overview on these hallmarks is illustrated [11].

Cancer is right now and also will be in the coming years one of the major burdens on human and animal health. Veterinary oncology is actually mainly focussing on companion animals such as cats and dogs which suffer from many of the same types of cancer like humans do and are often treated with the same drugs [12]. But animals themselves have been widely used to develop and test anti-cancer therapeutics. For the main part of them rodents were taken which represent a widely used model in the fight against cancer. They represent a proper model because their anatomy, physiology and genetics are well-understood. Their genetic, biological and behavior characteristics are similar to those of humans. Rodents are relatively easy to handle, they adapt to new conditions very fast, they reproduce very quickly and have a short lifespan (two to three years), so several generations of mice can be observed in a relatively short period of time. Among laboratory mice, a greater variety of different strains with or without deficiencies compared to all other animals is existing, additionally there is the possibility to create knock-out or knock-in mouse models which are increasingly established in cancer research. This offers the possibility to choose the most adequate mouse model for a tumor experiment [13]. In vivo models are one of the most important steps during the long process of drug development for cancer therapy, they constitute the transition of pure in vitro results to real therapeutic use.

This thesis focuses exclusively on the establishment of murine tumor models to evaluate new promising anti-cancer approaches, the use of natural and synthetic compounds as

chemotherapeutics in cancer therapy, partly in regard to the influence of an inhibition of cyclin dependent kinase 5 (Cdk5) as a target. Our lab concentrates on a variety of in vitro projects to evaluate the anti-cancer properties of different experimental compounds. The establishments of corresponding animal experiments to substantiate these in vitro data and to generate profound knowledge on the efficacy of these compounds in vivo are the content of this thesis.

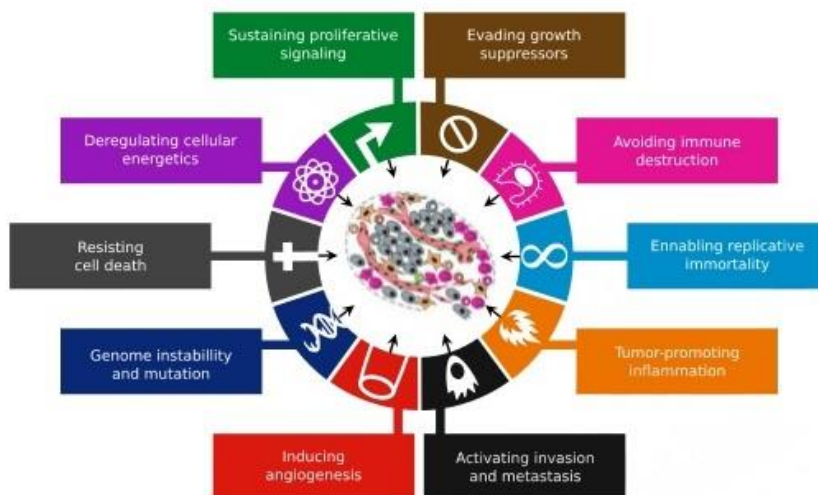


Figure 1: Hallmarks of cancer according to Weinberg et al. [11] [10]

1. Investigated experimental anti-cancer drugs

Our lab works with a variety of compounds, either natural ones (DFG, FOR 1406) or synthetic ones, in order to evaluate their anti-cancer properties. In this thesis, mouse models were used for a variety of in vivo experiments with both types of these experimental drugs.

1.1. Natural compounds

A natural product is defined as a compound or substance produced by a living organism. They can possess pharmacological or biological activity which makes them useful for drug development [14]. Nature itself has been a source of medicinal products for millennia, in this context animals, plants, microorganisms and organisms from the sea play important roles as sources [15]. Natural products have always been the origin of many ingredients in medicine, even more than 80% of drug substances were natural products themselves or were inspired by a natural compound [16]. The amount of drugs of natural origin in development is immense. At the end of 2013, more than 100 natural products and natural product derived compounds were arranged in clinical trials or in registration processes. The area of indications ranges from oncology, anti-infectives,

cardiovascular and metabolic diseases to inflammatory and neuronal illness [17]. In the field of anti-cancer and anti-infective agents even two-thirds of all drugs are derived from natural products. Hence, such drugs continue to make great contributions to human and animal health [18]. One of their key features is their enormous structural and chemical diversity. Their frequent use in therapy, the huge number of diseases which are treated or prevented by them and the rate of wide structural diversity, including their application as templates for semi-synthetic and total synthetic modification speak for the importance of natural compounds in modern medicine [14]. Prominent representatives are e.g. paclitaxel which was isolated from the bark of a yew tree in 1967 and is now clinically approved and widely used to treat breast and ovarian cancer [19] and bendamustine, a nitrogen mustard, which is approved for the treatment of chronic lymphocytic leukemia (CLL) and lymphomas [20]. Natural compounds mostly show their effective properties, the basic challenge is to evaluate the mechanism behind them. However, synthetic drugs are designed to work according a specific mode of action and their effectiveness has to be proven.

The focus of this thesis is the establishment of in vivo models for the evaluation of natural compounds as chemotherapeutics. The effects of several substances will be evaluated concerning their effects on tumor development, growth and dissemination.

In the following sections the natural substances used in this thesis will be described in more detail.

1.1.1. Archazolid A

Archazolids A and B were first isolated from cultivated myxobacteria *Archangium gephyra* and its related genus *Cystobacter violaceus*, they consist of a macrocyclic lactone ring with a thiazole side chain [21]. Next to argyrins [22], tubulyisin [23] and gephyronic acids [24], they are the fourth compound which was isolated from these specific myxobacteria. The mode of action of archazolids is based on their inhibitory effect on the V-ATPase activity of cells [21].

Vacuolar (H⁺)-ATPases (V-ATPases) are proton pumps which are ubiquitously expressed on various membranes, including lysosomes, endosomes, vesicles and the plasma membrane. They depend on adenosine triphosphate (ATP) and play a crucial role in endo- and exocytotic processes of the cell [25] [26]. They regulate pH homeostasis in endomembrane systems by translocating protons across the plasma membrane. In cancer tissues, this proton pump is overexpressed within the plasma membrane [27], the extrusion of protons via V-ATPase causes extracellular acidification and contributes to the maintenance of an aberrant pH gradient between the alkaline cytosol and the acidic extracellular environment. The low pH of tumor extracellular microenvironment may induce the increased secretion and activation of proteases. In fact, the promoting effect of V-ATPases on cancer invasion and metastasis mainly relies on their ability to maintain an acidic pH of extracellular microenvironment [28]. This enables tumor cells to be invasive and to migrate into other tissues [29].

V-ATPases are consisting of the V_0 complex which is membrane bound and responsible for the translocation of protons and the catalytic V_1 complex which is oriented towards the cytosol [30]. Archazolid binds to the subunit c of V_0 which forms an H^+ binding rotor ring that transports protons from the cytoplasm to the endosomal/lysosomal lumen or the extracellular space. It was already shown that archazolid A reduces tumor cell proliferation and migration through the inhibition of V-ATPase in vitro and in vivo [31]. This has to be the initial point for further in vivo investigations to enlarge the spectrum where archazolid can be used.

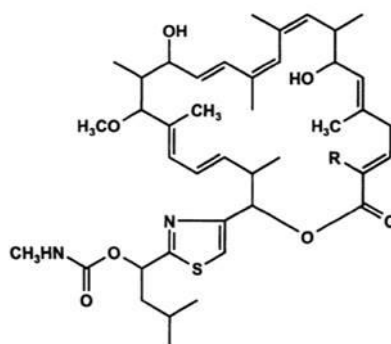


Figure 2: Chemical structure of archazolids [21] Archazolid A: R = CH₃, Archazolid B: R = H

1.1.2. Tetrandrine

Tetrandrine was originally isolated from the root of creeper *Stephania tetrandra*, a Chinese herb which has been used in oriental medicine for several decades [32] [33]. It is an alkaloid with a variety of pharmacological activities such as immunomodulating, anti-hepatofibrogenic, anti-inflammatory, anti-arrhythmic, anti-portal hypertension, neuroprotective and anti-cancer activities [34] [35] [36]. Depending on the cell line, tetrandrine induces cell cycle arrest in different phases and it also induces apoptosis in a variety of cancer cells [34]. It has received considerable attention during the past decade owing to its interesting pharmacological property as a Ca^{2+} antagonist, especially with its action as an L-type Ca^{2+} channel inhibitor [37]. It also interacts with non-voltage dependent Ca^{2+} channels in blood vessels, based on contractility experiments [38]. In recent studies it was shown that tetrandrine is a potent inhibitor of nicotinic acid adenine dinucleotide phosphate (NAADP)-stimulated calcium release. NAADP is a highly potent intracellular calcium-mobilizing agent which makes intracellular calcium channels to release Ca^{2+} from endosomes and lysosomes. So-called two-pore channels (TPCs), which belong to the family of voltage-gated ion-channels, are the major calcium channels activated by NAADP, and tetrandrine was found to be a very potent agent to block TPC1 and TPC2 [39] [40]. It was also shown that tetrandrine has potency as a multidrug resistance modulator by using it as anti-cancer drug in combination with other anti-cancer agents [41]. Based on already performed in vivo experiments with tetrandrine [42] where it showed clear anti-cancer effects, we established a murine tumor dissemination model to

investigate the function of TPC1 and TPC2 in cancer processes, tetrandrine was used as a tool within these experiments.

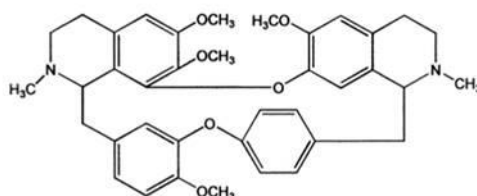


Figure 3: Chemical structure of tetrandrine [33]

1.1.3. Soraphen A

Originally, soraphen A was isolated from the culture broth of soil-dwelling myxobacterium *Sorangium cellulosum* [43]. The first focus of this polyketide natural product lay on its anti-fungal activity [44]. During recent years, this focus concerning use and effectiveness of soraphen A switched to its ability to also inhibit acetyl Coenzyme A carboxylase (ACC) activity in other beings than fungi [45]. ACCs are responsible for the adenosine triphosphate (ATP) dependent catalyzation to transform acetyl-CoA to malonyl-CoA, which is the first step of fatty acid biosynthesis and it is responsible for the speed rate of the mechanism. Two major domains are part of this enzyme, first the biotin carboxylase domain (BC) and second, the carboxytransferase domain (CT), both are connected through the biotin carboxyl carrier protein (BCCP) [46]. ACC has two isoforms, ACC1 is present in lipogenic tissues (liver, adipocytes) and ACC2 exists in oxidative tissues (liver, heart, skeletal muscle), both share on overall amino acid identity of 75% [47]. When one or both ACC isoforms are inhibited, the amount of intracellular malonyl-CoA lowers which causes an increase in the rate of fatty acid oxidation and it lowers the rate of fatty acid synthesis in cells [46]. Different ACC inhibitors have already shown promising results concerning treatment of insulin resistance and obesity. Soraphen A itself inhibits fungal and other eukaryotic ACC systems as well as mammalian ACCs [48]. It binds to the biotin carboxylase domain dimer and disrupts the oligomerization of ACC and inhibits its activity [49]. So, soraphen A has the potency to be used for treatment of obesity, diabetes and cancer [50]. It was shown that development and progression of cancer depends on the expression and activity of proteins which are involved in the fatty acid synthesis. The addition of soraphen A to cancer cells, even in nanomolar concentrations, blocks the fatty acid synthesis and stimulates their oxidation which leads to the situation that cancer cells lack phospholipids, they stop their proliferation and apoptosis starts because cancer cells depend on ACC activity to guarantee their sufficient supply [49]. We evaluated the in vivo effect of soraphen A concerning tumor growth and dissemination in different murine models.

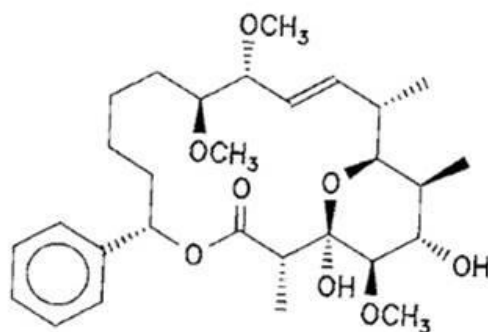


Figure 4: Chemical structure of soraphen A [43]

1.2. Synthetic compounds

Chemical synthesis is a tool which has been successfully used for many decades to produce and establish a variety of compounds, many of them are in clinical use now. Chemical synthesis is the preparation of a compound by performing various chemical reactions, it can also be used to prove the chemical structure of a compound or to improve its properties [51] [52] [53]. Traditionally, synthetic chemistry in drug discovery has been a main source of new structural classes. Since analogy plays an important role in applied research, it is not surprising that it became a crucial strategy in medicinal chemistry [54]. Compounds are also synthesized to test a chemical theory, to create a new or better chemical, or to confirm the structure of a material isolated from a natural source. Chemical synthesis can also be used to supplement the supply of a drug that is commonly isolated in small amounts from natural sources [51].

In our lab we focus on the evaluation of natural and synthetic compounds for their use as novel chemotherapeutics in cancer therapy, the synthetic substances used in this thesis will be described in the following sections in more detail.

1.2.1. PS89

PS89 is a close analogue to T8 which was found during a screening of a commercial compound library on search of a chemosensitizer of etoposide-induced apoptosis in various cancer cell lines. PS89 is a completely new compound which was first described in 2014 [55]. Resistance against chemotherapeutic drugs is a serious problem in effective anti-cancer therapy. There are two categories of resistance, first the acquired one, which develops during the treatment with an initially sensitive drug because of adaption, mutation and usage of sub-pathways and second, the intrinsic one, in which the resistance is already present before start of the therapy which makes the treatment ineffective right from the beginning [56]. The consequence is that tumor cells do not succumb programmed cell death or apoptosis and that therapy fails [57]. The solution for this problem might be to dispose a combinatorial treatment or to use sensitizing compounds together with chemotherapeutic drugs. PS89 is one of those sensitizers. It inhibits the

protein disulfide isomerase (PDI) and triggers the chemosensitization of cancer cells [55]. PDIs are enzymes which catalyze the formation of disulfid bonds in the oxidative folding pathway which takes place in the endoplasmatic reticulum (ER) of eukaryotic cells [58]. It is organised in four thioredoxin-like domains (a b a`b`), the sites with the redox activity are the a- sides [59]. Cancer cells require an increased protein synthesis which results in imbalance between the load and capacity of protein folding and leads to a cellular condition known as ER stress. That is the trigger for a variety of processes to restore homeostasis, termed as unfolded protein response (UPR) [60]. This is mediated by so-called chaperones, PDI is one of them. They maintain the ER homeostasis and support cancer cell survival, so they are a potential target to fight chemoresistance [55]. PDI family proteins were already demonstrated to be involved in a wide range of physiological and disease processes [61]. Here, we wanted to evaluate the effects of PS89 in vivo for the first time.

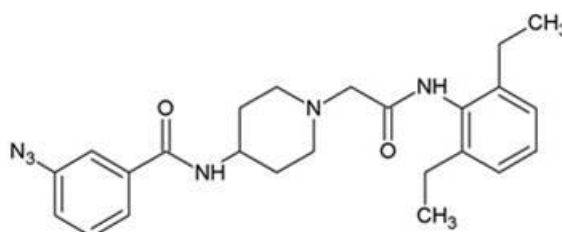


Figure 5: Chemical structure of PS89 [55]

1.2.2. Roscovitine and its analogue LGR 2674

Roscovitine (CYC-202, (R)-roscovitine, seliciclib) is a small molecule which inhibits cyclin-dependent kinases (Cdks) through direct competition at the ATP-binding site by interacting with the amino acids that line up the ATP binding pocket of the Cdk catalytic domain. It belongs to a family of purines which all share a basic ring structure. It inhibits Cdk1, Cdk2, Cdk5, Cdk7 and Cdk9 [62] [63]. Roscovitine is a close analogue to olomoucine which is one of the earliest potent and specific inhibitors of Cdks [64] [65]. But in comparison to the forerunner olomoucine, roscovitine shows a 10-fold higher efficiency towards Cdk2 and a 20-fold higher efficiency towards Cdk5. A lot of human tumors are associated with an abnormal overexpression of Cdk proteins and their regulators which makes it indispensable to lay the focus on an active search for chemical Cdk inhibitors. Amongst them, roscovitine is one of the most promising because it holds a great variety of effects on tumor cells [66] [64]. Roscovitine was shown to induce cell cycle arrest in the G2/M and G1/S phase [66] and leads to induction of apoptosis in many cancer cell lines at all phases of the cell cycle. It was also evaluated that roscovitine has synergistic effects with other anti-cancer agents. It also showed its potency in a variety of in vivo experiments [67]. So, it is widely inserted as a biological tool in cell cycle, cancer, apoptosis and neurobiology studies [63].

LGR 2674 is an analogue of roscovitine which has been synthesized by Dr. Vladimír Krystof (Palacký University, Czech Republic). Next to other analogues (EU Project

collaboration PROKINASE No. 503467), it is claimed to show a higher potency and selectivity in comparison to (R)-roscovitine. This is what we wanted to evaluate in our experiment. The differences concerning the original substance is that the purine scaffold has been changed to pyrazolo [4,3-d] pyrimidine and an alteration of the side chain at the position C5.

Roscovitine was used as a Cdk5 inhibitor in combination with mice carrying an inducible endothelial Cdk5 knock-out to evaluate their effects on tumor growth while LGR 2674 was chosen for a xenograft model concerning growth reduction of HCCs.

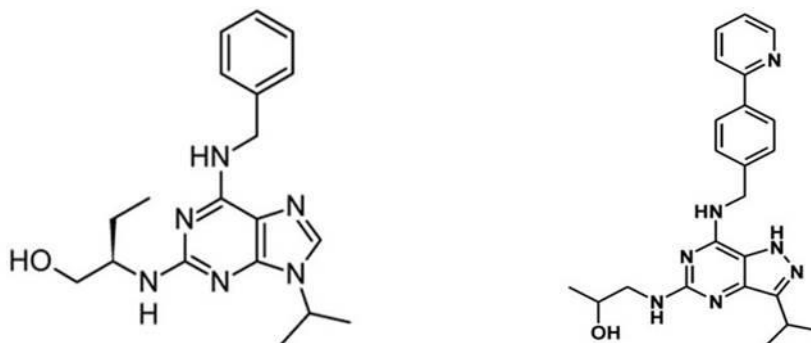


Figure 6: Chemical structures of R-roscovitine (left) and LGR 2674 (right) [68]

1.2.3. Dinaciclib

Dinaciclib (SCH727965) is also a potent small molecule inhibitor of cyclin-dependent kinases (Cdks), it intensely affects Cdk1, 2, 5 and 9 [69]. It was developed during a screening for proper candidates which integrated efficacy and tolerability parameters to identify potential Cdk inhibitors with a suitable balance of activity and tolerability. The inhibition of Cdks in general is more and more used in cancer therapy. Flavopiridol and roscovitine are two clinically studied and common used Cdk inhibitors, which are also based on the pyrazolo-pyrimidine scaffold as dinaciclib is [70]. It was shown that dinaciclib detracted volume of established solid tumors in a variety of murine models with used dosages below the maximally tolerated level [71]. Dinaciclib is used in clinical trials for a range of solid-organ malignancies. Currently, it is undergoing clinical phase II trial in the treatment of non-small-cell lung cancer [72]. Compared with flavopiridol, it inhibits Cdk1 and Cdk9 with equal potency, but with 12-fold higher potency Cdk2 and 14-fold higher potency Cdk5, in which we were interested in [71]. Dinaciclib binds to the ATP side of Cdks through a complex network of binding interactions [73] and it interferes in the unfolded protein response (UPR) whose dysregulation plays a role in cancer pathogenesis. This mechanism is based on Cdk1 and Cdk5 [74]. Dinaciclib was used in its function as an inhibitor of Cdk5 in the limiting dilution experiment with 4T1-luc cells (murine breast cancer).

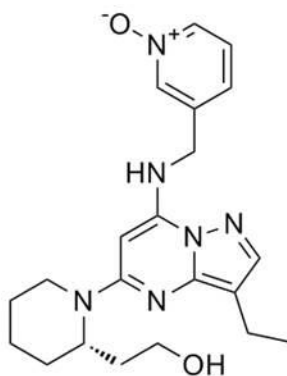


Figure 7: Chemical structure of dinaciclib [75]

2. Compounds used for combinatorial treatment

Next to the natural and synthesized compounds we were mainly interested in, some other drugs were used for combination in the *in vivo* experiments due to their mode of actions or their consisting establishment for certain indications. The intent of these combinations was to reach synergistic effects.

Concerning the combinatorial use of drugs, additive, synergistic and antagonistic effects have to be differentiated. Additive effect means to get the sum of the effect from one drug plus the effect of the combinatorial drug while a synergistic combination leads to effects which are higher than the sum of the effects of the individual drugs [76]. An antagonistic effect would lead to an abolition of the effect of two drugs, so there is less or no outcome. The compounds which were just used for combinatorial treatment are illustrated in the following.

2.1. Nutlin-3a

Nutlin-3a is a small-molecule inhibitor of the interaction between tumor suppressor p53 and its negative regulator mouse double minutes clone 2 (MDM2) [77]. In recent years, the disruption between MDM2 and p53 interaction turned out to be a promising therapeutic strategy [78]. Nutlins are *cis*-imidazoline analogues which were identified during screening of synthetic chemical libraries and then optimized for potency and selectivity. Nutlin-3a showed the highest effectivity [77] [79]. P53 is a very important protein concerning tumor suppression, its pathway is always disturbed in cancer cells either by inactivating mutations or by other mechanisms which lower the p53 level, e.g. MDM2 overexpression [80]. MDM2 itself shows an overexpression in a variety of tumors [81] and is associated with a high aggressiveness in cancer disease [82]. The nutlin strategy is to displace p53 from the binding pocket of MDM2 by docking on the N-terminal of MDM2 [81], so the p53 level increases again and p53 is able to attend its functions [83]. Nutlin-3a already showed proper results within combinatorial treatment and it was successfully tested *in vivo* before [84] [85]. Our data suggest that V-ATPases also influence p53, so we combined V-ATPase inhibition through archazolid A and p53

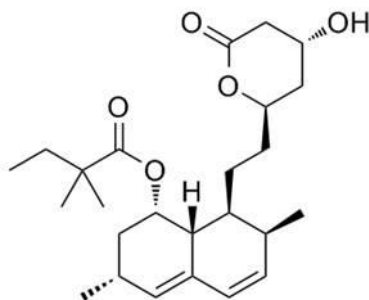


Figure 9: Chemical structure of simvastatin [75]

2.3. Sorafenib

Sorafenib is a multiple kinase inhibitor which has been established on the market as Nexavar® (Bayer Pharmaceuticals) since 2006 [96]. It belongs chemically to a class that can be described as bis-aryl ureas [97]. Sorafenib is able to inhibit the serine-threonine kinase Raf which is part of the Ras/MEK/ERK pathway [98]. In addition, it is able to block the auto-phosphorylation of a variety of receptor tyrosine kinases [99]. It is effective against tumor growth through its anti-proliferative, anti-angiogenesis, anti-metastatic and pro-apoptotic properties [100] [101]. Sorafenib is the only drug with clinical approval for patients suffering from advanced stage hepatocellular carcinoma (HCC) [102]. HCC is an epithelial liver tumor, mostly with poor prognosis. Sorafenib is used as a cytotoxic drug for systemic treatment. It is orally administered and relatively well tolerated by patients up to a dosage of 400 mg which was tested in a phase III study with over 600 participants [103]. Sorafenib was able to improve the overall survival rate of patients suffering from advanced hepatocellular carcinoma [104]. This drug was already tested in a variety of in vitro and in vivo models. In murine models it showed the induction of vascular regression and inhibition of tumor growth, orally administered in dosages up to 100 mg/kg via gavage [105] [106]. But there are also other data on in vivo experiments which show proper results with an intraperitoneal application [107]. Since Cdk5 is known to play a role in HCC, we investigated the effect of sorafenib in combination with Cdk5 inhibition on Huh7 tumors.

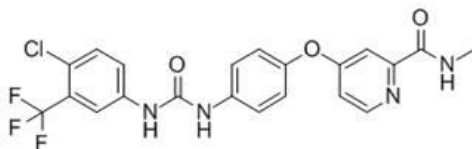


Figure 10: Chemical structure of sorafenib [75]

3. The role of Cdk5 in cancer development

Some projects of our lab focus on the effects of Cdk5 inhibition in cancer therapy. I contributed to some of these projects with *in vivo* experiments, so the role of Cdk5 in cancer development is explained in more detail in this section.

Cyclin-dependent kinases (Cdks) are a family of serine/threonine kinases which are activated by cyclins. Nine Cdks and ten cyclins have been identified in humans but there are additionally several Cdk related kinases whose cyclin partner is not yet identified [108]. Cdk5, which is expressed in all tissues, is a very special member of this family because its kinase activity is activated by binding to the non-cyclin proteins p35 and p39 which induces changes in the conformation of the kinase [109]. These activators are predominantly expressed in post-mitotic neurons which is the reason why Cdk5 is mainly associated with the central nervous system (CNS) [110]. These two activators regulate themselves through transcription and ubiquitin-mediated degradation. P35 and p39 can get cleaved to the more stable products p25 and p29 which increases the Cdk5 activation [111]. Cdk5 itself was first discovered during the 1990s to have certain functions in the CNS [112]. Its main influence concerns neuronal migration, axonal guidance and synaptic plasticity and it is also associated with a variety of neurodegenerative and neuropsychiatric diseases [113]. Its dysregulation by binding to p25 is associated with the development of amyotrophic lateral sclerosis and Alzheimer's disease [114] [115]. Since the 1990s, a variety of other functions of Cdk5 have been evaluated. There are many molecular mechanisms Cdk5 uses to affect cellular processes in different cell types, associated with aberrant Cdk5 activity. It was shown that it regulates differentiation, exocytosis, gene expression and transcription, cell-cell and cell-matrix adhesion, cell migration, tissue regeneration, wound healing, senescence, angiogenesis, apoptosis and hormone regulation in non-neuronal cells [116] [117]. Cdk5 was discovered to play a significant role in different cancer types including lung cancer, prostate cancer, pancreatic cancer, breast cancer and glioblastomas [118]. Our group was able to show the profound functions of Cdk5, that it is increased in human HCC tissues [111] and that it plays a role in vascular development [113].

Several murine tumor experiments in this thesis were established to investigate the potential of Cdk5 inhibition as anti-cancer strategy.

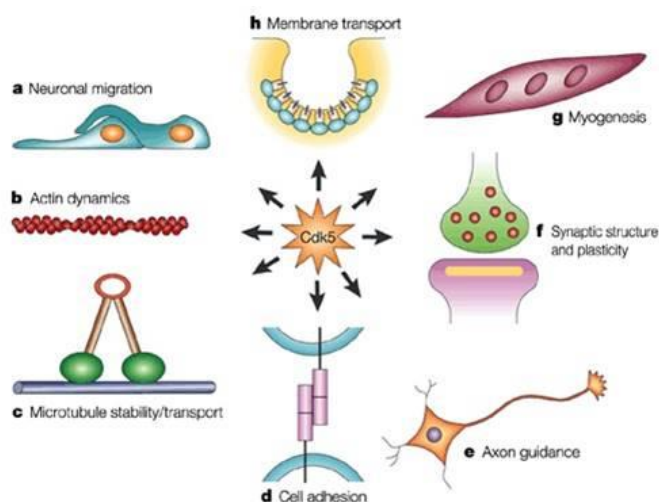


Figure 11: Cellular processes regulated by Cdk5 [112]

4. Murine tumor models in cancer research

Laboratory animals are widely used in research, according to the BMEL, 2.798.463 animals were used in its purpose in Germany in 2014. 83% of all of them are allotted to rodents as mice and rats.

Murine models have always played a significant role in cancer research for many decades and are indispensable in the drug discovery and developmental process for new anti-cancer drugs, small molecules and biologics [119]. Models which are mostly used include xenografts, meaning that a graft of tissues is taken from a donor of one species and is grafted into a recipient of another species, and allografts, meaning that a graft of tissues is taken from a donor of one species and is grafted into a recipient of the same species, grown in either immune competent or immune deficient mice. But nowadays, transgenic, knock-out and knock-in mouse models become established more and more to evaluate the pathways and targets in anti-cancer therapy [120]. Animal models can provide information on pharmacodynamics and pharmacokinetics and provide pharmacological and biological information on anti-cancer drugs. They are used to identify the pathophysiology of cancer including new target identification, to identify novel therapeutic agents, to explore the utility of novel therapeutics combined with established therapeutic regimes and to study mechanisms of intrinsic and acquired resistance to cytotoxic and targeted therapies [119]. There exist a variety of animal models in cancer research, beginning with toxicology tests to determine parameters such as LD₅₀ (median lethal dose), TD₅₀ (median toxic dose), LOEL (lowest observed effect level) and NOEL (no observed effect level) to evaluate the toxicity of a certain anti-cancer drug *in vivo*, followed by studies on pharmacokinetics and dynamics to evaluate the behavior of the substance in the body and to find an adequate administration regime. According to this, we performed experiments concerning pharmacokinetics with the compounds archazolid A and roscovitine. After this, planning an experiment leads to the decision which dosage is suitable enough to use it in a murine tumor model. In this thesis, these kind of

experiments are called “dose finding“ because we wanted to evaluate suitable dose rates which the mice would tolerate during long-term experimental periods. We conducted this with many of our compounds. The next step was to establish tumor models concerning tumor growth or dissemination. Two classes of animal models are used widely, the ectopic tumor model where the mouse receives tumor cells via subcutaneous, intraperitoneal or intravenous injection, not into the original organ of tumor cells. Within the other one, the orthotopic model, the tumor cells are implanted into the organ of their origin [119]. In this thesis, ectopic xenografts with a variety of human cancer cell lines and two ectopic allograft models with luciferase-tagged murine breast cancer cells or murine melanoma cells were used. Partly using bioluminescence imaging for their evaluation. The advantage of our murine tumor models is that the experimental drugs were able to be tested under the physiological influences of a living organism, e.g. the general condition of the animals, their gender or corresponding hormones. This is not possible with in vitro experiments where cell layers are used. For the use of murine cancer cell lines we chose the mouse strains where they originated from to work with syngeneic models. But a variety of human cancer cell lines were also used to evaluate our experimental compounds. This was even possible because we used immuno-deficient mouse strains in which human cancer cells were able to grow. In this way, information can be gained in murine experiments to enable conclusions how human cancers could respond to a certain treatment. But it has to be mentioned that murine models alone are not suitable for a complete preclinical evaluation of an experimental drug. This is the reason why in preclinical studies always two different animal species have to be used for testings. Murine models are established as a start, they are very important to gain first in vivo results and to lay the foundations for further experiments.

5. Aim of the thesis

Our lab focuses on new pharmaceutical anti-cancer approaches, namely the use of natural compounds (DFG, FOR 1406) and synthetic compounds as potential novel anti-cancer drugs. A variety of in vitro experiments were performed by my colleagues to investigate the anti-cancer potential of the experimental drugs. I carried out the next step, namely the corresponding animal experiments. The aim of this thesis was the establishment, realisation and evaluation of all performed murine tumor experiments. In detail, the establishment of the experimental setups, the choice of mouse strains, the realisation of all experiments up to the generation and interpretation of the results. The profound testing of the anti-cancer compounds was enabled through the in vivo experiments in this thesis. Additionally, all methods for the usage of the bioluminescence imager IVIS® Spectrum within the murine experiments were established for the very first time at our lab and offered the possibility to use a non-invasive and repeatable imaging tool for tumor dissemination models. It is very important to visualize the dissemination of tumor cells in the body to identify the organs they invade and where they are able to form new growths. The demonstration of tumor cell dissemination in a living animal over time, where mice

do not have to be sacrificed, was realised for the first time in our lab by use of this bioluminescence imager.

In general, all of the animal experiments in this thesis can be described as models to investigate attempts to hamper tumor growth or dissemination through natural and synthetic chemotherapeutics *in vivo*, partly with closer inspection on the influence of Cdk5 in cancer processes. The aim was to provide tools to develop new anti-cancer strategies and to reach profound results through *in vivo* experiments.

When an experimental compound was used *in vivo* for the first time, a dose-finding experiment was performed in the beginning. The aim of these trials was to evaluate a suitable treatment regime and a dosage mice tolerate during long-term experiments. Studies on pharmacokinetics were performed to evaluate the concentration of a substance in the blood over time after injection and to adjust our treatment regimes according to the results.

The aim of this thesis was to establish suitable murine tumor models for our projects. Suitable allograft and xenograft models were needed for the evaluation of the effects on tumor growth of some of the experimental compounds (archazolid A, LGR 2674, PS89 and soraphen A). Additionally, two murine models were established to investigate the potential of the experimental compounds tetrandrine and soraphen A on hampering tumor dissemination.

To evaluate the influence of cancer stem cells on tumor development and growth, two murine limiting dilution experiments were performed. And to further investigate Cdk5's role in cancer different murine tumor growth experiments were established.

All in all, the aim of this thesis was to establish and use *in vivo* models in order to investigate the effects of experimental compounds on tumor growth and tumor dissemination.

II. Materials and Methods

1. Materials

1.1. Compounds

Archazolid A	Prof. Dirk Menche (University of Bonn, Germany)
Dinaciclib	Selleckchem (Munich, Germany)
LGR 2674	Dr. Vladimir Krystof (Palacky University of Olomouc, Czech Republic)
Nutlin-3a	MedChemExpress (Princeton, USA)
PS89	Prof. Uli Kazmaier (University of Saarland, Germany)
Roscovitine	LC Laboratories (New Boston, USA)
Simvastatin	Sigma Aldrich (Taufkirchen, Germany)
Sorafenib	LC Laboratories (New Boston, USA)
Soraphen A	Prof. Rolf Müller (University of Saarland, Germany)
Tetrandrine	Santa Cruz Biotechnology (Santa Cruz, USA)

1.2. Cell culture

B16F1 cells	ATCC (Wesel, Germany)
Huh7 cells	DSMZ (Braunschweig, Germany)
Huh7 nt shRNA cells	generated by Dr. Sandra Ehrlich (University of Munich, Germany)
Huh7 Cdk5 shRNA cells	generated by Dr. Sandra Ehrlich (University of Munich, Germany)
U87MG cells	Prof. Adrian Harris (Oxford University, United Kingdom)
Jurkat-luc cells	Dr. Irmela Jeremias (Helmholtz Centre Munich, Germany)
T24 nt shRNA cells	generated by Dr. Siwei Zhang (University of Munich, Germany)

II. Materials and Methods

T24 Cdk5 shRNA cells	generated by Dr. Siwei Zhang (University of Munich, Germany)
4T1-luc cells	Perkin Elmer (Rodgau, Germany)
RPMI 1640 medium	Pan Biotech (Aidenbach, Germany)
DMEM medium	Pan Biotech (Aidenbach, Germany)
McCoy's 5A medium	Pan Biotech (Aidenbach, Germany)
Glutamine	Roth (Karlsruhe, Germany)
Collagen G	Biochrom AG (Berlin, Germany)
Fetal calf serum (FCS)	Biochrom AG (Berlin, Germany)
Puromycin	Sigma Aldrich (Taufkirchen, Germany)
Pyruvate	VWR (Ismaning, Germany)
Cremophor® (solutol)	Sigma Aldrich (Taufkirchen, Germany)
DMSO	AppliChem (Darmstadt, Germany)
NaCl	Bernd Kraft (Duisburg, Germany)
Na ₂ HPO ₄	Grüssing (Filsum, Germany)
KH ₂ PO ₄	Merck (Darmstadt, Germany)
EDTA	Roth (Karlsruhe, Germany)
Trypsin	Pan Biotech (Aidenbach, Germany)
PBS (pH7.4)	NaCl 132.2mM + Na ₂ HPO ₄ 10.4 mM + KH ₂ PO ₄ 3,2 mM + H ₂ O (in house)
Trypsin/EDTA (TE)	Trypsin 0.05 % , EDTA 0.20% , PBS (in house)
Cell culture flasks/plates	Sarstedt (Nümbrecht, Germany)

1.3. In vivo experiments

NaCl 0,9%	Braun AG (Melsungen, Germany)
Acetone	Brenntag GmbH (Munich, Germany)
Ethanol	Brenntag GmbH (Munich, Germany)
Bepanthen®	Bayer Vital GmbH (Leverkusen, Germany)

Isothesia®	Henry Schein Vet (Hamburg, Germany)
Lasal 2003 Oxygen	Air Liquide (Munich, Germany)
Ketamine 10%	beta-pharm (Vechta, Germany)
Xylarium®	Ecuphar (Oostkamp, Belgium)
Tamoxifen	Sigma Aldrich (Taufkirchen, Germany)
Syringes	Henry Schein Vet (Hamburg, Germany)
Needles	Terumo (Leuven, Belgium)
Scalpels	Dahlhausen (Cologne, Germany)
Matrigel®	Corning (Bedford, USA)
D-Luciferin, potassium salt	Perkin Elmer (Waltham, USA)
Paraformaldehyde (PFA)	AppliChem (Darmstadt, Germany)
EDTA blood tubes	Sarstedt (Nümrecht, Germany)

1.4. Laboratory mouse strains

1.4.1. C57BL/6

These black mice (C57BL/6J OlaHsd) were purchased from Envigo, former Harlan Laboratories (Eystrup, Germany) or taken from our own breeding. This is an inbred strain which has a competent innate and adaptive immune system.

1.4.2. BALB/c

These albino mice (BALB/c OlaHsd) were purchased from Envigo, former Harlan Laboratories (Eystrup, Germany). This is an inbred strain which has a competent innate and adaptive immune system.

1.4.3. BALB/c nu/nu

These nude mice (BALB/c OlaHsd-Foxn1^{nu}) were purchased from Envigo, former Harlan Laboratories (Eystrup, Germany). They are hairless with an albino background. These mice are T-cell deficient and the nu allele on chromosome 11 holds an autosomal recessive mutation which is responsible for the hairlessness.

1.4.4. Scid

This albino immunodeficient strain (CB17/lcr-Prkdc^{scid}/lcrCr1) was purchased from Charles River Laboratories (Sulzfeld, Germany). They hold the autosomal recessive scid mutation (severe combined immunodeficiency). This mutation affects B- and T-cell production, while their innate immune system is intact.

1.4.5. Nod Scid

These albino immunodeficient mice (Nod.CB17-Prkd^{scid}/NCrHsd) were purchased from Envigo, former Harlan Laboratories (Eystrup, Germany). They hold the scid mutation, so they have no mature B- and T-cells. They also have a reduced innate immune system including deficits in macrophages, dendritic and natural killer cells and the complement system.

1.4.6. NSG (Nod Scid Gamma)

This albino immunodeficient strain (Nod.Cg-Prkd^{scid}Il2rg^{tm1Wjl}/SzJ) was purchased from Charles River Laboratories (Sulzfeld, Germany). Their scid mutation prevents maturation of T- and B-cells, they hold deficiencies in their innate immune system as the absence of hemolytic complement, reduction of dendritic cell function and defective macrophages. There is also a deficit in Il2rg which prevents the signaling from six interleukins and blocks the development of natural killer cells.

1.4.7. Housing

Mice were housed in a special air-conditioned room within individual ventilated cages (IVC, type II long, Tecniplast). A 12h day- and night cycle was provided. All of the mice had ad libitum access to autoclaved water (in bottles) and autoclaved standard food (producer: Ssniff). The maximum occupancy was five animals per cage. The cages, inclusive litter and bedding inlets, were changed once a week.

Mice were purchased at an age of five weeks and used at the earliest with six weeks in the experiments to have enough time to acclimatize and to adapt to the new housing conditions. In the animal facility, the health status was checked quarterly according to FELASA recommendations.

All animal experiments were performed according to German legislation for the protection of animals and were approved by the government of Upper Bavaria.

1.5. Instruments

Canon Digital IXUS 70	Canon (Krefeld, Germany)
Digital Caliper	Emil Lux (Wendelskirchen, Germany)
Grundig MC4541 shaver	Grundig (Fürth, Germany)
IVIS® Spectrum	Caliper Life Sciences (Rüsselsheim, Germany)
Megafuge 1. ORS	Heraeus (Hanau, Germany)
Olympus CK30 microscope	Olympus (Hamburg, Germany)
Scale TE601	Sartorius (Göttingen, Germany)
UV- lamp	Philips (Hamburg, Germany)

Vi-Cell TM XR Beckmann Coulter (Fullerton, USA)

1.6. Software

Graph Pad Prism 5.04 Graph Pad (San Diego, USA)

Living Image 4.4 Caliper Life Sciences (Rüsselsheim, Germany)

2. Methods

2.1. Cell culture

All tumor cell lines which were used for our animal experiments were chosen according to prior in vitro experiments. Human hepatocellular carcinoma cells (Huh7) were cultivated in DMEM medium, supplemented with 10% FCS. The stable lentiviral knock-down in Huh7 nt shRNA and Huh7 Cdk5 shRNA was generated by Dr. Sandra Ehrlich (University of Munich, Germany), these cells were grown in DMEM medium which contained 10% FCS and 1% puromycin. B16F1 (murine melanoma cells) were cultured in DMEM medium, supplemented with 10% FCS. Stable luciferase expressing murine breast adenocarcinoma cells (4T1-luc) and the human glioblastoma cell line (U87MG) were cultivated in RPMI 1640 medium containing 10% FCS. The stable luciferase-expressing human leukemia cells (Jurkat-luc) were grown in RPMI 1640 medium containing 10% FCS and 1% pyruvate. The stable lentiviral knock-down in the human urinary bladder cancer cells T24 nt shRNA and T24 Cdk5 shRNA was generated by Dr. Siwei Zhang (University of Munich, Germany). These cells were grown in McCoy's 5A medium which contained 10% FCS, 1% glutamine and 1% puromycin. All cells were cultured under constant humidity at 37°C and with 5% CO₂ in an incubator. The culture flasks for all Huh7 lines were first coated with collagen G (0.001% in PBS) before seeding.

For all animal experiments 150 cm² flasks were used. Adherent cells were used when they were confluent, their medium was removed and cells were washed two times with PBS before incubation with trypsin/EDTA (TE) for about 2 min at 37°C to harvest them. This reaction was inactivated again with growth medium. Afterwards the cells were counted via Vi-Cell TM XR cell counter. The required amount of cells was taken off and centrifuged (1.000 rpm, 5 min, 20°C), then the cell pellet was solved again with PBS. U87MG cells and T24 cells were diluted 1:1 in Matrigel® and PBS in terms of better propagation of tumors prior to injection.

Cells in suspension (Jurkat-luc) were cultivated in growth medium, then counted via Vi-Cell TM XR. The required amount was taken off and centrifuged (1.000 rpm, 5 min, 20°C), afterwards the cell pellet was re-suspended in PBS.

2.2. In vivo experiments

All laboratory mice were purchased at an age of five weeks. They were used at the earliest with an age of six weeks for the experiments. Tumor cells for all in vivo experiments were cultured and prepared as described above.

Hairy mice were locally shaved before cell inoculation. Subcutaneous (s.c.) injections of tumor cells into the mice' flanks and intraperitoneal (i.p.) injections of substances were carried out with 1 ml syringes in combination with 27 Gauge (G) needles. Before intravenous (i.v.) injections, the tail veins were dilated with an UV lamp and 1 ml syringes and 27 G needles were used for this procedure. General condition of the mice was checked daily, body weight was measured at least once a week with a scale and tumor growth was measured every second to third day with a caliper. For intravenous applications, the injection volume did not exceed 100 μ l while the volume for subcutaneous and intraperitoneal injections varied between 100 μ l and 200 μ l. In the end of all in vivo experiments mice were sacrificed through cervical dislocation. Solid tumors were removed, weighed, photographed and split into two parts, one for storage at -80°C and one for conservation in 1% paraformaldehyde (PFA).

2.2.1. In vivo imaging system (IVIS®)

For bioluminescence imaging experiments with the IVIS® Spectrum, all mice were anesthetized with isoflurane in oxygen, during the beginning with 2-3 % in a chamber and for maintenance with 1.5-2 % through nose cones. Eye ointment (Bepanthen®) was used to prevent the cornea drying out. During imaging, mice lay on a warm board. Five to ten minutes before imaging 6 mg K-luciferin per mouse, solved in 100 μ l PBS, were intraperitoneally injected. Adjustments for the IVIS® Spectrum: 3-6 sequenced pictures with a delay time of 0.5-2 min were taken. Exposure time 1 sec, Binning 8, F-Stop 1, if not indicated otherwise. For evaluation of bioluminescence signals ROIs (region of interest) were defined and the total signal per ROI was calculated as photons/second/cm² (total flux/area). Shown is always one picture out of a sequence.

Method is based on the reaction between the luciferase in the cells and the injected luciferin which led to a bioluminescence signal the imager can detect [121]. Luciferin is oxidized by the enzyme luciferase under ATP spending and under the presence of oxygen to form an electronically excited oxy-luciferin structure. Visible light is emitted following the relaxation of excited oxy-luciferin to its ground state. Because this light can be transmitted through mammalian tissues, it is possible to use bioluminescence for non-invasive and quantitative monitoring of tumor burden [122].

2.2.2. Preliminary dose finding experiments

Dose finding experiments were performed for the compounds simvastatin, PS89, LGR 2674, soraphen A, archazolid A and nutlin-3a, partly within combinatorial treatment regimes. For evaluating their toxicity in living mice and to find a proper dosage, all substances were solved in 5% DMSO, 10% solutol and 85% PBS and were intraperitoneally injected using 1 ml syringes and 27 G needles. Volume of injection always amounted 100 µl per mouse. For all experiments, female mice at an age of six weeks were used. Mice were controlled at least directly after injection, 30 minutes later, two hours later, 24 hours later and then daily. Their general condition was evaluated by their breathing, behavior, posture, weight and body condition score (BCS), by signs of pain as bent position, closed eyes and isolation of the group and by their fur and color of the skin and mucosa (eyes and anus). Mouse strains were chosen according to the cell lines they should get applied in the main trials.

2.2.2.1. Simvastatin

For the dose finding test with simvastatin, two female Scid mice received a daily dose of 10 mg/kg over five days, method is described above. They received the first dosage on day 0 and the experiment was ended on day 4 through cervical dislocation. A second experiment was performed with another two female Scid mice that received 10 mg/kg simvastatin in combination with 0.2 mg/kg archazolid A via daily intraperitoneal injection, also over five days. Mice were kept under close meshed surveillance, all mice were sacrificed at the end of the experiment (d4) through cervical dislocation.

2.2.2.2. LGR 2674

The roscovitine derivative LGR 2674 was tested in two dose rates over five days, 1.5 mg/kg and 15 mg/kg per day. In both settings two female Scid mice were used which received a daily intraperitoneal injection. At the end of the experiment (d4) mice were sacrificed through cervical dislocation

2.2.2.3. Archazolid A and nutlin-3a

Archazolid A was tested four times, dosages lay at 0.25 mg/kg/d, 0.3 mg/kg/d, 0.45 mg/kg/d and 0.6 mg/kg/d.

First, from a group of three BALB/c nu/nu mice, always one mouse received either 0.3 mg/kg archazolid A or 5 mg/kg nutlin-3a or a combination of both via daily i.p. injection over five days (d0, d1, d2, d3, d4).

Afterwards, the dosage of archazolid A was varied, 0.3 mg/kg, 0.45 mg/kg and 0.6 mg/kg were tested, each in one mouse via daily i.p. injection over five days.

In the third part of this experiment, 0.25 mg/kg and 0.3 mg/kg archazolid A were tested daily over five days via i.p. injection, each in one BALB/c nu/nu mouse. At last, 0.25 mg/kg archazolid A in combination with 5 mg/kg nutlin-3a and 0.3 mg/kg

archazolid A in combination with 5 mg/kg nutlin-3a were evaluated, each combination in one BALB/c nu/nu mouse daily over five days.

Their vitality was checked close meshed. On final days mice were sacrificed through cervical dislocation.

2.2.2.4. PS89

The substance PS89 was tested in three different dose rates, 10 mg/kg, 20 mg/kg and 30 mg/kg. In each experiment two female Scid mice received a daily intraperitoneal injection. 10 mg/kg and 20 mg/kg were tested over four days (d0-d3), and the 30 mg/kg dosage was evaluated over seven days (d0-d6). Afterwards a combination of 30 mg/kg PS89 and 10 mg/kg sorafenib was tested in two female Scid mice daily over three days (d0-d2). On final days, mice were euthanised through cervical dislocation.

2.2.2.5. Soraphen A

A 5 mg/kg, a 10 mg/kg and a 20 mg/kg dosage was used for soraphen A testing. In each experiment two BALB/c mice received a daily i.p. injection over four days (d0-d3). We also tested 20 mg/kg and 40 mg/kg of soraphen A in two female Scid mice each, which received a daily i.p. injection over five days (d0-d4). All mice were euthanised through cervical dislocation afterwards.

2.2.3. Murine models concerning pharmacokinetics

2.2.3.1. Archazolid A

To evaluate the blood concentration of archazolid A after i.p. and i.v. injection, ten C57BL/6 mice, female and 12 months old, were used. Eight of these mice were divided into two groups (n=4), in the one group each mouse received an intraperitoneal injection of archazolid A (0.3 mg/kg), in the other group they received the same dosage intravenously via tail vein. In both groups, archazolid A was solved in an amount of 100 µl, consisting of 5% DMSO, 10% solutol and 85% PBS. 30 min, 1 hour, 2 hours and 6 hours later blood was taken via heart puncture with 3 ml syringes and 27 G needles, for that mice were anesthetized with a combination of ketamine and xylazine (1 ml ketamine + 0.25 ml xylazine + 6 ml NaCl, then using 0.1 ml per 10g body weight). At each time-point blood was taken from one intraperitoneally treated and one intravenously treated mouse. After heart puncture mice were euthanized through cervical dislocation. The other two mice did not get an archazolid A injection, but blood was also taken from them via heart puncture, method is mentioned above. One sample stayed clear and was used as an internal standard (0% value) and the second one was armed with 10 µM archazolid A and was used as the 100 % value. All blood samples were centrifuged, serum phase was taken off and mixed 1:1 with acetone, centrifuged again and then, the upper phase containing archazolid A was taken off and frozen at -80° C for analysis. All

analyses, high performance liquid chromatography (HPLC) and mass spectrometry were performed by Dr. Jennifer Herrmann (University of Saarland, Germany). For our calculation of theoretical values which should be found in the blood, the formula $n = m/M$, (n = blood concentration, m = amount of the substance, M = molecular weight) was used. Based on the assumption of 1600 μl blood per mouse, consisting of 800 μl serum and 800 μl blood cells. The calculation we made is described in detail in the following: Molecular weight of archazolid A lays at 737.98 g/mol, we injected 0.3 mg/kg archazolid A which equates 6 μg archazolid A per 20g mouse (standard mouse). The 6 μg are contained in 800 μl serum, following that 1 μl serum contains 7.5 ng archazolid A. Using the formula $n = m/M$, $n = 7.5 \text{ ng} / 737.98 \text{ g/mol}$, $n = 10 \mu\text{M}$. All results were compared with this calculated value.

2.2.3.2. Roscovitine

To evaluate the concentration of roscovitine in murine blood samples after i.p. injection, 21 C57BL/6 mice, female and six weeks old, were used. 18 of these mice received an intraperitoneal injection of 150 mg/kg roscovitine, solved in 100 μl consisting of 5 % DMSO, 10 % solutol and 85 % PBS. 10 minutes, 20 minutes, 30 minutes, 60 minutes, 2 hours and 4 hours later blood was taken from three mice at each time-point via puncture of the heart, mice were anesthetized for that with the ketamine/xylazine combination mentioned before. Used were 3 ml syringes and 27 G needles. After the blood take, mice were sacrificed through cervical dislocation. The blood of the other three mice was taken in the same way, it was used as an internal standard, those mice were all vehicle treated before. All blood samples were taken into EDTA blood tubes to prevent coagulation. All following analyses, HPLC and mass spectrometry were performed by Dr. Christoph Müller (University of Munich, Germany). We performed calculations on the theoretical concentration which should be found in the blood, method is described in the following: We injected 150 mg/kg roscovitine per mouse which equates 3 mg/ 20g mouse (standard mouse). Based on the assumption of 1600 μl blood per mouse, there are 3 mg roscovitine in 1.6 ml blood equating 1.875 mg in 1 ml blood. All results were compared with this calculated value.

2.2.4. Murine tumor models for tumor growth evaluation

These experiments were performed following a general procedure. Hairy mice were shaved one to two days before the experiment started. All mice received the cells via subcutaneous injections into the left flank using 1 ml syringes and 27 G needles, if not indicated otherwise. Tumor growth was measured every second day with a caliper using the formula $\pi/6 \times L \times W \times H$ (L = length, longest side of the tumor, W = width, widest side vertical to L , H = height). On final days of the experiments, all mice were sacrificed through cervical dislocation. Tumors were resected, weighed,

photographed and split into two parts, one for freezing at $-80\text{ }^{\circ}\text{C}$ and one for conservation in 1 % PFA.

2.2.4.1. Effect of archazolid A treatment on murine breast cancer shown in an allograft tumor model

For evaluating the effect of archazolid A on tumor growth of 4T1-luc cells, eight BALB/c nu/nu mice, female and six weeks old were used. 1×10^6 4T1-luc cells per mouse, solved in 100 μl PBS, were injected. After that, mice were randomly divided into two groups (n=4). Therapy started on day six after cell inoculation. Archazolid A, solved in 5% DMSO, 10% solutol and 85 % PBS, was daily given in a dose of 0.3 mg/kg via intraperitoneal injection, volume lay at 100 μl . Therapy was conducted seven times after cell application (d6, d7, d8, d9, d10, d11, d12), one group was treated with archazolid A, the other group was vehicle treated at the same points of time. Over a period of 12 days the average tumor volumes of both groups were measured and compared. Final day of experiment was day 13.

2.2.4.2. Combinatorial effect of simvastatin and archazolid A on HCC tumors evaluated in a xenograft tumor model

Regarding the combinatorial effect of simvastatin and archazolid A, a Scid mouse model was used. 32 female and six weeks old Scid mice received 3×10^6 Huh7 cells for injection. Tumor bearing mice were randomly divided into four groups (n=8). Concerning therapy, volume of injection amounted 100 μl , both substances and the combination of both were solved in 5% DMSO, 10% solutol and 85% PBS. One group of mice was treated as a control and received vehicle, the simvastatin group got 10 mg/kg while the archazolid A group got 0.2 mg/kg. The fourth group was the combinatorial group which received both compounds in the dosage mentioned before. The intraperitoneal treatment started on day seven after cell injection and was daily continued until day 17. Mice received an injection 11 times (d7, d8, d9, d10, d11, d12, d13, d14, d15, d16, d17). Experiment was ended on day 17.

2.2.4.3. Effects of combinatorial treatment of nutlin-3a and archazolid A on glioblastoma tumors using a xenograft model

The combinatorial effect of nutlin-3a and archazolid A was tested in a xenograft BALB/c nu/nu mouse model. 32 female BALB/c nu/nu mice at an age of six weeks got 5×10^6 U87MG cells injected. Volume of injection amounted 100 μl , cells were solved in 50% PBS and 50% Matrigel®. All mice were separated into four groups (n=8). One group was vehicle treated and used as control, another group was treated with archazolid A (0.2 mg/kg), the third group received a daily dosage of nutlin-3a (5mg/kg) and the last one received a daily combinatorial dosage of archazolid A (0.2mg/kg) and nutlin-3a (5 mg/kg), all substances were solved in 5% DMSO, 10% solutol and 85% PBS. Therapy started on day seven after cell application and was

performed 16 times, that means daily until day 25. Experiment was ended on day 25. The evaluation of tumor growth over time was performed by jun.-Prof. Thorsten Lehr (University of Saarland, Germany). The modeling was performed using the non-linear mixed effects modeling technique with the software NONMEM 7.3. [123], nutlin-3a PK model was built based on literature data. [84] Tumor growth curves were normalized to control.

2.2.4.4. Effect of LGR 2674 on HCC tumors using a xenograft setup

The effect of the roscovitine derivative LGR 2674 on tumor growth was evaluated with Huh7 cells using a Scid mouse model. 20 female mice at an age of six weeks were chosen. 3×10^6 Huh7 cells per mouse were solved in 100 μ l PBS and then s.c. injected. Tumor bearing mice were randomly divided into two groups, one control group (n=10) and a LGR 2674 treatment group (n=10). The control group was daily vehicle treated while the therapy group received LGR 2674 in a dosage of 1.5 mg/kg solved in 5% DMSO, 10% solutol and 85% PBS every day. Therapy started on day eight after tumor cell inoculation, mice got their daily intraperitoneal injection 13 times (d8, d9, d10, d11, d12, d13, d14, d15, d16, d17, d18, d19, d20). One mouse of the control group and one mouse of the LGR 2674 treated group had to be taken out of the experiment on day 17 because their tumor's volume exceeded 1000 mm³. Final day for the other animals was day 20.

2.2.4.5. Evaluation of the effect of PS89 in combination with sorafenib on HCC tumors using a xenograft model

For evaluating the effect of PS89 in combination with sorafenib on tumor growth, 3×10^6 Huh7 cells were injected into Scid mice. These 32 female and six weeks old mice received the cells solved in a volume of 100 μ l PBS. Afterwards, mice were divided into four groups (n=8). Both substances and the combination of both were solved in 5% DMSO, 10% solutol and 85% PBS, the control group received intraperitoneal injections of the vehicle, the PS89 treated group received 20 mg/kg and the sorafenib treated group 10 mg/kg. The fourth group got a combination of both substances, dosage as mentioned before. Treatment was carried out three times a week, it started on day ten and ended on day 19, so mice received five injections (d10, d12, d14, d17, d19). Experiment ended on day 19.

2.2.4.6. Effect of soraphen A on HCC tumors shown in a xenograft tumor model

For this experiment, 20 Scid mice, female and six weeks old were used. They received 3×10^6 Huh7 cells. Volume of injection amounted 100 μ l, cells were solved in PBS. Tumor bearing mice were divided into two groups (n=10). Therapy with soraphen A (40 mg/kg) started on day seven after cell inoculation. Mice received a daily dose of 40 mg/kg soraphen A, solved in 5% DMSO, 10% solutol and 85% PBS via intraperitoneal injection. The second group was treated as a control and received

solvent. Therapy started on day seven after cell application and was performed nine times (d7, d8, d9, d10, d11, d12, d13, d14, d15). Over a period of 15 days the average tumor volumes of both groups were measured and compared. On day 16 the experiment was ended.

2.2.5. Murine tumor experiments concerning tumor dissemination

2.2.5.1. Searching for a murine tumor model within a leukemia project

For the Jurkat-luc leukemia experiment, three different mouse strains were used, Scid, Nod-Scid and Nod Scid Gamma (NSG) mice. From each strain we worked with three mice, female and six weeks old. 1×10^6 Jurkat-luc cells per mouse were solved in 100 μ l PBS and were injected via the tail vein. Veins were dilated by holding an UV lamp for circa 20 sec over the tail. We used 1 ml syringes and 27 G needles to inject the cells. For bioluminescence imaging, the imager IVIS® Spectrum was used, each group (n=3) was imaged together, the setup for imaging was described before. Imaging was performed several times. Nod-Scid and Scid mice were imaged six times (d4, d7, d11, d13, d19 and d21) up to final day (d21) after cell inoculation while NSG mice were imaged nine times (d2, d5, d8, d12, d15, d19, d22, d26, d29) until final day (d29). After the last imaging procedures, mice were sacrificed through cervical dislocation

2.2.5.2. Effect of tetrandrine on tumor dissemination evaluated in three different murine experiments

The dissemination of 4T1-luc cells under tetrandrine treatment was evaluated via three different experimental setups. For all of them, we used BALB/c mice, female and six weeks old. 1×10^5 4T1-luc cells, solved in 100 μ l PBS, were intravenously injected into the tail vein of each mouse. Tetrandrine was intraperitoneally applied, injection volume lay at 100 μ l. The IVIS® Spectrum was used for bioluminescence imaging. Setup is described before. Ventrodorsal imaging positions were chosen, meaning mice lay on their backs during the imaging procedure.

In the first setup 20 BALB/c mice were randomly divided into two groups (n=10), tetrandrine was solved in 5% DMSO, 10% solutol and 85% PBS. One group received tetrandrine (100 mg/kg) three times, 24h and 4h before cell application and 24h after it. The other group, used as a control, was vehicle treated at the same points of time. On day eight after cell injection bioluminescence imaging was conducted with IVIS® Spectrum and the experiment was ended through cervical dislocation of all mice. Lungs were extracted, imaged with IVIS® Spectrum and photographed. Organs were fixed in 1% PFA.

Concerning the second setup, 24 BALB/c mice were randomly divided into three groups (n=8), tetrandrine was solved in sterile filtered 0.1 molar HCl this time. One group was vehicle treated and one group was treated with tetrandrine (100 mg/kg),

each group four hours before application of cells, directly after it and 20 hours after it a third time, both groups received just vehicle (DMSO) pre-treated 4T1-luc cells. While the third group got 4T1-luc cells injected which were pre-treated with tetrandrine (10 μ M, 24h), those animals received one extra dose of tetrandrine directly after cell injection, at the other two points of time (4h before and 20h after cell application) they were vehicle treated. Imaging was performed eight days after cell inoculation with IVIS® Spectrum, four mice at a time. After imaging, all mice were euthanised through cervical dislocation.

For the third setup 16 BALB/c mice were used, divided into two groups (n=8). One group, as a control, received vehicle (DMSO) pre-treated 4T1-luc cells, the other group received cells which were tetrandrine pre-treated (10 μ M, 24h) via tail vein injection. We imaged on day five and on day seven after tumor cell injection with the IVIS® Spectrum bioluminescence imager. Directly after the second imaging (d7) mice were sacrificed through cervical dislocation.

2.2.5.3. Effect of soraphen A on tumor dissemination shown in an allograft tumor model

In the metastasis experiment with soraphen A, 24 BALB/c mice were randomly divided into three groups (n=8), one as a control group received vehicle (ethanol) pre-treated 4T1-luc cells, one group received 4T1-luc cells with six hours pre-treatment with soraphen A (1 μ M) and a third group received cells with 72 hours pre-treatment with soraphen A (25 nM). 1×10^5 cells per mouse were solved in 100 μ l PBS and were injected via tail vein, four days respectively seven days later, mice were imaged with IVIS® Spectrum bioluminescence imager and the experiment was ended through cervical dislocation on day seven.

2.2.6. The influence of Cdk5 in cancer processes evaluated in murine tumor experiments

2.2.6.1. Effect of Cdk5 knock-down in cells in combination with sorafenib treatment on HCC tumors evaluated in a Scid mouse model

The effect of Cdk5 knock-down in tumor cells on tumor growth was tested in a Huh7 and Scid mouse xenograft model. All cells for this experiment were generated by Dr. Sandra Ehrlich (University of Munich, Germany) through lentiviral transduction. 24 female Scid mice at an age of six weeks were divided into four groups. In two groups each mouse got 3.3×10^6 Huh7 nt shRNA cells, solved in 100 μ l PBS, injected into the left flank, after being locally shaved. The other two groups received the same amount of Huh7 Cdk5 shRNA cells. In the first Huh7 nt shRNA group (n=5, because one mouse did not develop a tumor) mice were treated as a control and received solvent consisting of 5% DMSO, 10% solutol and 85% PBS, the second group (n=6) received 10 mg/kg sorafenib solved in 5% DMSO, 10% solutol and 85% PBS via intraperitoneal injection. In the groups (n=6) which received the Huh7 Cdk5 shRNA

cells, one group was also treated with solvent as a control, the other group received 10 mg/kg sorafenib. Daily intraperitoneal treatment started on day 11 after cell inoculation and lasted until day 18, so all mice received vehicle respectively sorafenib eight times during the experiment. Tumor volume was measured every second day with a caliper and calculated with the formula $\pi/6 \times L \times W \times H$. On day 18 all mice were sacrificed through cervical dislocation. Tumors were resected, weighed, photographed and split into two parts, one for freezing at -80 C° and one for conservation in 1 % PFA.

2.2.6.2. Using Cdk5 knock-out mice and roscovitine treatment to evaluate their effects on melanoma cells

For evaluating the effect of mice carrying an inducible endothelial Cdk5 knock-out in combination with roscovitine treatment on tumor growth, six Cdk5 knock-out mice (Cdk5^{fl/fl} VECCre+) were used. All mice were provided by Dr. Johanna Liebl (University of Munich, Germany), for their creation a Cre-lox system was used. To induce the Cdk5 knock-out, mice were treated with tamoxifen (5mg/ml, 100 μ l i.p. injection) over five days. After being locally shaved, each mouse received 1×10^6 B16F1 cells via subcutaneous injection into the left flank. Cells were solved in 100 μ l PBS. For this, 1 ml syringes and 27 G needles were used. Two groups of mice were formed. Three knock-out mice (Cdk5^{fl/fl} VECCre+) were treated as a control and received solvent while the other three knock-out mice (Cdk5^{fl/fl} VECCre+) were treated with roscovitine (150 mg/kg). Roscovitine was solved in 5% DMSO, 10% solutol and 85% PBS, an amount of 100 μ l was intraperitoneally injected into the mice three times a week. Therapy started on day seven after cell inoculation. Tumor growth and tumor volume were measured three times a week with a caliper, using the formula $\pi/6 \times L \times W \times H$. Experiment lasted 14 days altogether. On day 14, mice were sacrificed through cervical dislocation. Tumors were preserved as mentioned before.

2.2.6.3. Limiting dilution experiment with T24 cells

Regarding the effect of Cdk5 knock-down in T24 cells on tumor growth, 30 female BALB/c nu/nu mice at an age of six weeks were used. They were separated into two groups (n=15) which were divided again in three equal subgroups. All animals in one of the large groups (n=15) received T24 nt shRNA cells but each subgroup received a different amount of cells. The subgroups consisted of five animals, the first got just 5×10^6 cells subcutaneously injected into the left flank, the second group received 2.5×10^6 into their left flank and 1×10^5 into their right flank, while the third group got 1×10^6 cells injected into the left flank and 5×10^5 cells into the right flank. Always used were 1 ml syringes and 27 G needles for the application. The same distributions were made for the 15 animals which received T24 shRNA Cdk5 cells. All cells were generated by Dr. Siwei Zhang (University of Munich, Germany) using lentiviral transduction. Each time, the cells were solved in 100 μ l PBS mixed with

100 μ l Matrigel®. Tumor volume was measured three times a week with a caliper, using the formula $\pi/6 \times L \times W \times H$. Measurement started on day four and lasted until day 42 after tumor cell inoculation. Mice were euthanized through cervical dislocation, tumor were preserved as mentioned above.

2.2.6.4. Limiting dilution experiment with 4T1-luc cells

In this experiment 50 BALB/c mice, female and six weeks old were locally shaved on their left flanks and got a subcutaneous application of 4T1-luc cells. Ten groups with five mice each were formed, two groups at a time received the same amount of 4T1-luc cells. Injected were 1×10^6 , 1×10^5 , 1×10^4 , 1×10^3 and 1×10^2 cells, each solved in 100 μ l PBS per mouse, using 1 ml syringes and 27 G needles for that. One of these two groups was then vehicle treated (100 μ l, consisting of 5% DMSO, 10% solutol and 85% PBS), the other one received dinaciclib (30 mg/kg). Treatment was performed three times a week starting on the day of tumor cell application (d0) and was stopped on day 14. Tumor volumes were measured three times a week with a caliper in use of the formula $\pi/6 \times L \times W \times H$. Bioluminescence pictures were taken with the IVIS® Spectrum on d3, d8, d15, d23 and d28. On day 25 after cell application, mice of both groups (control and dinaciclib) which received either 1×10^6 , 1×10^5 or 1×10^4 cells were taken out of the experiment. The other mice, which received 1×10^3 and 1×10^2 cells were kept in the experiment and sacrificed on day 30. The experiment was performed over 30 days altogether, ending with euthanasia through cervical dislocation on final day (d25 or d30), tumors were preserved as mentioned before.

2.3. Statistical analysis

Results are expressed as mean value \pm S.E.M. Statistical analysis were performed with GraphPadPrism™, using unpaired t-tests for experiments with two groups and One-way ANOVA (Dunnett) for experiments with three or more groups to compare, if not indicated otherwise. P-values < 0.05 were considered as significant.

III. Results

1. Preliminary dose finding experiments in murine models

The aim of the following experiments was to find dose rates of simvastatin, LGR 2674, archazolid A, nutlin-3a, PS89 and soraphen A which different mouse strains would tolerate in our long-term main experiments with these experimental compounds concerning tumor growth and dissemination. All animal experiments were performed together with Kerstin Loske (technician, University of Munich, Germany) at the animal facility of AK Vollmar and AK Biel on the campus of the University of Munich in Großhadern.

All of these substances have already shown promising results *in vitro* or were even evaluated in animal studies before. That was the basis for us to realize the following *in vivo* experiments. Dose rates were chosen according to former *in vivo* experiments performed at our lab, according to publications or in dependence on results of *in vitro* experiments with these substances. The toxicity and the tolerance of the compounds *in vivo* were evaluated with regard to the effects on the mice' general condition concerning their breathing, behavior, posture, signs of pain as bent position, closed eyes and isolation of the group, fur and color of the skin and mucosa (eyes and anus), body condition score (BCS) and body weight, which is the most meaningful parameter.

For these preliminary experiments the same mouse strain we also wanted to use for the main experiment was chosen. This choice depended on the cell line which should subsequently be applied. Substances were solved in the same way as they were used afterwards for the injections in the main experiments (5% DMSO, 10% solutol, 85% PBS, composition is due to proper tolerance and solubility of substances in former *in vivo* experiments). After these preliminary dose finding experiments, simvastatin, LGR 2674, PS89 and soraphen A should be used in xenograft tumor models with Huh7 cells. This is a human cancer cell line, which only grows in immunodeficient mouse strains. Scid mice are B- and T-cell deficient and Huh7 cells grow very fast and reliable in this mouse strain, this is the reason why they were chosen and why we also performed these dose finding tests with them. The choice of a BALB/c nu/nu strain for the evaluation of archazolid A and nutlin-3a depends on the human glioblastoma cells (U87MG) which should be used for the corresponding tumor growth experiment. This is a human cell line which grows best in the T-cell deficient BALB/c nu/nu strain. Soraphen A should also be used for a tumor dissemination model with 4T1-luc cells, these murine breast cancer cells originate from BALB/c mice, so this is a syngeneic combination, which is why we chose this strain for such experiments.

Due to the aim to minimize the numbers of experimental animals, we chose not more than two mice per dose finding test, because these experiments are just about preliminary information finding on which dosage could be suitable. Nevertheless, the

preliminary data gained in all of these experiments were useful tools for the planning of the corresponding main experiments because they gave us an orientation.

1.1. Simvastatin

Scid mice were chosen to evaluate the tolerance for simvastatin after intraperitoneal injections. The following therapy regime was performed over five days:

n=2: 10 mg/kg simvastatin

n=2: 10 mg/kg simvastatin combined with 0.2 mg/kg archazolid A

All mice showed a proper general condition over the whole time of the experiment. The body condition score (BCS) retained at a value of 3, no loss of weight was detectable in the group receiving combinatorial treatment, mice receiving single simvastatin treatment constantly gained weight. (Figure 12) Both groups tolerated their treatments well. The consequence was to use exactly these dose rates of simvastatin, archazolid A and their combination for the main experiment (3.3. in this thesis).

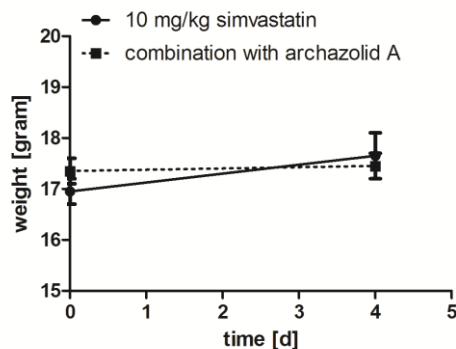


Figure 12.: Weight development over time. Weight of mice during the whole experimental period (d0-d4) either with daily simvastatin treatment (10 mg/kg) or daily combinatorial treatment (10 mg/kg simvastatin and 0.2 mg/kg archazolid A). Weight was assessed on first (d0) and last day (d4) of the experiment. Represented is the mean \pm S.E.M. of two mice per group.

1.2. LGR 2674

To find a proper dosage for intraperitoneal injections of LGR 2674, Scid mice were chosen. Treatment regime over five days:

n=2: 1.5 mg/kg LGR 2674

n=2: 15 mg/kg LGR 2674

In the group receiving 1.5 mg/kg, mice showed a reduction of body weight from the beginning of the treatment on, which still decreased during the ongoing experiment. Both mice showed signs of pain as horrent fur and a bent position. In the group

receiving 15 mg/kg, one mouse was found dead in the cage after the third treatment with substance, the other one suffered from harmful reduction of body weight (Figure 13) and also showed indications of pain as horrent fur and a bent position. These results led to the decision to use the lower dosage of LGR 2674 (1.5 mg/kg) for the main experiment (3.2. in this thesis) because this dosage was much better tolerated.

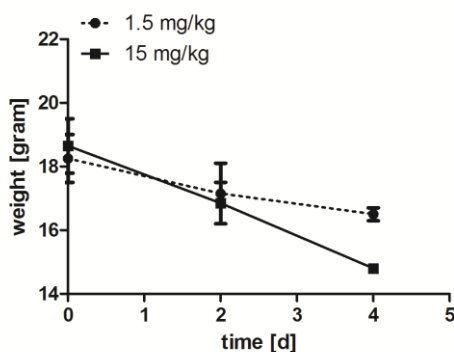


Figure 13: Weight development over time. Weight loss of mice daily treated either with 1.5 mg/kg or 15 mg/kg LGR 2674 over five days (d0-d4). Weight was measured on day 0, day 2 and day 4 of the experiment. Represented is the mean \pm S.E.M. of two mice per group (one within the 15 mg/kg treatment group on day 4).

1.3. Archazolid A and nutlin-3a

In this dose finding experiment, BALB/c nu/nu mice were chosen. Concerning archazolid A, four different dose rates were evaluated: 0.25 mg/kg, 0.3 mg/kg, 0.45 mg/kg and 0.6 mg/kg. Nutlin-3a was single tested in a dose of 5 mg/kg and in combination with archazolid A. All compounds were intraperitoneally injected.

Treatment regime in the first part of this experiment over five days (d0-d4):

n=1: 0.3 mg/kg archazolid A

n=1: 5 mg/kg nutlin-3a

n=1: 0.3 mg/kg archazolid A combined with 5 mg/kg nutlin-3a

Mice tolerated all of these dose rates well, no abnormalities in their general condition were detected. (Figure 14 A)

In the second experiment, we administered a higher dosage of archazolid A because of the good tolerance in the prior experiment. Treatment regime in the second part of this experiment over five days (d0-d4):

n=1: 0.3 mg/kg archazolid A

n=1: 0.45 mg/kg archazolid A

n=1: 0.6 mg/kg archazolid A

Mice receiving 0.3 mg/kg and 0.6 mg/kg showed no changes in their behavior or wellness until the third treatment, on the fourth day of the experiment both mice were

III. Results

found dead in their cage. The mouse receiving 0.45 mg/kg had unchanged parameters during the five day period of the experiment. (Figure 14 B)

Concerning the deviant results of the 0.3 mg/kg dosage, a third experiment was performed. Treatment regime in this part of the experiment over five days (d0-d4):

n=1: 0.25 mg/kg archazolid A

n=1: 0.3 mg/kg archazolid A

In this try, both mice showed an unchanged general condition during the experiment. (Figure 14 C)

In a fourth part of this experiment, further combinations of archazolid A and nutlin-3a were evaluated. Treatment regime over five days (d0-d5):

n=1: 0.25 mg/kg archazolid A combined with 5 mg/kg nutlin-3a

n=1: 0.3 mg/kg archazolid A combined with 5 mg/kg nutlin-3a

Both compositions were tolerated well. Mice did not lose weight over time. (Figure 14 D)

The consequence of this experiment for us was to choose a 0.2 mg/kg dosage of archazolid A in the main experiment (3.6. in this thesis) to make sure that mice survive the long-time archazolid A treatment. This dose finding experiment also confirmed that 5 mg/kg of nutlin-3a is a dosage mice will tolerate over several days.

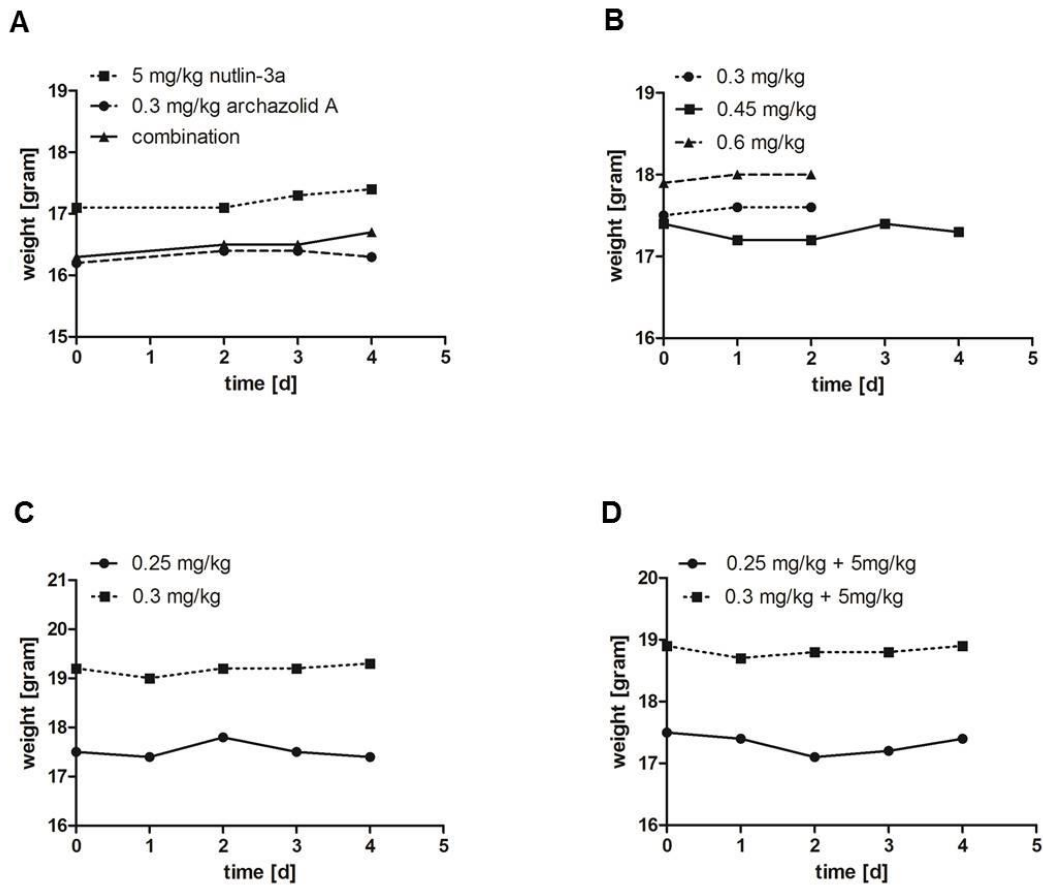


Figure 14: Weight development over time. **A)** Weight of mice in part one of this dose finding experiment, 0.3 mg/kg archazolid A, 5 mg/kg nutlin-3a and a combination of both were tested in one mouse each over five days. Weight was assessed on day 0, day 2, day 3 and day 4. Each curve represents one single mouse. **B)** Mice of part two, 0.3 mg/kg, 0.45 mg/kg and 0.6 mg/kg archazolid A were tested over five days. Weight was measured daily. Each curve represents one single mouse. **C)** Part three, 0.25 mg/kg and 0.3 mg/kg archazolid A were tested over a five day period, each dosage in one mouse. Weight was assessed daily. **D)** Part four, two combinatorial treatments were evaluated. 0.25 mg/kg archazolid A with 5 mg/kg nutlin 3a and 0.3 mg/kg archazolid A with 5 mg/kg nutlin-3a, both over five days. Weight was assessed daily. Each curve represents one single mouse.

1.4. PS89

To assess a proper dosage for the i.p. use of PS89 in our tumor experiments, we evaluated three different dose rates over four days (d0-d3) in Scid mice:

n=2: 10 mg/kg PS89

n=2: 20 mg/kg PS89

n=2: 30 mg/kg PS89

Additionally, a combination of PS89 with sorafenib which was necessary for the main experiment (3.4. in this thesis) was evaluated over seven days (d0-d6):

n=2: 30 mg/kg PS89 combined with 10 mg/kg sorafenib

III. Results

During all these dose finding experiments, mice showed unchanged parameters concerning their general condition and a relatively constant body weight. BCS retained at a value of 3. Mice receiving 10 mg/kg and 20 mg/kg of PS89 gained little weight during the experimental period. (Figure 15) All dose rates of PS89 and the combination with sorafenib were tolerated well. For the main experiment (3.4. in this thesis) with PS89, we decided to use the medium dose rate of 20 mg/kg of PS89 and the evaluated 10 mg/kg of sorafenib to make sure all mice would endure the whole experimental period.

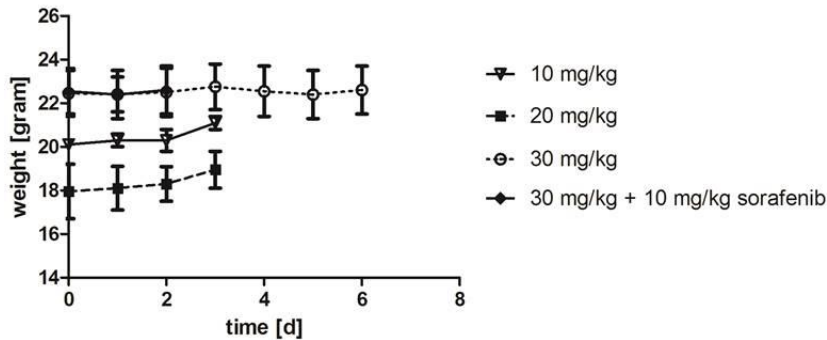


Figure 15: Weight development over time. Mice were treated with different dosages (10 mg/kg, 20 mg/kg, 30 mg/kg) of PS89 single or 30 mg/kg PS89 in combination with 10 mg/kg sorafenib. Weight was assessed daily. Represented is the mean \pm S.E.M. of two mice per group.

1.5. Soraphen A

This compound was evaluated in a BALB/c strain as well as in a Scid strain performing i.p. injections, because it should be used later in different experiments. Treatment regime to evaluate the tolerance of soraphen A in BALB/c mice over four days (d0-d3):

n=2: 5 mg/kg soraphen A

n=2: 10 mg/kg soraphen A

n=2: 20 mg/kg soraphen A

All animals showed a proper general condition over the whole experimental period and changes in weight range were physiological. (Figure 16 A) All dose rates we evaluated were tolerated well.

Treatment regime to evaluate the tolerance of soraphen A in Scid mice over five days (d0-d4):

n=2: 20 mg/kg soraphen A

n=2: 40 mg/kg soraphen A

All animals showed a good general condition and weight fluctuated in physiological ranges during the five days of treatment. (Figure 16 B) For the main experiment (3.5. in this thesis) we used Scid mice and the higher dosage (40 mg/kg) of soraphen A.

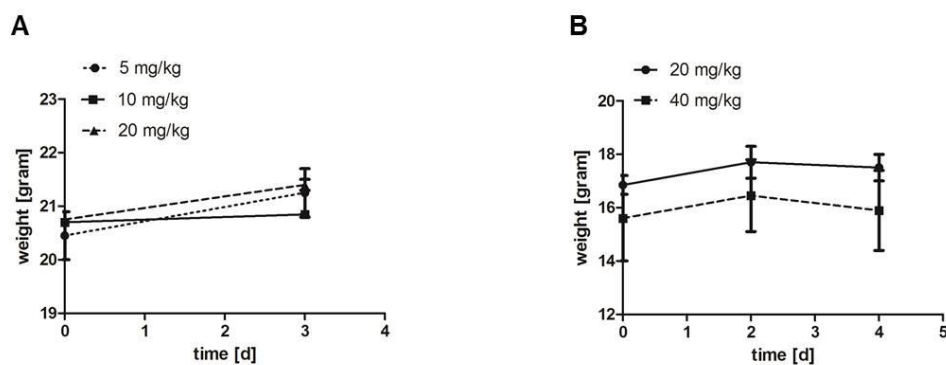


Figure 16: Weight development over time: **A)** Weight of BALB/c mice daily treated with sorafenib A (5 mg/kg, 10 mg/kg, 20 mg/kg) over four days. Weight was assessed on first (d0) and last (d3) day of experiment. Represented is the mean \pm S.E.M. of two mice per group. **B)** Weight of Scid mice daily treated with sorafenib A (20 mg/kg or 40 mg/kg) over five days. Weight was measured three times (d0, d2, d4). Represented is the mean \pm S.E.M. of two mice per group.

2. Murine experiments for pharmacokinetic studies

These kind of animal experiments were established to extend our knowledge on the pharmacokinetic properties of V-ATPase inhibitor archazolid A and Cdk inhibitor roscovitine to evaluate their blood levels after intraperitoneal or intravenous injections. Such experiments were performed for the first time in our lab, both substances were chosen because they are frequently used in our projects. The aim of these studies was to determine suitable treatment regimes for our experiments with these compounds. We performed theoretical calculations on the expected blood concentration based on the assumption of a total amount of 1600 μ l blood per mouse, consisting of 800 μ l serum and 800 μ l cellular compounds. The blood concentration reached in our experiments was then compared to the expected value calculated before. For these experiments, the very common and widely used C57BL/6 mouse strain was chosen. These animals have a competent immune system and so they were suitable for such experiments due to creation of standard conditions.

2.1. Archazolid A distribution

To evaluate the concentration of archazolid A in murine serum after i.v. and i.p. injection, a C57BL/6 mouse model was chosen. Animals (n=8) were divided in two equal groups (n=4), mice in one of these groups received an intraperitoneal injection of 0.3 mg/kg archazolid A, while the other group received the same amount intravenously. Blood of two other mice was used for internal standards. After i.v. respectively i.p. treatment, blood was taken from one mouse each via heart puncture at certain time points (0.5h, 1h, 2h, 6h) after the application, serum was separated of all probes afterwards. The evaluation of this experiment was performed by Dr.

III. Results

Jennifer Herrmann (University of Saarland, Germany) using HPLC and mass spectrometry.

Regarding the resulting graph, it is recognizable that the concentration of archazolid A increases directly after application, reaches its peak after 2h and lowers again afterwards in both forms of application (Figure 17 A), but the total concentration (in μM) in the serum was higher in probes of i.v. treated mice than in i.p. treated ones. Based on the dosage 0.3 mg/kg archazolid A meaning 0.6 μg / 20 g mouse (standard mouse) and based on 800 μl serum per mouse, there should be 7.5 ng of archazolid A found in 1 μl serum. Interpretation is based on the following: Archazolid A holds a molecular weight of 737.98 g/mol. Using the formula $n=m/M$, we calculated that there should be 10 μM archazolid A in the total serum. In the experiment the highest reachable value with i.p. treatment lay at 4.0 μM and at 16.5 μM with i.v. treatment. (Figure 17 B) The concentration in the blood of archazolid A in i.p. treated animals did not reach the expected value of 10 μM while the values in the i.v. treated group exceeded 10 μM , this might be due to an impureness with polyethylene glycols of the i.v. probes which disturbed the measurements.

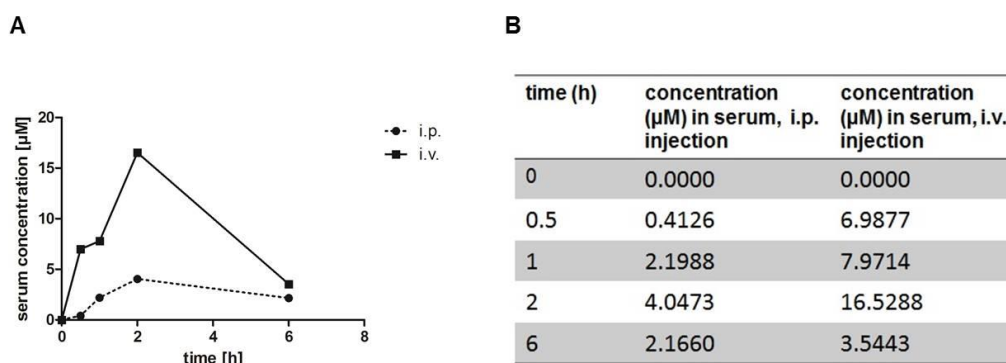


Figure 17: Concentration of archazolid A in murine serum over time. A) Shown is the concentration (in μM) of archazolid A in murine serum 0h, 0.5h, 1h, 2h and 6h after intraperitoneal (i.p.) respectively intravenous (i.v.) injection. B) Shown are the exact values archazolid A reaches in the serum at certain time points after i.p. respectively i.v. application.

2.2. Roscovitine distribution

For this experiment, we also used a C57BL/6 mouse model. To evaluate the concentration in the blood of Cdk inhibitor roscovitine, blood was taken via heart puncture from 18 C57BL/6 mice which were intraperitoneally treated with roscovitine (150 mg/kg). A blood take was performed at consecutive time points after application (10 min, 20 min, 30 min, 1h, 2h, 4h). We had to mix the blood of three mice per time point due to reduced blood exploitation after roscovitine treatment. Another three mice were just vehicle treated and used as internal standard. Blood was collected in EDTA coated sample tubes to prevent coagulation. The evaluation of the probes was carried out by Dr. Christoph Müller (University of Munich, Germany) performing HPLC and mass spectrometry.

III. Results

The resulting graph shows an increasing blood concentration directly after injection which reaches its peak 30 min after i.p. application, from 30 min on, the roscovitine concentration lowers again. After 4h, the blood concentration seemed to reach a plateau. (Figure 18 A) We performed calculations on theoretical finding of roscovitine in the blood before. Based on the given dosage of 150 mg/kg roscovitine meaning 3 mg/ 20 g mouse (standard mouse) and based on 1600 μ l blood per mouse, there should be 1.875 mg in 1 ml blood. 30 min after application, we were able to detect 178.1 μ g in 100 μ l blood equating 1.78 mg in 1 ml blood. (Figure 18 B) So, the detected value almost reaches the theoretical value. Therefore, we categorized i.p. injections as suitable and used them in our experiments with roscovitine.

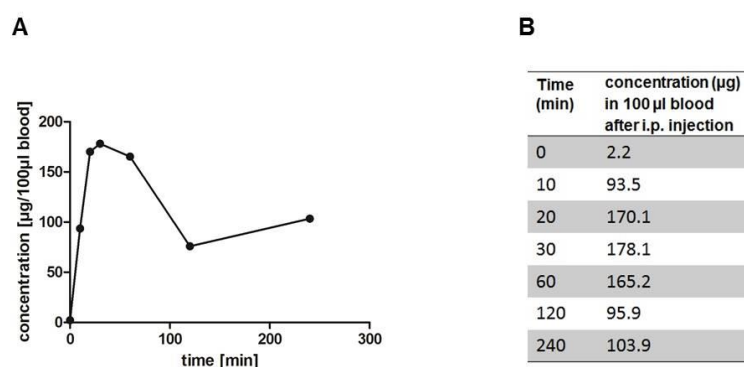


Figure 18: Distribution of roscovitine in murine blood over time. A) Shown is the concentration (in μ g/ 100 μ l blood) of roscovitine in blood 10 min, 20 min, 30 min, 1h, 2h and 4h after intraperitoneal injection. B) Shown are the exact values roscovitine reached in 100 μ l blood at different time points during the experiment.

3. Murine tumor models to evaluate the reduction of tumor growth through various compounds

In this chapter different approaches were evaluated to hamper the growth of tumors through treatment with potential anti-cancer compounds. For this, different animal experimental setups were established. First, we analyzed the effect of V-ATPase inhibitor archazolid A on murine breast cancer cells (4T1-luc) in an allograft BALB/c nu/nu mouse model and afterwards its combinatorial properties together with cholesterol synthesis inhibitor simvastatin in a Scid mouse experiment and then the effect of its combination with the MDM2 inhibitor nutlin-3a in another experiment with BALB/c nu/nu mice. Furthermore, the roscovitine analogue LGR 2674, PDI inhibitor PS89 and ACC inhibitor soraphen A were evaluated concerning their anti-cancer efficacy in Huh7 xenograft Scid mouse experiments.

Therapy started when all or most of the mice bore a tumor, end points were chosen due to the mice' general condition and due to tumor's size, a critical mark of 1000

mm³ should not be exceeded to prevent mice from pain and limitations in their physiological course of motions.

3.1. Evaluation of the effect of archazolid A treatment on murine breast cancer in an allograft tumor experiment

Due to a project in our lab where the potential of archazolid A to initiate apoptosis of cancer cells as a consequence of disturbed iron metabolism was focused [124], we evaluated the influence of this V-ATPase inhibitor on tumor growth of murine breast cancer tumors. A murine allograft tumor model, using eight BALB/c nu/nu mice, was chosen. 4T1 cells originate from BALB/c mice, a strain which is similar to the chosen BALB/c nu/nu mouse model. Mice were divided into two groups (n=4) and received 1×10^6 murine breast cancer cells (4T1-luc). Tumor bearing mice were daily and intraperitoneally treated either with archazolid A (0.3 mg/kg) or vehicle seven times altogether, starting on day six after tumor cell inoculation.

Treatment with archazolid A lowered tumor volume over time compared to the control group. On day 11, tumor volume in the archazolid A treated group was significantly lower in comparison to control. (Figure 19 A) Tumor volumes were measured last on day 12 while on final day of the experiment (d13) tumors were resected and weighed. Weighing of tumors after resection led to no significant differences between both groups. (Figure 19 B)

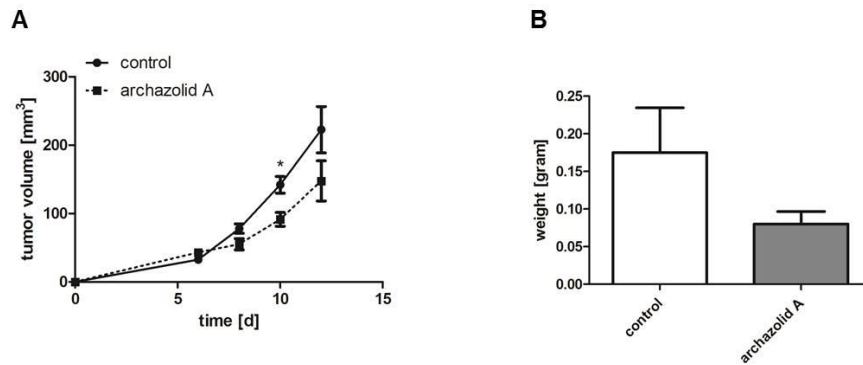


Figure 19: Tumor growth over time and tumor weight after resection. **A)** Development of tumor volume over time, group with daily archazolid A (0.3 mg/kg) treatment compared to vehicle treated control group. Represented is the mean \pm S.E.M. of four mice per group. Statistical analyses were performed using t-test (* $p < 0.05$, ** $p < 0.01$). **B)** Comparison of tumor weight in both groups after tumor resection (d13). Represented is the mean \pm S.E.M. of four mice per group. Statistical analyses were performed using t-test (n.s. = not significant).

All mice showed an unchanged general condition during the whole experiment, both groups did not show non physiological variations in weight. (Figure 20)

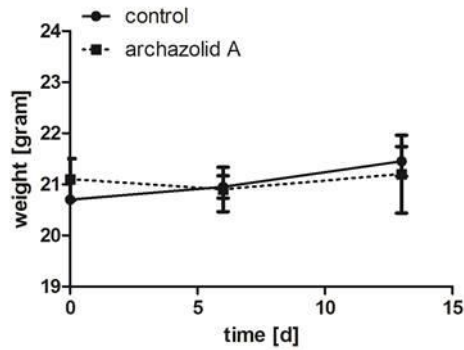


Figure 20: Weight over time. Development of mice' weight during the experiment, measured three times, starting with injection of cells (day 0) and ending with euthanasia (day 13). Represented is the mean \pm S.E.M. of four mice per group.

3.2. Examination of combinatorial effects of simvastatin and archazolid A on HCC using a xenograft model

This experiment was performed due to an in vitro project where the focus was laid on the effects of archazolid A on cholesterol metabolism in cancer cells. The aim of this experiment was to evaluate the effect on hampering tumor growth in vivo using the established cholesterol synthesis inhibitor simvastatin and our natural compound archazolid A, on the one hand in single use and on the other hand in combination. A Scid mouse xenograft model with 32 animals was chosen to evaluate this. The in vitro experiments were performed with Huh7 cells and led to promising results, so we chose this cell line for the in vivo experiment, too. Scid mice are T-cell and B-cell deficient and the human Huh7 cell line grows very fast and very reliable in this strain. Mice were divided into four groups (n=8), one group was treated with solvent as a control, one group was treated with simvastatin (10 mg/kg), one group was treated with archazolid A (0.2 mg/kg) and one group was treated with a combination of both. 3×10^6 hepatocellular carcinoma cells (Huh7) were injected (day 0), daily therapy of tumor bearing mice started on day 7 after cell inoculation und lasted until day 17.

One mouse of the control group and two mice in the simvastatin treated group did not develop any tumor over time. The tumor volume in the archazolid A treated group was significantly lower compared to control group in the last two measurements of the experiment, d15 (Figure 21 C) and d17 (Figure 21 D). Single simvastatin treatment and combinatorial treatment with archazolid A led to no significant differences in tumor volume compared to the control group. (Figure 21 A) On final day of experiment (d17) mice were sacrificed through cervical dislocation, after that all tumors were resected and weighed. The weight of tumors showed no significant differences between the groups. Simvastatin treated mice developed the most heavy tumors while the archazolid treated ones developed the lightest tumors. (Figure 21 B)

III. Results

Figure 22 shows that mice in all groups kept a healthy general condition and showed just physiological fluctuations in weight over the whole experimental period.

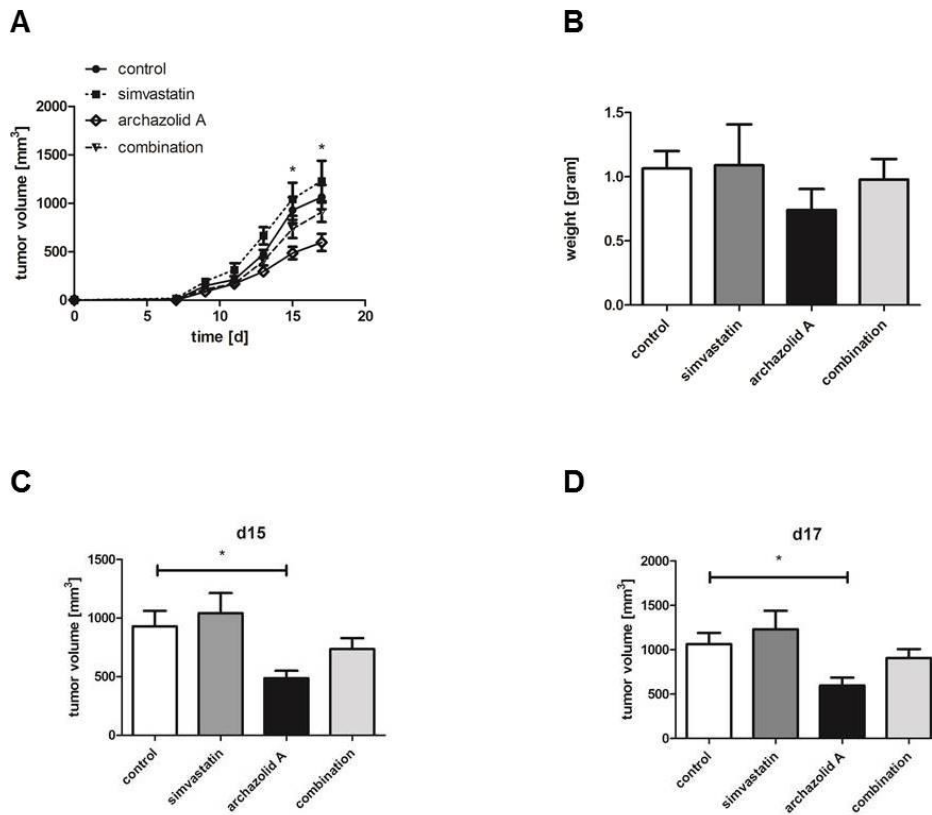


Figure 21: Tumor volume and weight during experimental period. **A)** The graph shows the average tumor volume of each group, control, simvastatin (10 mg/kg) treated, archazolid A (0.2 mg/kg) treated and combinatorial treatment. On day 15 and day 17 the archazolid A treated group showed a significantly lowered tumor volume compared to the control. Represented is the mean \pm S.E.M. per group. Differences were evaluated with One-way ANOVA test (* $p < 0.05$, ** $p < 0.01$). **B)** Tumor weight after resection (day 17) in all groups. Represented is the mean \pm S.E.M. per group. Differences were evaluated via One-way ANOVA test (n.s.). **C)** Shown is the tumor volume of all groups on day 15 of the experiment. Tumor volume in single archazolid A treated group was significantly lowered compared to control. Represented is the mean \pm S.E.M. per group. Differences were evaluated with One-way ANOVA test (* $p < 0.05$, ** $p < 0.01$). **D)** Shown is the tumor volume of all groups on day 17 of the experiment. Tumor volume in single archazolid A treated group was significantly lowered compared to control. Represented is the mean \pm S.E.M. per group. Differences were evaluated with One-way ANOVA test (* $p < 0.05$, ** $p < 0.01$).

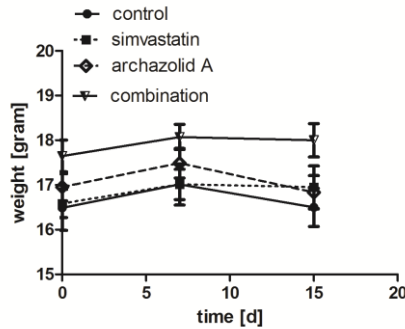


Figure 22: Weight development over time. Weight of mice during experimental period was assessed on day 0, day 7 and day 15 and is shown for all four groups. Represented is the mean \pm S.E.M. per group.

3.3. Effects of combinatorial treatment of nutlin-3a and archazolid A on glioblastomas shown in a xenograft tumor model

This *in vivo* experiment contributed to a project of our lab where we showed that the inhibition of V-ATPases influences p53 levels positively *in vitro*. So, we analyzed the single and combinatorial effect of p53 activator nutlin-3a and V-ATPase inhibitor archazolid A in a xenograft model using BALB/c nu/nu mice and glioblastoma cells. The T-cell deficient BALB/c nu/nu strain was chosen according to its good growth properties for this human cell line. 32 BALB/c nu/nu mice got an injection of 5×10^6 U87MG cells into the left flank and were divided into four groups (n=8) afterwards. Tumor bearing mice were daily intraperitoneally treated either with solvent, with 0.2 mg/kg archazolid A, with 5 mg/kg nutlin-3a or with a combination of both. Therapy started on day seven after cell application and lasted until day 25. Two mice in the control group, one mouse in the archazolid A treated group and one mouse in the nutlin-3a group died during the experiment.

The evaluation of the experiment was realised by jun.- Prof. Thorsten Lehr (University of Saarland, Germany) through specific modeling (description in 2.2.4.6. of this thesis). In Figure 23 A the tumor growth over time is shown. Growth rate of tumors treated with combination was significantly reduced compared to control. Moreover, the combination of archazolid A and nutlin-3a was most effective in reducing tumor volume (50.4%). (Figure 23 B)

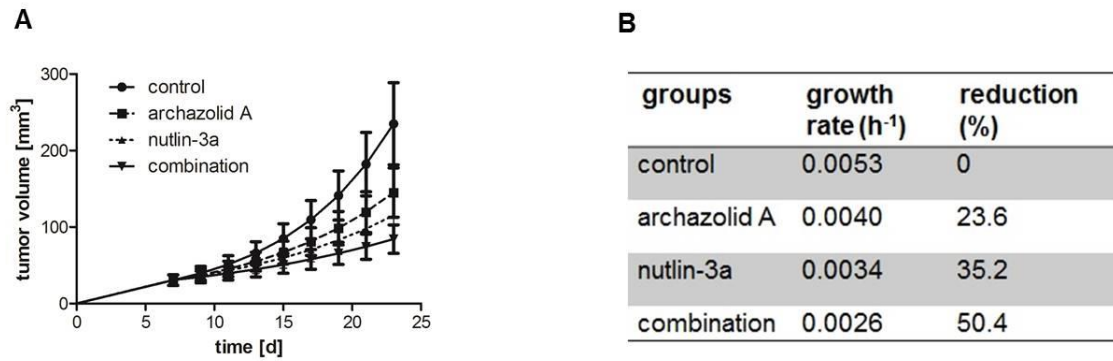


Figure 23: Tumor volume and growth rate. **A)** Shown is the tumor growth curve over time of four groups, one treated with solvent (control), one treated with archazolid A (0.2 mg/kg), one treated with nutlin-3a (5 mg/kg) and one treated with a combination (0.2 mg/kg archazolid A and 5 mg/kg nutlin-3a). Represented is the mean \pm S.D. per group. **B)** Shown is the growth rate (h⁻¹) and the reduction of tumor volume (%) in all four groups.

Surviving mice kept a proper general condition during the experimental period and gained weight. (Figure 24)

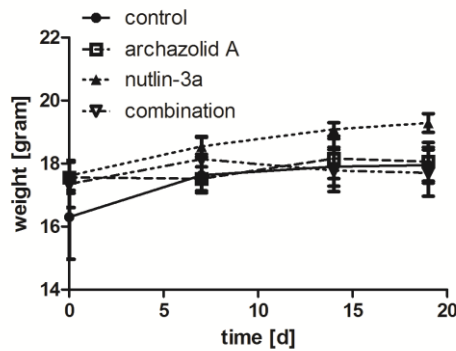


Figure 24: Weight development over time. Surviving mice kept their weight during experimental period. Starting with tumor cell application (day 0) ending with euthanasia (day 25). Weight was assessed four times (d0, d8, d14, d19). Represented is the mean \pm S.E.M. per group.

3.4. Effect of LGR 2674 on HCC tumors evaluated in a xenograft model

LGR 2674, an analogue of the established Cdk inhibitor roscovitine, was evaluated *in vivo* for the very first time. According to promising *in vitro* results concerning the inhibition of Huh7 proliferation in one of our current projects [68], it should be evaluated *in vivo*. Its effect on tumor growth was evaluated in a Huh7 xenograft model. Scid mice were chosen according to prior experiments where the cells grew very good in this strain and formed tumors very fast. 3×10^6 tumor cells were injected. Mice were divided into two groups (n=10). With appearing of tumors on day eight after cell application, daily treatment with LGR 2674 (1.5 mg/kg) started in one group, the other one received a daily intraperitoneal injection of solvent. The experiment lasted until day 20 after cell inoculation.

III. Results

One mouse in the control group did not develop any tumor at all. One mouse of the control group and one mouse of the LGR 2674 treated group had to be taken out of the experiment on day 17, because their tumor volume reached the critical mark of 1000 mm^3 . Comparison of tumor volume in the control group and in the LGR 2674 treatment group showed that intraperitoneal therapy of Scid mice with LGR 2674 significantly reduced the volume of tumors on day 17. (Figure 25 A) The resection of the tumors after euthanasia showed no significant reduction of tumor weight in LGR 2674 treated mice compared to the control group. (Figure 25 B)

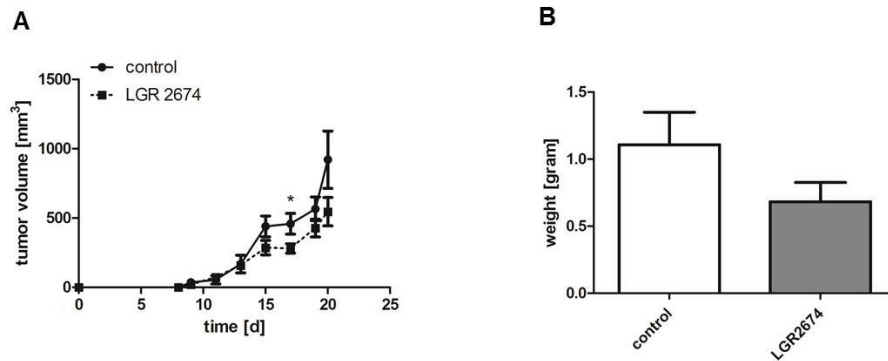


Figure 25: Development of tumors over time and weight after resection. A) Shown is the growth of Huh7 tumors during the whole experimental period until day 20 in both groups, control and LGR 2674 (1.5 mg/kg) treated. Represented is the mean \pm S.E.M. per group. Differences were evaluated with t-test (* $p < 0.05$, ** $p < 0.01$). B) Tumors were weighed on day 20 and both groups were compared. Represented is the mean \pm S.E.M. per group. Differences were evaluated with t-test (n.s.).

Control mice showed a healthy general condition over the whole experimental period, in contrast to that, mice in the LGR 2674 group lost weight with beginning of treatment on day eight (Figure 26). On day 19, one mouse in the LGR 2674 treatment group was found dead in the cage. Mice in this therapy group showed signs of reduced general condition, e.g. fur clotted with feces around the anus, horrent fur and reduced activity.

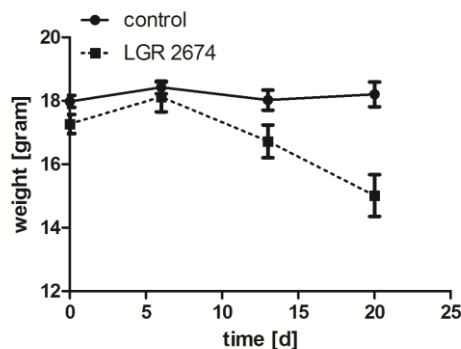


Figure 26: Weight of mice over time. Shown is the constant weight of mice in the control group and weight loss of mice in the LGR 2674 treated group during the experimental period. Weight was assessed four times at all, starting with tumor cell injection (day 0) and ending with euthanasia (day 20). Represented is the mean \pm S.E.M. per group.

3.5. Effect of PS89 in combination with sorafenib on HCC tumors shown in a xenograft model

Sorafenib is an established therapeutic agent in HCC treatment, but resistances occur more and more. So, we wanted to analyze if the new PDI inhibitor PS89 would have a sensitizing effect on tumor cells for sorafenib treatment to hamper tumor growth. For this experiment a xenograft model using Scid mice, which are very suitable for Huh7 models, was chosen. We injected 3×10^6 Huh7 cells subcutaneously in 32 Scid mice. These animals were divided into four groups (n=8), control, single PS89 (20 mg/kg) treated, single sorafenib (10 mg/kg) treated and combinatorial treated. Mice were intraperitoneally treated three times a week, therapy started on day 10 after cell inoculation and lasted until day 19 ending with euthanasia.

One mouse in each group and two mice in the control group did not develop any tumor over the whole experimental period at all. Tumor development over time showed an almost equal volume in all of the groups, there was no significant difference in tumor volume between them. (Figure 27 A-B) The experiment was ended on day 19 with euthanasia because tumors reached the 1000 mm^3 mark. Results of weighing of tumors showed that the lightest tumors are developed by mice of the control group, while tumors of mice in PS89, sorafenib and combinatorial group showed a higher and almost equal weight. So, there were no significant differences in tumor weight. (Figure 27 C) Mice kept a healthy general condition during the experiment and weight loss and gain are fluctuating in a physiological range. (Figure 27 D)

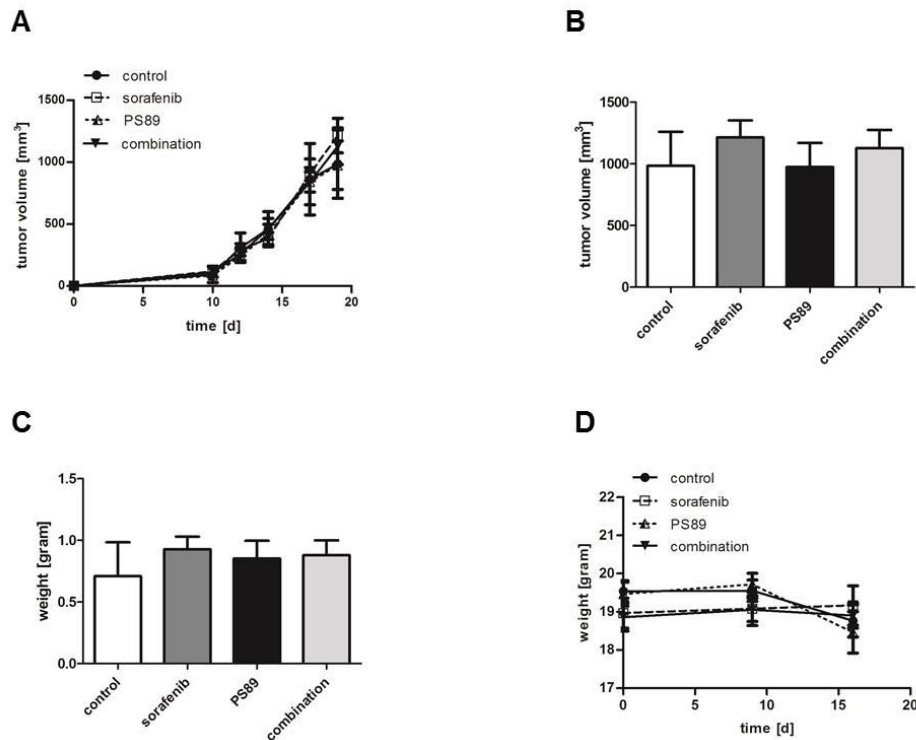


Figure 27: Tumor development over time and weight of mice. **A)** Shown is tumor volume over time of Scid mice bearing subcutaneous tumors in a control group, a sorafenib (10 mg/kg) treated group, a PS89 (20 mg/kg) treated group and a combinatorial treatment group. Represented is the mean \pm S.E.M. per group. Differences were evaluated with One-way ANOVA test (n.s.). **B)** Shown is tumor volume of all groups on final day of experiment (day 19). Represented is the mean \pm S.E.M. per group. Differences were evaluated with One-way ANOVA test (n.s.). **C)** Weight of tumors on final day of the experiment (day 19) is shown. Represented is the mean \pm S.E.M. per group. Differences were evaluated with One-way ANOVA test (n.s.). **D)** Weight of mice during the whole period of the experiment, starting with tumor cell inoculation (day 0) and ending with euthanasia (day 19). Measurements performed on day 0, day 9 and day 16. Represented is the mean \pm S.E.M. per group.

3.6. Use of a xenograft tumor model to evaluate the effect of soraphen A on HCC tumors

Within a soraphen A project of our lab, we wanted to evaluate the efficacy of the natural compound soraphen A on hampering tumor growth. So, a xenograft tumor model was chosen. Such an experiment was performed for the first time with this experimental drug, it corresponds with an in vitro project performed in our lab, where soraphen A inhibited the proliferation of Huh7 cells in cell culture. That is why Huh7 cells were chosen for this animal experiment. Scid mice are suitable for this human tumor cell line. 3×10^6 hepatocellular carcinoma cells (Huh7) were subcutaneously injected into Scid mice. Tumor bearing mice were separated into two groups (n = 10), two mice in the soraphen A treated group did not develop any tumor over time. One group was treated with solvent and the other group was treated with soraphen A (40 mg/kg). Daily therapy started on day seven after tumor cell application and mice received therapy for nine times altogether. Treatment with

III. Results

soraphen A mediated a lower tumor size compared to the control group, volume of tumors in the soraphen A treated group was significantly lower compared to control group on the last three days of the experiment (d14, d15 and d16). (Figure 28 A) On day 16 all mice were euthanised, the comparison of tumor weight of both groups after resection showed no significant difference between soraphen A treated mice compared to control. (Figure 28 B).

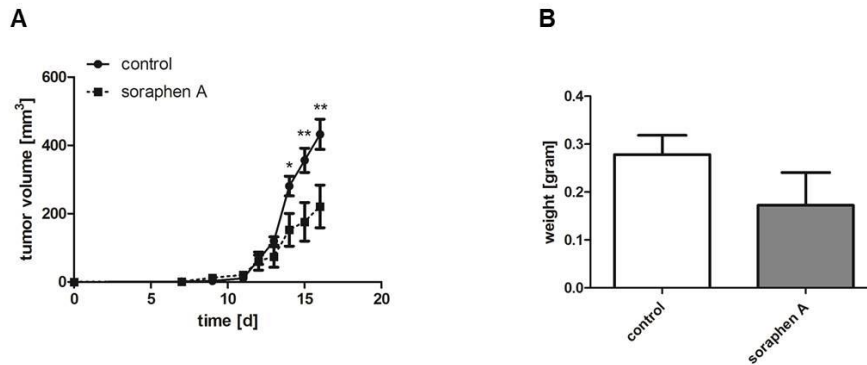


Figure 28: Tumor volume and weight **A**) Shown is the growth of Huh7 tumors over time in both groups, control and soraphen A (40 mg/kg) treated. Represented is the mean \pm S.E.M. per group. Results are statistically evaluated with t-test (* $p < 0.05$, ** $p < 0.01$ **B**) Shown is tumor weight after resection out of the body on day 16. Represented is the mean \pm S.E.M. per group. Results are statistically evaluated with t-test (n.s.).

Figure 29 shows that all mice kept a healthy general condition and that the weight loss and gain fluctuated in a physiological range.

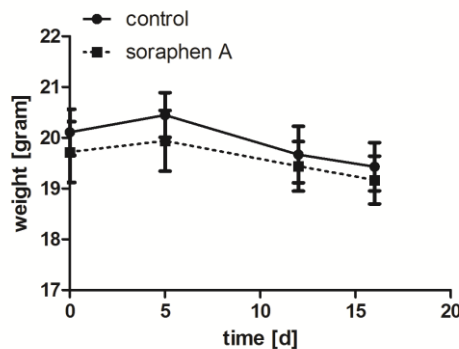


Figure 29: Weight over time: Mice did hardly lose weight during experimental period. Weight was assessed four times (d0, d5, d12, d16). Represented is the mean \pm S.E.M. per group.

4. Murine tumor models to evaluate tumor dissemination

In this kind of experiments, the aim was to evaluate the dissemination of tumor cells after i.v. injection. Three different methods were established with a variety of different experimental setups. For all of them, luciferase tagged cells (4T1-luc and Jurkat-luc) were used which made it possible for us to detect the distribution of tumor cells in the body of living mice with our bioluminescence in vivo imaging

system (IVIS®). We evaluated the distribution of human leukemia cells (Jurkat-luc) in three different murine models (Scid, Nod-Scid and NSG mice) without any treatment to find out in which model the cells were able to disseminate at all and to establish a suitable mouse model for a leukemia project. The effects of sorafenib treatment and likewise tetrandrine treatment on murine breast cancer cells (4T1-luc) were evaluated both in allograft tumor models using BALB/c mice, because 4T1 cells originate from this strain.

4.1. Evaluation of suitable mouse models for a leukemia project

Concerning a leukemia project in our lab, Jurkat-luc cells should be tested *in vivo*. Due to the fact that there exist, to our knowledge, no published data on the most suitable mouse strain for leukemia models in general, this experiment was performed with three different strains. We used three Scid mice, three Nod-Scid mice and three Nod-Scid-Gamma (NSG) mice. Each of these animals received 1×10^6 Jurkat-luc leukemia cells via injection into the tail vein. Bioluminescence imaging started on day four after cell inoculation with the Scid and Nod-Scid animals and on day two with NSG mice, all Scid and Nod-Scid mice lay in ventrodorsal position during the procedure, the NSG mice in ventrodorsal and dorsoventral positions.

The bioluminescence signals the imager detected are represented in Figure 30 A-B, always one picture out of the sequence was chosen. Scid and Nod-Scid mice were imaged six times altogether (d4, d7, d11, d13, d19, d21), no bioluminescence signals equating tumor cell dissemination were detectable. Mice were euthanised on day 21. NSG mice were imaged nine times altogether (d2, d5, d8, d12, d15, d19, d22, d26, d29), the first bioluminescence signals were detected on day five after cell inoculation. The first one was remarkable in dorsoventral position in the region of the tail base in one mouse. Three days later, we noticed a daily increase of the signal and from day 15 on, all three mice showed a strong bioluminescence signal in different parts of the body in both imaging positions. We continued the imaging process until day 29 after cell application, strong bioluminescence signals were presented in ventrodorsal positions as well as in dorsoventral positions. Concerning mice' anatomy, the strongest signals detected at dorsoventral imaging positions came from medulla and brain and from lungs, heart, liver, stomach, femurs and bladder, imaged in ventrodorsal positions. After the last procedure on day 29, all mice were sacrificed.

During the trial, all mice were in a healthy general condition and did not show any weight loss (Figure 31).

The consequence of this experiment was that just NSG mice can be used in bioluminescence imaging experiments with Jurkat-luc cells and other leukemia models.

III. Results

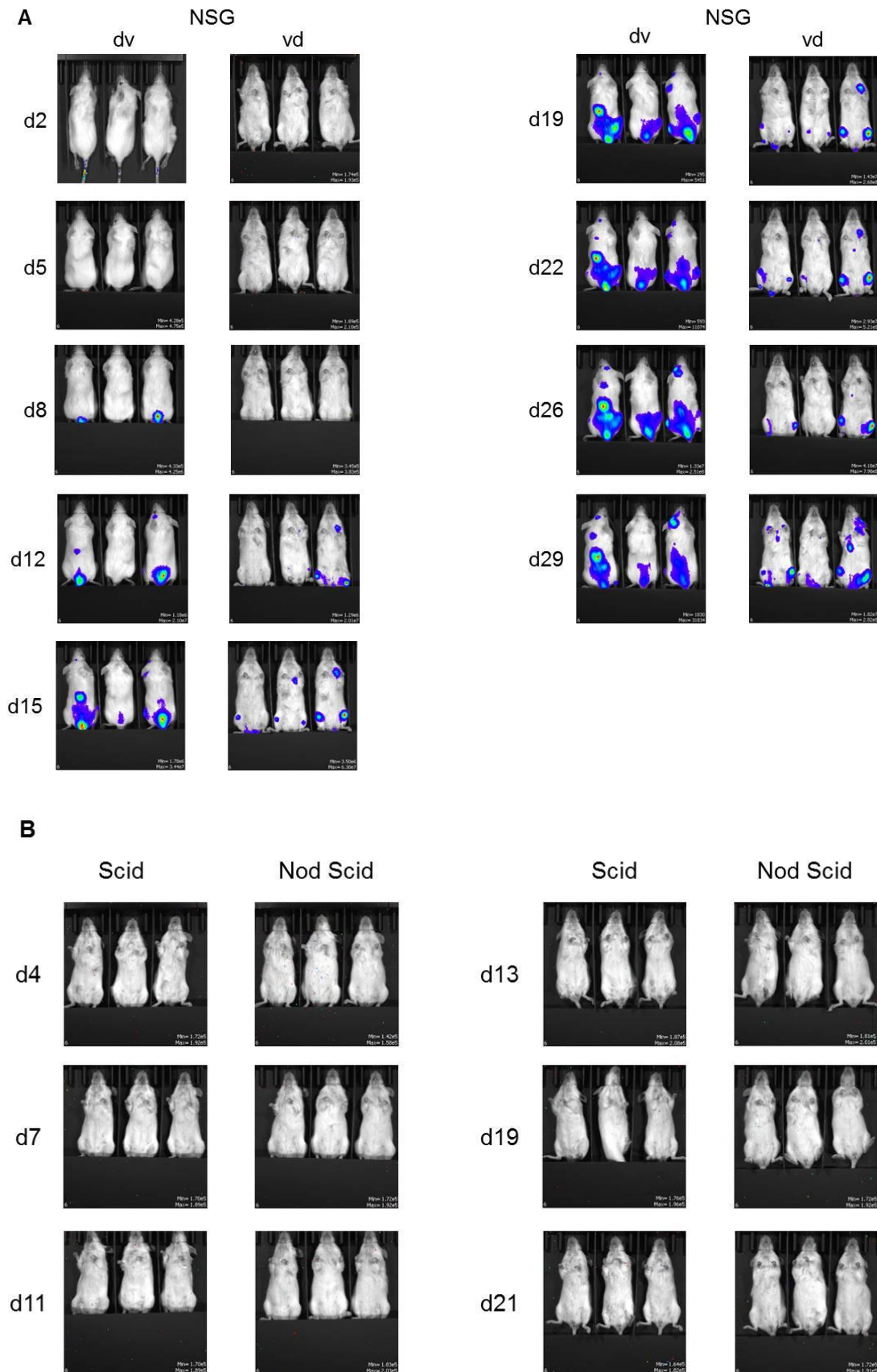


Figure 30: Bioluminescence images. **A)** Pictures of tumor burden in NSG mice until day 29 after Jurkat-luc cell inoculation, taken on day 2, 5, 8, 12, 15, 19, 22, 26, 29, in ventrodorsal (dv) and dorsoventral (dv) imaging positions. **B)** Ventrodorsal bioluminescence pictures of Scid and Nod Scid mice taken on day 4, 7, 11, 13, 19 and 21 after cell application.

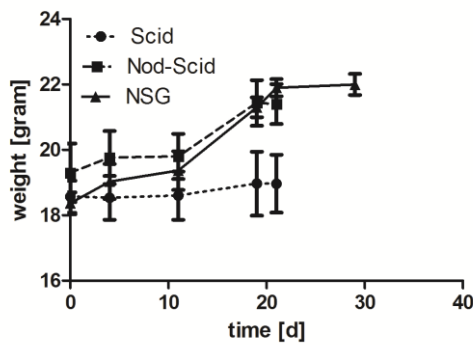


Figure 31: Weight over time. Weight of Scid and Nod-Scid mice over time, starting with tumor cell injection (day 0), ending with euthanasia (day 21). And weight of NSG mice starting with tumor cell injection (day 0) and ending with euthanasia (day 29). Weight was assessed on day 0, 4, 11, 19, 21 and 29 (d29 just for NSG mice). Represented is mean \pm S.E.M. of three mice per group.

4.2. Murine tumor models to evaluate the effect of tetrandrine on tumor dissemination

The *in vivo* dissemination of 4T1-luc cells under tetrandrine treatment was evaluated in three different setups due to a project in which the inhibition of two-pore channels through tetrandrine was focused.

In our first experiment, 20 BALB/c mice were separated into two groups (n=10), each mouse received 1×10^5 4T1-luc cells via *i.v.* injection. One group was treated with solvent as a control, the other one was treated with tetrandrine in a dosage of 100 mg/kg. Solvent respectively tetrandrine were intraperitoneally administered 24 hours and 4 hours before cell application and a third time 24 hours after it. On day eight after inoculation of cells, both groups were imaged with the IVIS® Spectrum in ventrodorsal imaging positions. One mouse of the control group died during the experiment.

Figure 32 represents the bioluminescence signal equating the tumor burden in the lungs on day eight after cell application. For evaluation, regions of interest (ROIs) were defined and the total signal per ROI was calculated as photons/second/cm² (total flux/area). The tumor burden in the lungs of the tetrandrine treated group was significantly higher compared to the control group, which was a controversial result for us.

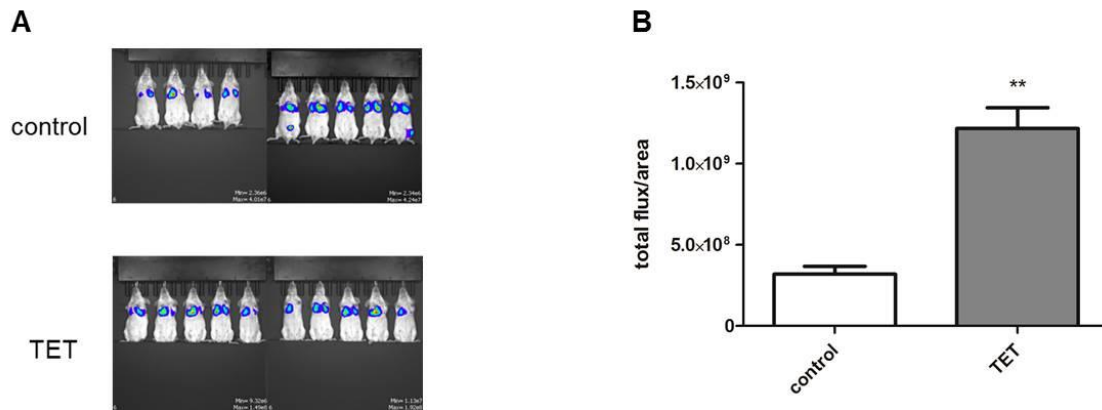


Figure 32: Average tumor burden in the lungs on day 8. **A)** The average bioluminescence signal of both groups is shown in ventrodorsal imaging positions. Represented are nine mice in the control and ten mice in the tetrandrine (TET) treated group. **B)** Regions of interest (ROIs) were defined and the total signal per ROI was calculated as photons/second/cm² (total flux/area). Represented is the mean \pm S.E.M. of nine/ten mice per group. Significance of the results was evaluated using t-test (* $p < 0.05$, ** $p < 0.01$).

The animals showed no changes in their general condition and did not lose weight during the experimental period which was ended on day eight. (Figure 33)

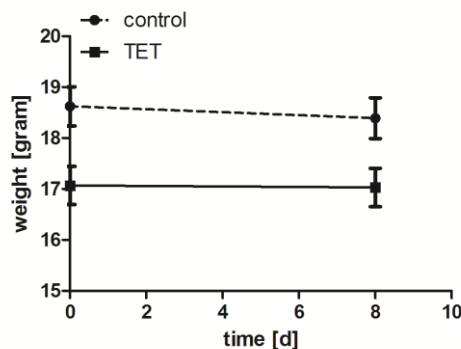


Figure 33: Weight over time. Shown is the weight development over eight days during the experiment, measured on day 0 and day 8. Represented is the mean \pm S.E.M. of nine/ten mice per group.

Subsequently, it was clear that this experimental setup was not suitable for such a dissemination experiment with tetrandrine. So, we established another setup within this trial. 24 BALB/c mice were divided into three groups (n=8), one group received with DMSO pre-treated 4T1-luc cells and was treated itself with solvent three times, another group also received with DMSO pre-treated 4T1-luc cells and was treated itself with tetrandrine (100 mg/kg solved in HCl) three times, and another group received cells, pre-treated with tetrandrine (10 μ M, 24h) and received just one treatment of tetrandrine (100 mg/kg) directly after cell injection. All animals passed through bioluminescence imaging on day eight after injection of cells. Each of them, except of one mouse in the three times tetrandrine treated group exhibited a thoracic

III. Results

luminescent signal reflecting the tumor burden in the lungs. All bioluminescence images were quantified by defining ROIs and then calculating the total signal per ROI as total flux/area. Figure 34 shows that the bioluminescence signal of control mice lay at 2.5×10^8 , while the group with three time tetrandrine treatment (TET) lay at 7.5×10^8 and the group with pre-treated cells and one time tetrandrine treatment lay at 2×10^9 . Mice which received pre-treated cells plus one tetrandrine therapy showed a significant higher bioluminescence signal compared to the control group, which actually was expected to be the group with the highest signal.

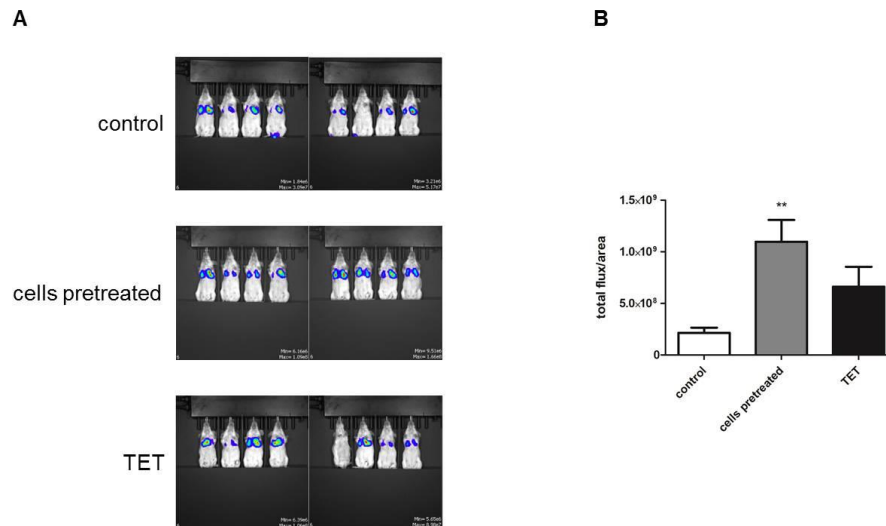


Figure 34: Average tumor burden in the lungs on day 8. A) The average bioluminescence signal of all groups is shown in ventrodorsal pictures, one group is consisting of eight mice. B) Regions of interest (ROIs) were defined and the total signal per ROI was calculated as photons/second/cm² (total flux/area). Represented is the mean \pm S.E.M. of eight mice per group. Significance of the results was evaluated using One-Way ANOVA test (* $p < 0.05$, ** $p < 0.01$).

The experiment was ended after imaging on day eight with euthanasia, all mice showed a proper general condition concerning their body weight during the experiment, although variabilities occurred. (Figure 35) But, some of the mice showed small wounds at the points of intraperitoneal injections, referable to HCl used as solvent. Mice with the highest tumor burden also showed the most weight loss.

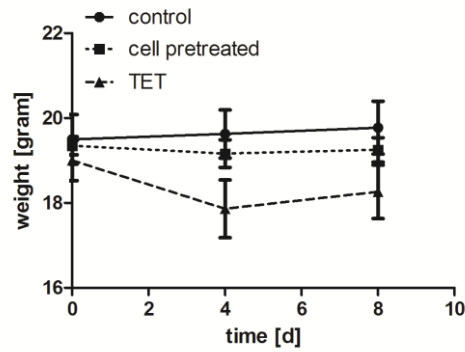


Figure 35: Development of mice' weight over time. Weight of all groups is shown from cell injection (day 0), over day 4 until euthanasia (day 8). Represented is the mean \pm S.E.M. of eight mice per group.

Due to these controversial results, the experimental setup had to be totally changed. So, another experimental setup was established within two groups of BALB/c mice, each group consisting of eight mice. One group received 1×10^5 with DMSO pre-treated 4T1-luc cells i.v. while the other one received 1×10^5 tetrandrine pre-treated cells ($10 \mu\text{M}$, 24h) intravenously injected. Bioluminescence imaging was performed five and seven days after cell application. All mice, except one in the tetrandrine group, showed a thoracic bioluminescent signal. Ventrodorsal images show the tumor burden in the lungs. The signal was calculated as total flux/area after defining ROIs. On day five, the group with tetrandrine pre-treated cells showed a significantly lower bioluminescence signal, equivalent to tumor burden, compared to the control group. (Figure 36) The result of day eight was not significant concerning the difference between both groups. (Figure 37) During the whole experimental period, all mice showed a good general health condition and even gained weight. (Figure 38)



Figure 36: Day 5, average tumor burden in the lungs. A) The average bioluminescence signal of both groups is shown in ventrodorsal pictures. B) Regions of interest (ROIs) were defined and the total signal per ROI was calculated as photons/second/cm² (total flux/area). Represented is the mean \pm S.E.M. of eight mice per group. Significance of the results was evaluated with t-test (* $p < 0.05$, ** $p < 0.01$).



Figure 37: Day 8, average tumor burden in the lungs. **A)** The average bioluminescence signal of both groups is shown in ventrodorsal pictures. **B)** Regions of interest (ROIs) were defined and the total signal per ROI was calculated as photons/second/cm² (total flux/area). Represented is the mean ± S.E.M. of eight mice per group. Significance of the results was evaluated with t-test (* p < 0.05, ** p < 0.01).

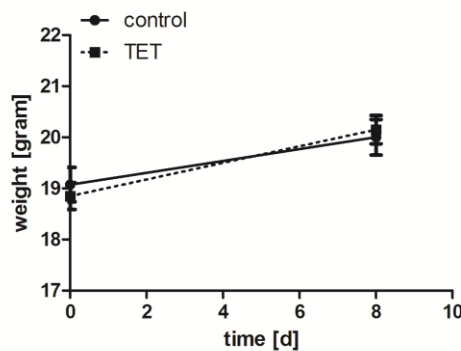


Figure 38: Weight over time diagram. Weight development of mice in both groups over experimental period, measured on day 0 and day 8. Represented is the mean ± S.E.M. of eight mice per group.

4.3. Using an allograft tumor model to evaluate the effect of soraphen A on tumor dissemination

Within a soraphen A project, we decided to use BALB/c mice for this allograft tumor experiment because they are syngeneic with the 4T1-luc cells we wanted to use. For the evaluation of the effect of ACC inhibitor soraphen A concerning the dissemination of murine breast cancer cells (4T1-luc) after i.v. injection into BALB/c mice, we compared mice which received soraphen A pretreated cells in two different concentrations with control mice which received vehicle pre-treated cells. Animals were divided into three groups (n=8), the control group received 1 x 10⁵ vehicle pre-treated 4T1-luc cells via i.v. injection, the second group received cells which were

III. Results

pre-treated with 1 μ M soraphen A for six hours and the third group received cells with a soraphen A pre-treatment of 25 nM over 72 hours. All mice passed through a bioluminescence imaging on day four and day seven after tumor cell inoculation, mice were imaged in ventrodorsal positions. On day seven all mice were euthanised. Seven out of eight mice in the control group showed a very strong bioluminescence signal on day four, three days later, all of the mice in the control group showed a firm signal. All animals in the six hours pre-treated as well as in the 72 hours pre-treated group evinced bioluminescence signals on day four and seven, whose total flux/area rates equating tumor burden in the lungs were lower compared to the burden in the control group. (Figure 39 A) Mice which received cells with soraphen A treatment over 72h showed a significantly reduced tumor burden compared to the control group on day four and day seven. (Figure 39 B)

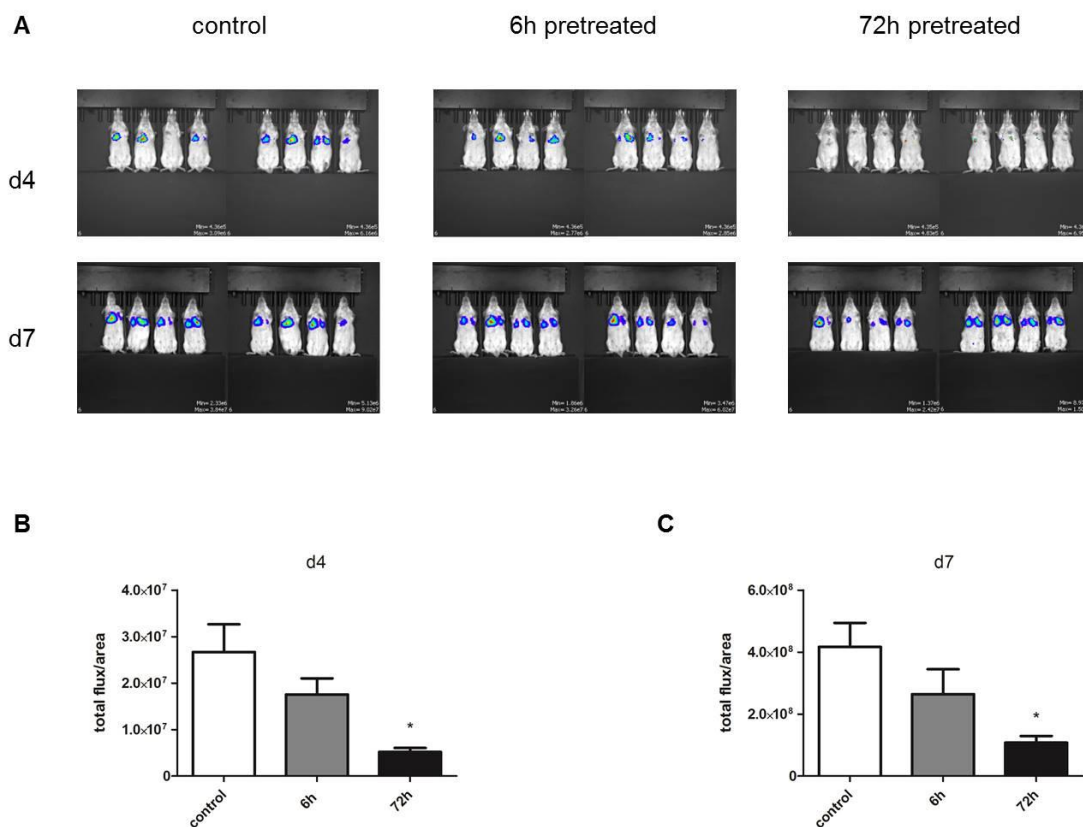


Figure 39: Dissemination of tumor cells in the body. A) Bioluminescence signals in the lungs in ventrodorsal imaging positions on day four and day seven after cell inoculation, three groups (n=8) are shown, one with vehicle pre-treated cells, one with soraphen A (1 μ M) pre-treatment over 6h and one with soraphen A (25 nM) pre-treatment over 72h. **B)** Regions of interest (ROIs) were defined and the total signal per ROI was calculated as photons/second/cm² (total flux/area), results of day 4. Represented is the mean \pm S.E.M. of eight mice per group. Significance of the results was evaluated using One-way ANOVA test (* p< 0.05, ** p< 0.01). **C)** Regions of interest (ROIs) were defined and the total signal per ROI was calculated as photons/second/cm² (total flux/area), results of day 7. Represented is the mean \pm S.E.M. of eight mice per group. Significance of the results was evaluated using One-way ANOVA test (* p< 0.05, ** p< 0.01).

All mice gained weight during the whole experimental period and stayed in a good general condition. (Figure 40)

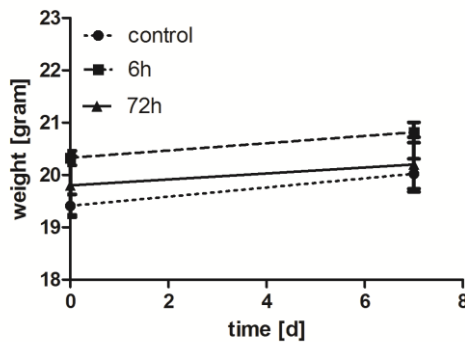


Figure 40: Weight over time. Weight development of mice in all groups, starting with i.v. injection of cells (day 0) until euthanasia (day 7). Represented is the mean S.E.M. of eight mice per group over time.

5. Murine tumor experiments to show the influences of Cdk5 on tumor development

The focus of this chapter lies on the establishment of *in vivo* experiments usable for the evaluation of the influences which the cyclin-dependent kinase 5 has on tumor development. We performed different experiments. We used a Cdk5 knock-down in Huh7 cells and treated the mice with the HCC therapeutic sorafenib, furthermore we used C57BL/6 mice with an inducible endothelial Cdk5 knock-out in combination with the Cdk inhibitor roscovitine. In addition, two murine limiting dilution experiments were performed, T24 Cdk5 knock-down cells as well as 4T1-luc cells in combination with Cdk5 inhibitor dinaciclib were used. Both trials were performed to evaluate the influence of cancer stem cells on tumor development and growth.

5.1. Evaluation of the effect of a Cdk5 knock-down in Huh7 cells in combination with sorafenib treatment in a xenograft model

The aim was the realisation of an *in vivo* experiment due to a current HCC project in our lab. To evaluate the effect of Cdk5 in HCC tumor development, 24 BALB/c mice received either Huh7 nt shRNA (n=12) or Huh7 cells with a Cdk5 knock-down (Huh7 Cdk5 shRNA) (n=12). After tumors arose, each group was divided a second time into a part which was vehicle treated and a part which was treated with the established HCC therapeutic sorafenib (10 mg/kg). Daily intraperitoneal therapy for tumor bearing mice started on day 11 after cell application and lasted until day 18, tumor volume was measured every second day. All groups, Huh7 nt shRNA cells receiving solvent treatment (n=5, because one mouse did not develop any tumor), Huh7 nt shRNA cells receiving sorafenib treatment (n=6), Huh7 Cdk5 shRNA cells

III. Results

receiving solvent (n= 6) and Huh7 Cdk5 shRNA receiving sorafenib treatment, were compared to each other.

The Cdk5 knock-down in Huh7 cells seemed to sensitize HCC tumors to sorafenib treatment *in vivo*, because the combination of Cdk5 knock-down and sorafenib treatment led to the lowest tumor volume. Differences are not significant. (Figure 41 A-C) All mice were in a good general condition and showed constant body weight. (Figure 41 D)

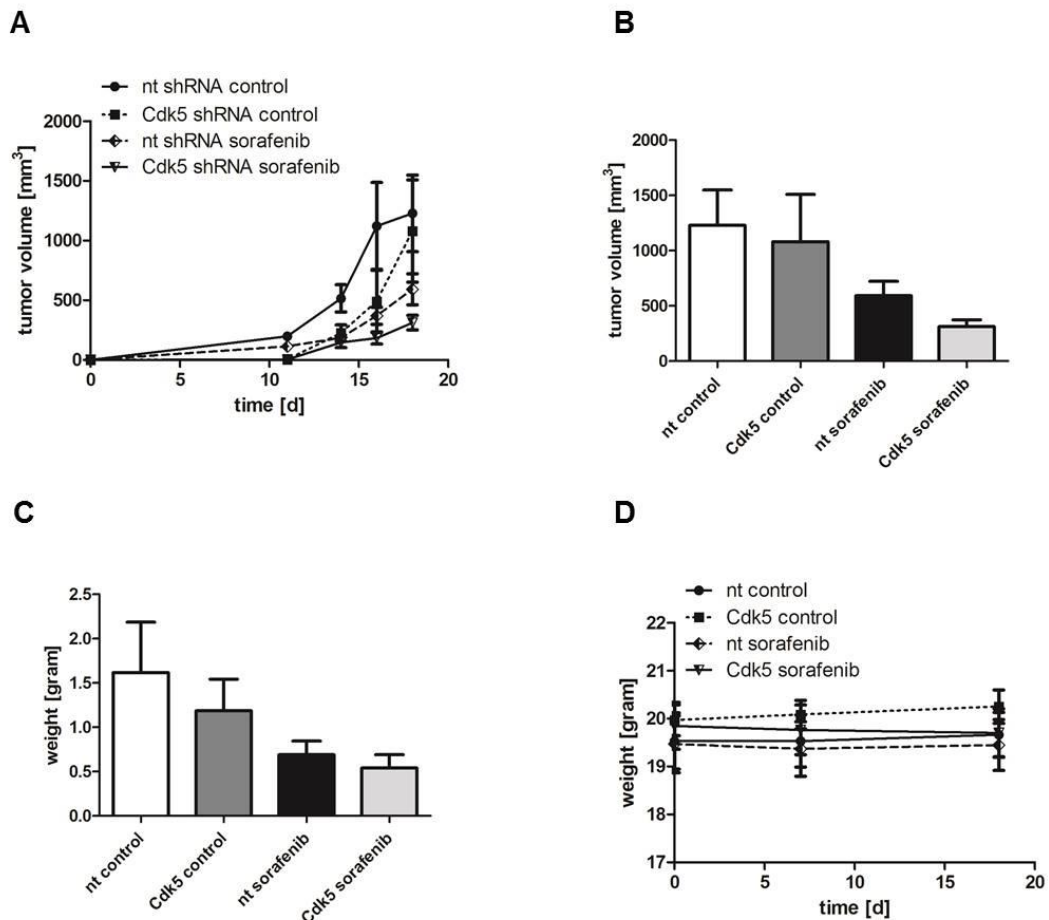


Figure 41: Tumor development and weight of mice A) Tumor development over time, four groups are shown, one with Huh7 nt cells and solvent treatment (n= 5), another with Huh7 nt cells and sorafenib treatment (10 mg/kg) (n=6), the third and fourth one with Huh7 Cdk5 shRNA cells and either solvent (n=6) or sorafenib (n=6) treatment. Shown is the development of tumors over time, starting with s.c. injection of cells (day 0) until euthanasia (day 18). Represented is the mean \pm S.E.M. per group. Results were statistically evaluated with One-way ANOVA test (n.s.). B) Shown is the tumor volume of all four groups on final day of experiment (d18). Represented is the mean \pm S.E.M. per group. Results are statistically evaluated via One-way ANOVA test (n.s.). C) Weight of tumors after resection. Shown is the weight of tumors on day 18 of experiment after resection from the body. Represented is the mean \pm S.E.M. of five respectively six mice per group. Results are statistically evaluated with One-way ANOVA test (n.s.). D) Weight of mice over time. Shown is the weight of mice in all of the four groups during the whole experimental period. Starting with injection of tumor cells (d0) until euthanasia (d18). Weight was assessed three times (d0, d7, d18). Represented is the mean \pm S.E.M. of five respectively six mice per group.

5.2. Effect of an inducible endothelial Cdk5 knock-out in mice in combination with roscovitine on melanoma tumors

Concerning a revision of a submitted manuscript focused on the reduction of tumor growth through the inhibition of endothelial Cdk5, we wanted to evaluate the effects of an inducible endothelial Cdk5 knock-out in mice in combination with roscovitine treatment on tumor growth of B16F1 cells. 6 C57BL/6 mice with Cdk5 knock-out (Cdk5^{fl/fl} VECCre+) were used for that. Mice were provided by Dr. Johanna Liebl (University of Munich, Germany). All mice received a subcutaneous injection of 1×10^6 B16F1 cells (murine melanoma cells) into the left flank (d0). When first tumors were visible and palpable (day 7), mice received either solvent or roscovitine (150 mg/kg) treatment three times a week, experiment was ended on day 14 after cell application. So, mice received therapy for four times (d7, d9, d11, d14). In Figure 42 is shown that Cdk5 knock-out mice receiving solvent (n=3) developed a higher tumor volume compared to Cdk5 knock-out mice receiving roscovitine (n=3). Differences between the groups were not significant. So, an endothelial Cdk5 knock-out sensitizes tumors for chemotherapy.

Mice were euthanised on day 14 after cell application, after resection, all tumors were weighed. Control group of Cdk5 knock-out mice developed heavier tumors than the roscovitine treated ones did. (Figure 42 C) During the whole experimental period, all mice kept a healthy general condition and they gained weight. (Figure 42 D)

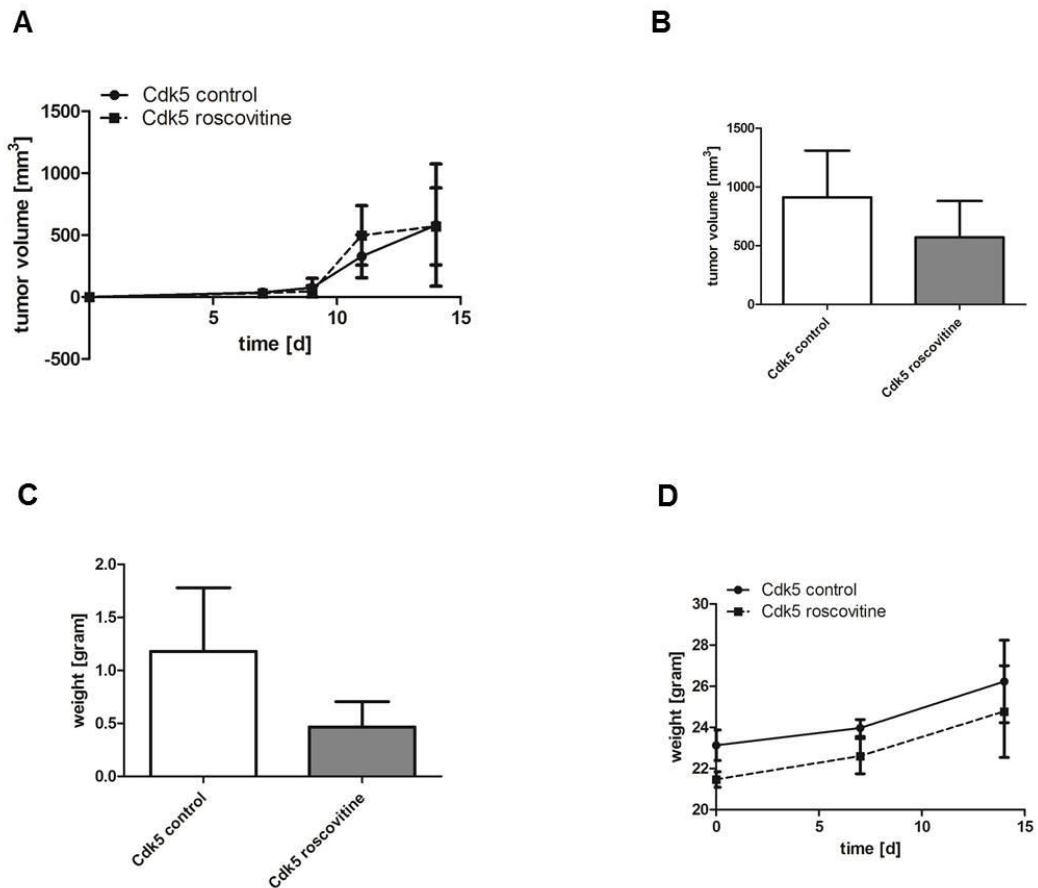


Figure 42: Tumor volume and weight of mice. **A)** Shown is the average tumor volume over the experimental period. Listed are mice with an inducible endothelial Cdk5 knock-out (Cdk5^{fl/fl} VECCre+), treated either with solvent or with roscovitine (150 mg/kg) (n=3 in each group). Therapy started on day seven after tumor cell application. Represented is the mean \pm S.E.M. of 3 mice per group. Results are statistically evaluated with t-test (n.s.). **B)** Shown is tumor volume of all groups on final day of experiment (d14). Represented is the mean \pm S.E.M. of 3 mice per group. Results are statistically evaluated with t-test (n.s.). **C)** Tumor weight on final day of experiment. Shown is tumor weight after resection on last day of experiment (day 14). Cdk5 knock-out mice were used. Represented is the mean \pm S.E.M. of 3 mice per group. Results are statistically evaluated with t-test (n.s.). **D).** Weight was assessed on day 0, day 7 and day 14. All mice gained weight during the experimental period. Represented is the mean \pm S.E.M. of 3 mice per group.

5.3. Limiting dilution experiment with T24 cells

The limiting dilution assay is applied to evaluate the tumor initiating potential of CSCs. So, to evaluate the influence of tumor initiating cells and their importance for tumor development and growth in combination with Cdk5 inhibition, a murine xenograft limiting dilution experiment was performed. T24 nt shRNA and T24 Cdk5 shRNA cells in different amounts were injected into BALB/c nu/nu mice subcutaneously into the left flank of the mice. Tumors were measured three times a week and so the tumor volume was evaluated, experiment lasted over 42 days, measurements started seven days after cell application when first tumors arise. Evaluated were 5×10^6 , 2.5×10^6 , 1×10^6 , 5×10^5 and 1×10^5 of each cell type, aside from the amount 5×10^6 , all other cell numbers were evaluated in pairs (2.5×10^6 and 1×10^5 ; 1×10^6 and 5×10^5), the higher one injected into the left flank of a mouse and the lower one injected into the right flank of the same mouse.

All in all, tumors arisen of T25 Cdk5 shRNA cells showed a higher volume during the experiment and on final day (d42) compared to tumors arisen of T24 nt shRNA cells (Figure 43 A-B), while the start of growing and the number of tumors that arose varied totally between the groups. (Figure 43 C) Numbers of tumors that arose are equal in all groups (n=5), except from 1×10^5 where 3 respectively 4 tumors arose. (Figure 43 C)

Weighing after the resection of all tumors also showed that those tumors arisen of T24 Cdk5 shRNA cells not only developed the higher tumor volume but also the higher tumor weight. (Figure 43 D) These results were not significant.

It is also noticeable, that in the T24 Cdk5 shRNA cell type the amount of 1×10^6 injected cells lead to the highest tumor volume and the highest tumor weight. So, 1×10^6 might be the best amount of cells for injection in tumor growth experiments with B16F1 cells.

III. Results

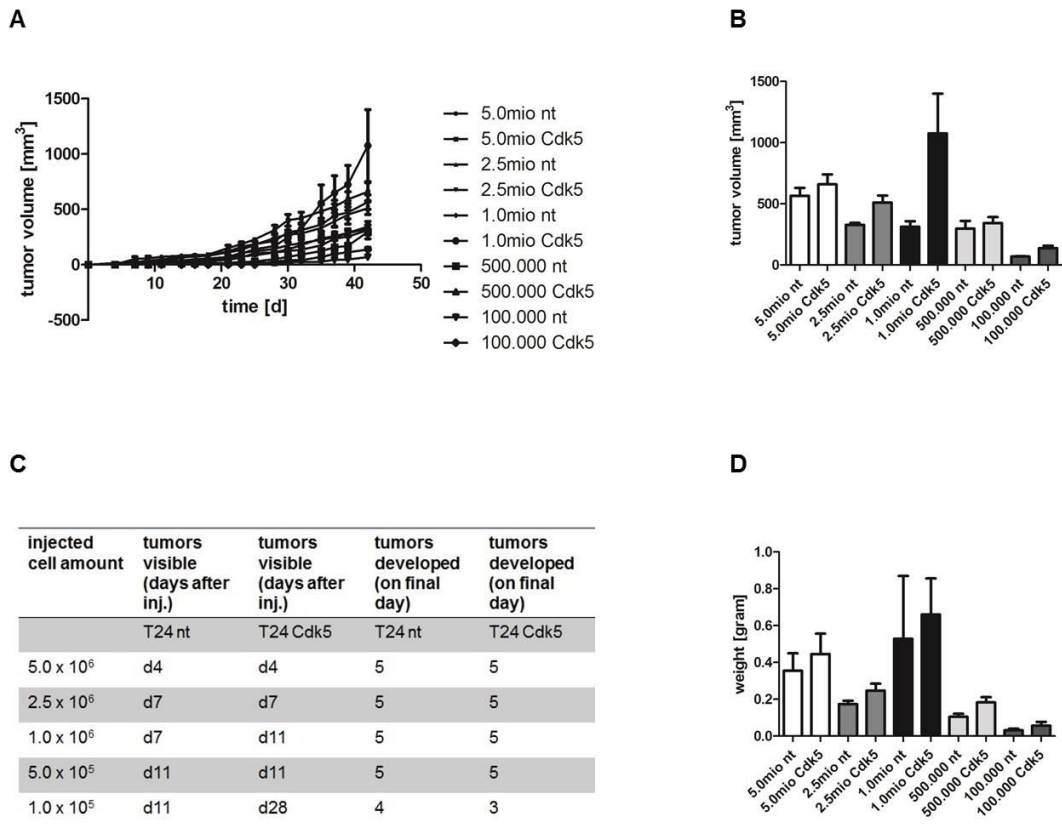


Figure 43: Tumor development and weight. T24 nt shRNA as well as T24 Cdk5 shRNA cells were subcutaneously injected into BALB/c nu/nu mice. We used five cell amounts of each cell line. Seven days after application, mice started to bear tumors, experiment lasted until day 42 after application and ended with euthanasia. **A)** Shown is the development of tumors of all cell amounts over time. Mice received either 5×10^6 , 2.5×10^6 , 1×10^6 , 5×10^5 or 1×10^5 cells (T25 nt shRNA or T24 Cdk5 shRNA). Represented is the mean \pm S.E.M. of five mice per group. Results are statistically evaluated with One-way ANOVA test (n.s.). **B)** Shown is the tumor volume on final day of experiment (d42). Represented is the mean \pm S.E.M. of five mice per group. Results are statistically evaluated with One-way ANOVA test (n.s.). **C)** Total amount of arisen tumors. Shown is a list of the accrument of tumors in days after the inoculation and the number of tumors developed until d42. **D)** Weight of tumors after resection. Shown is the tumor weight on final day of experiment (d42). Represented is the mean \pm S.E.M. of five mice per group. Results are statistically evaluated with One-way ANOVA test (n.s.).

All mice kept a good general condition during the whole experimental period and gained weight. (Figure 44) They were sacrificed through cervical dislocation on day 42.

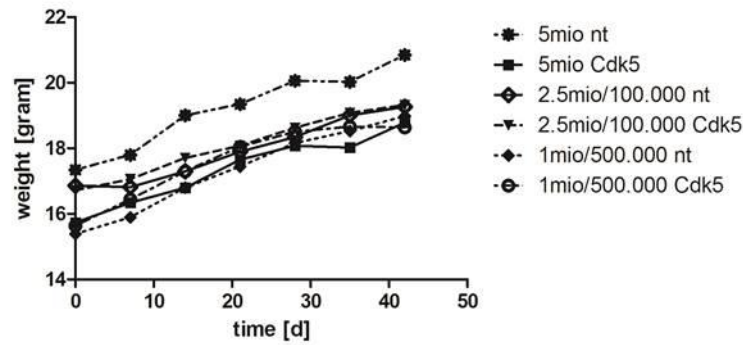


Figure 44: Weight of mice during experiment. Shown is the development of mice' weight during the whole experimental period. Starting with cell injection (d0) ending with euthanasia (d42). Shown is the group of mice receiving 5×10^6 cells (left flank), 2.5×10^6 and 1×10^5 cells (left and right flank) and 1×10^6 and 5×10^5 (left and right flank), these three groups for each cell type. Represented is the mean \pm S.E.M. of five mice per group.

5.4. Limiting dilution experiment with 4T1-luc cells

For the evaluation of tumor initiating cells in 4T1-luc tumors in combination with Cdk5 inhibition through dinaciclib, a murine allograft limiting dilution experiment was performed. 50 BALB/c mice received an application of different cell amounts and were then either treated with solvent or dinaciclib (30 mg/kg). 4T1-luc cells were subcutaneously injected into BALB/c mice. We used five cell amounts, each amount was injected into ten mice. These groups were divided into five mice which received either solvent or dinaciclib (30 mg/kg) three times a week. Treatment started on day of tumor cell application (d0). Experiment lasted until day 25 (in groups with 1×10^6 , 1×10^5 , 1×10^4 cells) because the bioluminescence signal the imager detected were saturated then and mice of these groups were euthanised because of the high tumor burden or it ended on day 30 (in groups with 1×10^3 or 1×10^2 cells) after application. One mouse in the 1×10^5 cells and vehicle treated group, two mice in the 1×10^5 cells and dinaciclib treated group and one mouse in the 1×10^3 cells and dinaciclib treated group died during the experiment. Figure 45 A shows the tumor development over time of ten groups. All mice with 1×10^6 tumor cells injection developed almost equal tumors in the control group and the dinaciclib treated group over time. On final day of experiment (d25) the control group showed a little higher tumor volume than the dinaciclib treated one. In the 1×10^5 and 1×10^4 cell amounts all mice developed a tumor, in each case the dinaciclib treated group developed the higher tumor volume compared to the control. (Figure 45 B)

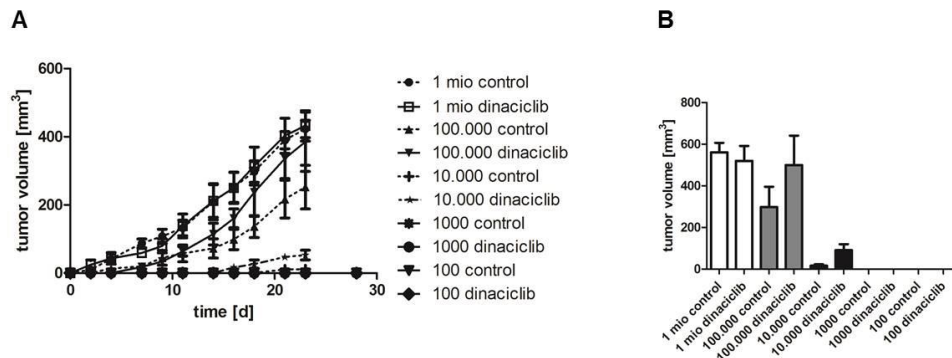


Figure 45: Tumor development over time. **A)** Shown is the development of tumors of all ten groups over time. Mice received either 1×10^6 , 1×10^5 , 1×10^4 , 1×10^3 or 1×10^2 cells and were either treated with dinaciclib or with vehicle. Represented is the mean \pm S.E.M. per group. Results are statistically evaluated via One-way ANOVA test (n.s.). **B)** Shown is the tumor volume of each group on final day of experiment (day 25 or day 30). Represented is the mean \pm S.E.M. per group. Results are statistically evaluated via One-way ANOVA test (n.s.).

Bioluminescence imaging with IVIS® Spectrum was performed on day 3, 8, 15, 23 and 28 after cell application. All mice with the 1×10^6 and 1×10^5 cell amounts developed visible and palpable tumors, the IVIS® imager detected strong bioluminescence signals at cell amounts of 1×10^6 and 1×10^5 from day 3 on and signals at the cell amount 1×10^4 from day 8 on, but here, one mouse in the control group did not develop a tumor at all, no signal was detectable. Mice which received 1×10^3 cells did not show any visible or palpable tumor during the whole experimental period, but in one mouse, treated with dinaciclib, the imager was able to detect a bioluminescence signal from day 15 onwards. Mice which received 1×10^2 tumor cells did not develop any visible or palpable tumors and the IVIS® was not able to detect any bioluminescence signal. (Figure 46) Signals were calculated as total flux/area. (Figure 47)

III. Results

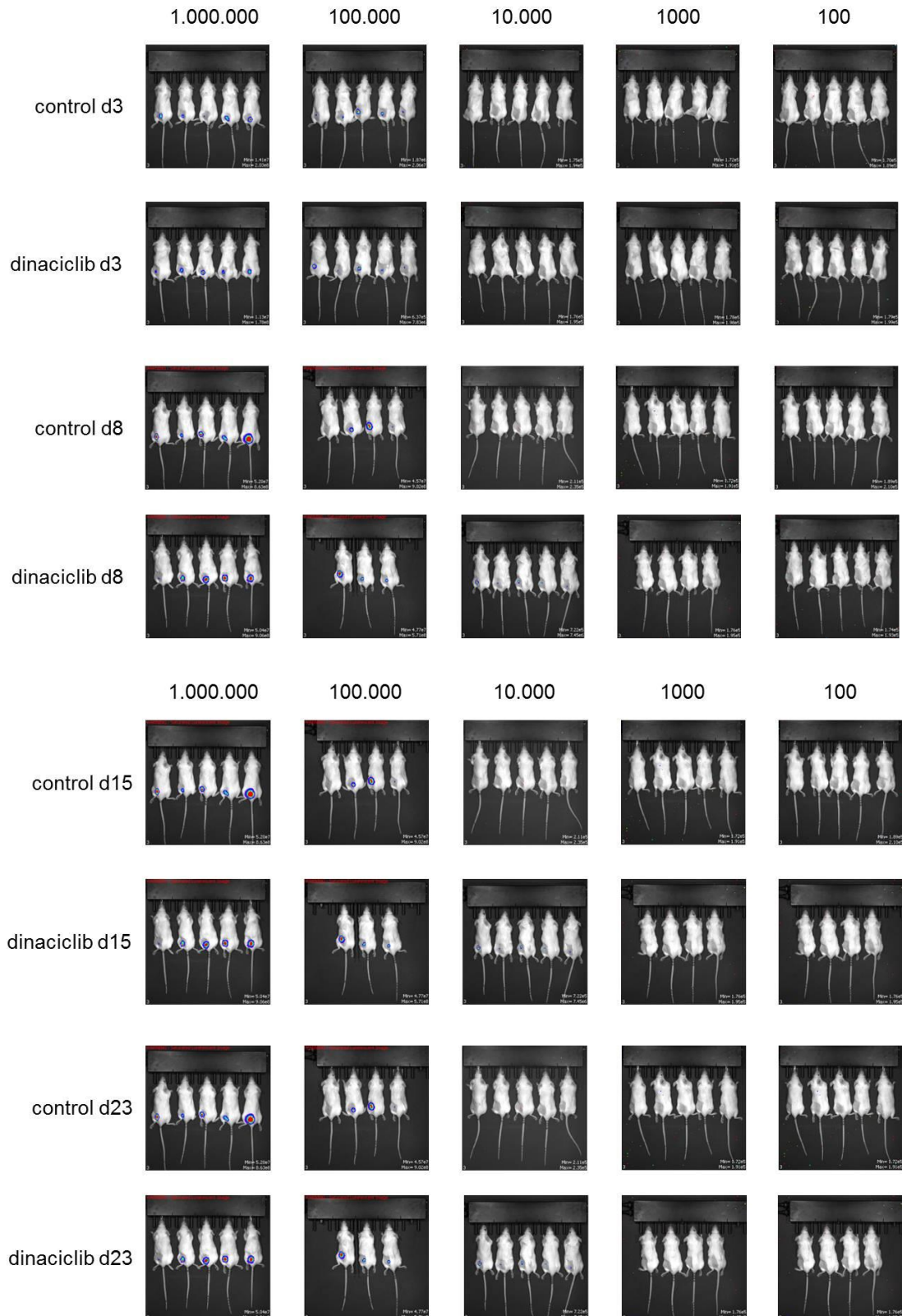


Figure 46: Bioluminescence signals of tumor bearing mice. 50 mice were divided into five groups, each group received another amount of cells (1.000.000, 100.000, 10.000, 1000, 100, shown in the horizontal legend), half of these groups was treated with solvent, the other half with dinaciclib (30 mg/kg). All mice were imaged with the IVIS® Spectrum in dorsoventral positions, shown is one

III. Results

luminescent image per group. Pictures were generated on day 3, 8, 15, 23 and 28. Imaging days are shown in the vertical legend.

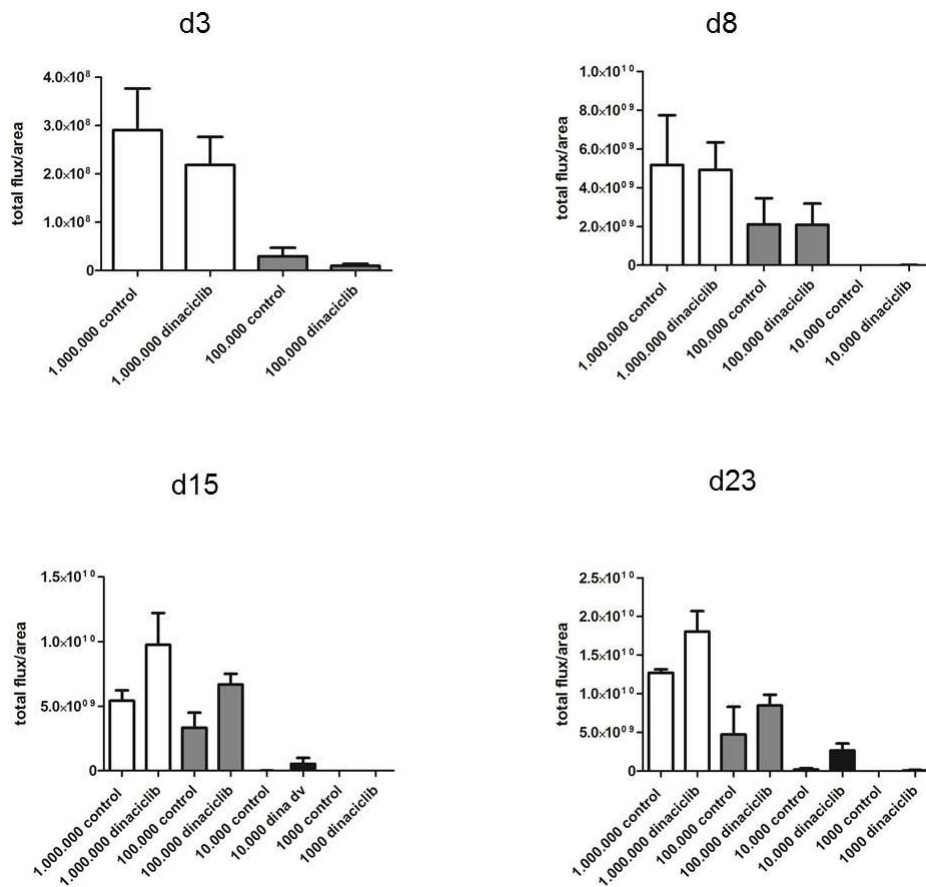


Figure 47: Evaluation of bioluminescence signals. For evaluation regions of interest (ROIs) were defined and the total signal per ROI was calculated as photons/second/cm² (total flux/area). All signals reached at imaging days (d3, d8, d15, d23) were compared with each other. Represented is the mean ± S.E.M. per group. Significance of the results was evaluated using One-way ANOVA test (n.s.).

On final days of experiment (day 25 or day 30), mice were euthanised and tumors were resected and weighed. Tumor weight was evaluated and results show that in the 1×10^6 cell amount group, the control group tumors were heavier while in 1×10^5 and 1×10^4 the dinaciclib treated groups developed heavier tumors. In the 1×10^4 and 1×10^2 cell amount groups, no tumors were palpable and so no tumors were removed. (Figure 48)

Mice in control group kept a good general condition during the whole experimental period. They also gained weight. (49) Mice with dinaciclib treatment showed no harmful changes in their body weight, but they showed a reduced general condition (horrent fur, isolation from the group, bent position) after dinaciclib injections.

According to these results, we cannot define any clear statement on effects of an Cdk5 inhibition through dinaciclib on reducing the development of 4T1-luc tumors. Results are too controversial to draw conclusions.

III. Results

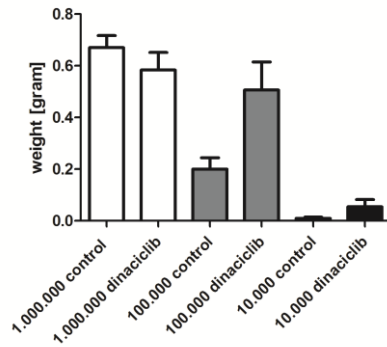


Figure 48: Tumor weight after resection. Shown is tumor weight of mice with 1×10^6 , 1×10^5 and 1×10^4 cells applied. Represented is the mean \pm S.E.M. of five mice per group. Significance of the results was evaluated using One-way ANOVA test (n.s.).

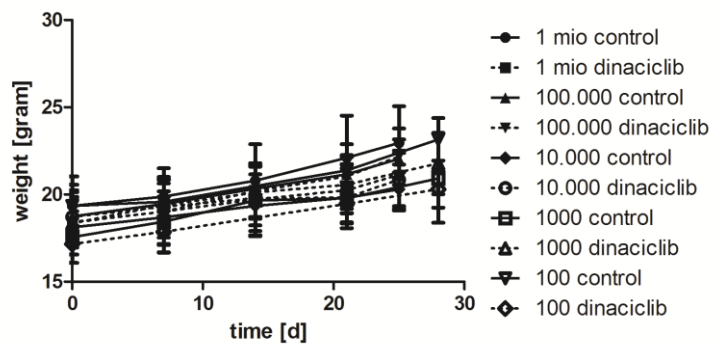


Figure 49: Weight of mice over time. Shown is the weight development of 50 mice over time, starting with cell application (d0) and euthanasia (d 25 /d30). Weight was assessed six times during the experiment. Represented is the mean \pm S.E.M. per group.

IV. Discussion

1. Murine models for preliminary dose finding experiments

One of the first steps in our in vivo experiments was to perform preliminary tests to find adequate dose rates which could be used in the main trials. Such experiments were realized with the compounds simvastatin, LGR 2674, archazolid A, nutlin-3a, PS89 and soraphen A. Mouse strains were chosen according to cell lines which should be used for the main experiments, possible accrument of injected cells and the duration of tumor growing were the key players in the decision process. All in all, simplified setups were used in this kind of experiments, we defined to perform daily intraperitoneal injections for all of the compounds in terms of simplification of animal handling and stress minimization for the mice.

Limited numbers of mice per group (n=1 or n=2) were chosen because these experiments were just performed to create an informative basis and to provide orientation which dosage would be possibly suitable for the main experiments.

Simvastatin is an established inhibitor of cholesterol synthesis, but more and more functions become known, among others its anti-cancer activity by activating apoptosis [125] [126]. A variety of daily dose rates were already evaluated concerning this compound during in vivo experiments by others, orally as well as intraperitoneally administered. In our lab we used simvastatin for the first time in a murine tumor model. For our HCC models with Huh7 cells the mouse strain of choice was Scid, because the human Huh7 tumor cells grow very fast and reliable in this B- and T-cell deficient strain. This was the reason why we performed this dose finding test exactly with these mice. All animals in the experiment tolerated 10 mg/kg/d simvastatin in single application and in combination with 0.2 mg/kg/d archazolid A well. (Figure 12) 10 mg/kg/d of simvastatin can be categorized as a medium dosage, mice would have probably tolerated a higher dose rate but for our combinatorial project this medium dosage was optimal.

LGR 2674, an analogue of Cdk inhibitor roscovitine, was evaluated in vivo for the very first time. It was compounded within the EU project PROKINASE No. 503467 and it is claimed to show a higher potency compared to roscovitine [64]. We geared our chosen dose rates to the dosage 150 mg/kg/d of roscovitine used in former tumor experiments performed in our lab [111]. Concerning the claim to be more effective, we decided to evaluate 15 mg/kg/d and 1.5 mg/kg/d for the compound LGR 2674, meaning dose rates in ten respectively a hundred times less concentrations. This experiment was performed using Scid mice as a suitable strain for Huh7 models. The higher dose rate (15 mg/kg/d) turned out to surmount the tolerance level of the mice. Using 1.5 mg/kg/d is possible in short time experiments, lasting not longer than a few days because mice suffer from weight loss and reduced general condition. (Figure 13) Concerning these results the suggestion for further approaches is a clear

reduction of the dosage because of the insufficient tolerance of 1.5 mg/kg/d LGR 2674 over a longer period.

V-ATPase inhibitor archazolid A is a natural compound frequently used in our lab. In former *in vivo* experiments, the authors chose a dosage of 1 mg/kg archazolid A. But those mice were treated just twice and the generated results showed no significance [127] [31]. Following after these trials, further *in vitro* and *in vivo* experiments were performed using archazolid A in our group. It emerged more and more that mice tolerate only very low concentrations of archazolid A when they were daily treated with it. In this thesis, it should be chosen for a long time experiment where mice receive a daily injection of the substance over a dozen days. The mice in the main trial should get U87MG cells injected, the most suitable strain for these cells are BALB/c nu/nu mice. That is why this strain was used in the dose finding experiments, too. So, a variety of dosages were tested, as a basic dosage 0.3 mg/kg/d archazolid A was chosen, but this led to deviant results. (Figure 14) Some mice tolerated the dosage and some mice did not. This was followed by the decision to lower the dosage for long-term trials to 0.2 mg/kg/d as a first step. The dosage of its combinatorial agent nutlin-3a was chosen according to Zhang et al. who tested a variety of dose rates higher than 5 mg/kg, so we played safe that our chosen dosage (5 mg/kg/d) would be tolerated [84]. An explanation for the controversial results concerning the 0.3 mg/kg/d archazolid A dosage might be our choice of mouse strain. We chose BALB/c nu/nu mice because they should also be used for the main experiment, a xenograft model with glioblastoma cells. But this strain is very sensible concerning its environment, e.g. temperature and housing conditions, and mice of this strain always seemed to be weaker compared to other strains we also purchase at an age of five weeks. Within this strain, there exist great discrepancies in the weight of single mice compared to each other. So, some mice suffered from a general weaker condition. This might be the reason why they were not able to tolerate the 0.3 mg/kg/d dosage of archazolid A, however their strain mates in other experimental groups tolerated the same dosage well. The consequence for us was to use 0.2 mg/kg/d of archazolid A for the mentioned main experiment to make sure all mice endure the long lasting trial. For further investigations, other mouse strains have to be chosen to evaluate how they tolerate archazolid A in a dose rate higher than 0.3 mg/kg/d.

The PDI inhibitor PS89 was evaluated *in vivo* for the very first time. It was planned to use PS89 in a Huh7 tumor model, so Scid mice were chosen for this dose finding experiment. Derived from the concentrations which were effective *in vitro*, we decided to evaluate dose rates from 10 mg/kg/d up to 30 mg/kg/d. (Figure 15) All of them were tolerated well. With a dosage of 30 mg/kg the limits of solubility were almost reached, an unsolved backlog of substance always remained. So, the most suitable dosage was 20 mg/kg/d for the usage in a main experiment, not dependent on tolerance of the mice but on problems with its solubility. In our case, it was

solved in DMSO, solutol and PBS, an approach to increase the possible dosage might be to try other solvent combinations.

Very little data exist on the *in vivo* use of soraphen A until now. Berod et al. described the use of soraphen A as a therapeutic agent in inflammatory processes [128], but concerning tumor growth and tumor dissemination there exist no data. So, we chose soraphen A for a main experiment concerning tumor growth with Huh7 cells using a Scid mouse strain and a dissemination model with 4T1-luc cells and BALB/c mice because they are syngeneic. These strains were used for the corresponding dose finding experiments, too. Concentrations were chosen according to *in vitro* data. All concentrations (5 mg/kg/d–20 mg/kg/d) we tested in BALB/c mice were tolerated well and we had no solubility problems. (Figure 16 A.)

Soraphen A should be also used in a xenograft tumor growth experiment with Scid mice. The highest dosage tested before lay at 20 mg/kg/d, we tried this one again and even doubled the dose rate for Scid mice. But with 40 mg/kg/d as dose rate we were almost reaching the limits of solubility little by little. (Figure 16 B) 40 mg/kg/d were tolerated and still soluble, so it was chosen for the main experiment.

This led to the suggestion that soraphen A might be a very tolerable substance for the usage in murine tumor experiments, independent from the mouse strain. Limitations persist because of solubility problems in concentrations higher than 40 mg/kg. The change of solvent might be an approach for further investigations.

2. Murine experiments to evaluate the pharmacokinetics of archazolid A and roscovitine

Pharmacokinetic is the umbrella term for all processes in the body which influence the applied compound, starting at the resorption, over distribution and metabolisation up to elimination [129]. Studies on pharmacokinetics of a substance are a very helpful tool to evaluate how long the injected substance stays in the circulation to find suitable regimes for the application form and its timed intervals. Namely, results strongly depend on the dosage of a substance and its form of application. The aim in this chapter was to establish two methods to evaluate the pharmacokinetic behavior of V-ATPase inhibitor archazolid A as well as of Cdk inhibitor roscovitine. Both substances are frequently used in our lab.

Archazolid A was intraperitoneally as well as intravenously administered, then 30 min, 1h, 2h, 4h and 6h later blood was taken and the substance concentration in the blood at the single points of time were evaluated. In both forms of application the concentration of archazolid A lowered after 2h and is almost vanished after 6h which led to the suggestion that the half-life of archazolid A is relatively short. (Figure 17 A) The consequence might be to administer archazolid A at least two times a day. The problem is that this substance affects the mice's general condition even in low dose rates very much, so we made the choice to inject it one time per day. To our

knowledge, 0.2 mg/kg/d were tolerated for several days without any bad complications. The high blood concentration of archazolid A after i.v. injection which surmounts the maximal theoretical value that should be found, can be constituted with a PEG impureness in the probes derived from solutol. According to Dr. Jennifer Herrmann, who performed the analyses, lay those in the range of the used internal standard and disturbed the measurements. A logical consequence for future experiments is to spare solutol in the injections and to solve archazolid A just in DMSO and PBS, then such an experiment on the pharmacokinetics of archazolid A should be repeated.

Roscovitine is an established Cdk inhibitor which is frequently used in tumor experiments. A variety of dose rates were used to treat cancer, starting from low dosage as e.g. 25 mg/kg [63] up to 150 mg/kg [111] which was used in our experiments [130]. Here, we evaluated its blood concentration after i.p. application. The concentration reached its peak 30 min after application and held a medium level in the blood up to the last measurement (4h). (Figure 18 A) The low value at the 2h point of time can be declared as a runaway value, but for future experiments it is necessary to choose points of time later than four hours after the application to evaluate how the concentration in the blood behaves afterwards. But this preliminary result encouraged us for now to adhere to our daily treatment regime because roscovitine seemed to reach and hold a plateau level in the blood after i.p. injection. But to really confirm this, such an experiment has to be repeated with more points of time later than four hours after injection.

3. Murine tumor models to evaluate the reduction of tumor growth through various compounds

Chemotherapy has been a widely used tool in the fight against cancer for years [131] and it is still one method of choice, in human medicine as well as in veterinary medicine. Choosing an anti-cancer compound depends on a variety of factors, e.g. the type of cancer, potential resistances and the possibility of combinatorial treatment regimes [132]. Our lab mainly focuses on natural compounds and their derivatives as anti-cancer agents. For this purpose, some of these compounds have been evaluated in animal experiments. All cells were injected subcutaneously to form a solid tumor whose growth was evaluated under the influence of the experimental anti-cancer agents. All experiments were terminated through the general condition of the mice and the tumors' size. We determined a ceiling of 1000 mm³ to exclude illness and limitations of physiological behavior and to prevent tumors from necrosis which is unflattering for further evaluation on biochemical levels.

3.1. Murine tumor models to evaluate the efficacy of archazolid A

The natural compound archazolid A inhibits the so-called V-ATPase which was shown to play an important role during cancer processes [133] [29]. In this thesis, it was used in three different experiments concerning tumor growth.

Within a project where the blockade of iron metabolism through the inhibition of V-ATPases led to therapeutic effects on breast cancer [124], we evaluated the potential of V-ATPase inhibitor archazolid A on hampering the growth of murine breast cancer tumors (4T1). Archazolid A (1 mg/kg, two times applied) was used in an in vivo experiment with BALB/c mice before, these animals also received injections with murine breast cancer cells. This experiment led to no clear and significant results [31]. That is why we established a totally different experimental setup. Therefore, the mouse strain BALB/c nu/nu was chosen and the application regime was changed to daily intraperitoneal injections (0.2 mg/kg/d). Therapy of the 4T1 tumors with archazolid A decreased their volume compared to the control group. (Figure 19) This shows that archazolid A has the potential to hamper the growth of breast cancer tumors [124]. It might be necessary to vary the experimental setup concerning the amount of mice in the groups, we just used n=4. For statistical analyses larger groups would be more suitable. Another improvement would be to extend the experimental period and to use BALB/c mice for long-term trials because they have a firmer general condition and tolerate daily applications better compared to the BALB/c nu/nu strain, at least according to our experiences. Furthermore, 4T1 cells are syngeneic with BALB/c mice where they originate from.

Within a project where the focus lay on the effects of archazolid A on cholesterol metabolism, the approach was to evaluate the properties of archazolid A in combination with the cholesterol synthesis inhibitor simvastatin (Merck Pharma) which is an established therapeutic successfully used in the treatment of high cholesterol levels and so reducing the risk for heart attack and stroke [134]. We wanted to evaluate with a Huh7 xenograft tumor model if there are any synergistic effects within a combinatorial treatment regime of both drugs. The expectation was that simvastatin and archazolid A in single therapy would both reduce tumor growth, but that the combination of both would reach a greater effect. Archazolid A alone hampered tumor growth significantly compared to the control group while the single simvastatin treated group showed the highest tumor volume of all groups, even a higher one than the control, so the effect of archazolid A in combination with simvastatin was worse compared to the single archazolid A treatment, which was a controversial result for us. (Figure 21) According to publications, simvastatin might promote angiogenesis. Asai et al. showed that systemic treatment with simvastatin stimulates wound healing which is impaired in diabetes and constitutes a major problem within this disease. Treatment with simvastatin promoted angiogenesis and lymphangiogenesis [135]. Furthermore, Fukui et al. showed that a therapy with simvastatin after bone fractures promotes neovascularisation and new bone formation which accelerates the healing [136]. This might be the explanation why our

simvastatin treated tumors reached their large size, instead of promoting the inhibitory effect of archazolid A, it stimulated angiogenesis which affected tumor growth positively. Especially Huh7 tumors are good vascularized which was even increased through simvastatin treatment. So, archazolid A showed its potential to hamper tumor growth again, but the combination of archazolid A and simvastatin is not suitable for this kind of tumor experiment.

The third *in vivo* experiment where the potential of archazolid A was evaluated was a xenograft model with U87MG (glioblastoma) cells. Glioblastomas belong into the group of brain tumors, their prognosis is very poor and almost all patients survive less than one year after diagnosis. Glioblastoma is the most malignant primary malignant brain tumor in adults. But the overall survival rate enhanced during the last decade because the understanding of glioblastomas and therapeutic approaches increased. The possibilities to treat them consist of surgery, radiotherapy and the use of temozolimide, a cytostatic [137] [138]. So, there is a great need to enlarge the therapy of these brain tumors.

Our lab showed that the inhibition of V-ATPase influences p53 levels positively, so we combined archazolid A, a V-ATPase inhibitor with nutlin-3a which was already shown to have anti-cancer effects in the fight against glioblastomas before [139], because we wanted to evaluate the combinatorial effect of the archazolid A usage with an additional p53 activation through nutlin-3a. This experiment showed that the growth rate of tumors treated with the combination of archazolid A and nutlin-3a was significantly reduced compared to control while the combination also was most effective in reducing tumor growth. (Figure 23) This might be a promising therapeutic approach against glioblastomas. But these results need further investigations, one might be to combine archazolid A with other p53 activators in murine tumor models to review if the positive effect is limited to nutlin-3a or if it is possible to confer this effect on other combinatorial therapies.

All in all, archazolid A showed anti-cancer effects in all of the evaluated tumor models we performed.

3.2. *In vivo* experiment to evaluate the anti-cancer potential of LGR 2674

HCC is an epithelial liver tumor which is the fifth frequent cancer in the world. It can develop from cirrhotic livers due to chronic hepatitis B and C infections or from a history of alcohol consumption [105]. The incidence of HCC is rising year by year, the prognosis is poor and the only established and admitted therapeutic agent for HCC is sorafenib (Bayer Pharmaceuticals) [96] [103]. Our lab already focused on the research on HCC treatment within Huh7 cells before [111] and now, in this thesis, different approaches to hamper the growth of HCC tumors through the usage of our experimental compounds were evaluated *in vivo*. In all of these experiments Scid mice were chosen because human Huh7 cells grow very reliable and fast in this mouse strain.

The roscovitine analogue LGR 2674 was evaluated in vivo for the first time, it is claimed to be more potent than its forerunner concerning the inhibition of Cdk5. According to the preliminary dose finding test we performed, 1.5 mg/kg/d were chosen as a dosage. LGR 2674 treatment lowered tumor volume significantly compared to control. (Figure 25) All mice treated with LGR 2674 lost around 10% body weight, showed a reduced general condition and signs of pain after the injections, e.g. a bent position, horrent fur and an isolation of single mice from the group. All in all, LGR 2674 showed its potential to hamper the growth of Huh7 tumors and that it seems to be more potent than roscovitine within this setup, because roscovitine had to be used in a dosage of 150 mg/kg/d in former experiments to reach similar effects. But further experiments are necessary to prove these results. But the setup in coming experiments has to be changed, for trials lasting longer than a few days, the dosage of LGR 2674 has to be lowered because mice do not tolerate 1.5 mg/kg over a longer period without retrenchments in their well-being. To evaluate the differences between LGR 2674 and roscovitine in detail, both compounds should be used within one tumor growth experiment to create equal experimental conditions.

3.3. Evaluation of PS89 as anti-cancer agent in a xenograft tumor model

Another approach for HCC therapy was evaluated in a xenograft tumor model. We combined the established HCC therapeutic sorafenib with the new PDI inhibitor PS89. Sorafenib is an anti-cancer agent that suppresses proliferation and angiogenesis of tumor cells through the inhibition of RAF kinase activity and the receptors of vascular endothelial growth factor and platelet-derived growth factor. It is able to improve the overall survival rate of patients suffering from advanced HCC [140]. It is mostly well tolerated and is a viable therapeutic approach, but patients with sorafenib treatment lived just three months longer on an average compared to placebo groups [141]. So, it is necessary to improve the efficacy of sorafenib and to evaluate more potential anti-cancer agents for HCC treatment. So, the combination of PS89 and sorafenib was evaluated. But PS89 did not show any sensitizing effect, even sorafenib treatment did not lead to any effect on hampering tumor growth. (Figure 27) Therefore, we concluded that the explanation lies within the experimental setup. Huh7 cells, subcutaneously injected, normally grow very fast and form solid tumors around seven days after application at latest. In this setup, the tumors grew slower than usual, so we were able to start therapy on day 10 first. Within the following days, tumors grew very fast and reached unequal sizes within the groups. Besides, mice received therapeutic injections just every second day. The combination of the late and then fast growing tumors and the reduced therapy regime led to the problem that the anti-cancer agents were not able to work fast and proper enough and the huge differences in tumor size within the groups themselves make this experiment not comparable with our other HCC trials. So, it is not possible to make a statement on the efficacy of PS89 as well as sorafenib. The experimental

setup for such an experiment has to be changed. PS89 and sorafenib either have to be injected daily when using Huh7 cells or another cell line has to be chosen.

3.4. Murine tumor model to evaluate the efficacy of sorafenib A

The use of ACC inhibitor sorafenib A, a natural compound derived from *Sorangium Cellulosum* is another approach for anti-cancer therapy, although very rare data exist concerning its use in vivo. ACCs are major key players in the fatty acid synthesis, there exist two isoforms, ACC1 and ACC2, in humans and other mammals. Sorafenib A is a specific inhibitor of both eukaryotic ACC isozymes [128]. Within one of our projects, we evaluated its therapeutic effect by hampering the growth of HCC tumors (Huh 7 cells) in Scid mice for the very first time and reached significant results. (Figure 28) So, this natural compound showed its potency to act as anti-cancer agent. These first results are promising but further experiments are necessary to evaluate this data, e.g. the usage of different types of tumor cell lines in combination with other mouse strains than Scid.

4. In vivo evaluation of new approaches to reduce tumor dissemination

For the in vivo experiments where tumor cell dissemination was the aim to evaluate, the bioluminescence imager IVIS® Spectrum was used. For this purpose, murine breast cancer cells (4T1) and human leukemia cells (Jurkat) were chosen. To track the tumor cell dissemination and the formation of new tumors by using bioluminescence imaging, we had to use cells tagged with stable expressing luciferase (4T1-luc and Jurkat-luc). When mice carrying 4T1-luc or Jurkat-luc tumors and they are injected with luciferin, the tumors emit a visual light signal that can be monitored using a sensitive optical imaging system like our IVIS® Spectrum [142].

This kind of bioluminescence imaging contains a variety of advantages within murine tumor models. Mice can be imaged several times, so the tumor dissemination over time can be reviewed. It can also be used to confirm that i.v. injections were performed properly. The imaging procedure itself is not invasive and the isoflurane narcosis is harmless and evaporates very fast. But it has to be mentioned that our performed experiments represent models for tumor cell dissemination not for tumor metastasis itself. Metastasis is defined as a spreading of tumor cells out of a cancerous growth into organs away from the original tumor. In our experiments the distribution of cells after i.v. injection was reviewed, the cells were injected right into the blood circulation, it was no active process as it is in metastatic processes. But with our model we were although able to show the main organs which were invaded by the injected tumor cells and how long it takes to reach such a tumor cell distribution. The dissemination of tumor cells over time was shown without the need to sacrifice the mice during the process, which limited the needed number of mice.

For a preliminary experiment concerning a leukemia model, we chose Jurkat-luc leukemia cells which we were able to get evaluated with the IVIS® Spectrum. As we never worked with a leukemia model in vivo before in our lab, the aim was to establish a new experimental setup because we wanted to evaluate the general cell dissemination after i.v. injection in vivo and to prove which kind of mouse strain is suitable for a leukemia model (Scid, Nod-Scid or NSG).

4T1-luc cells were chosen according to the possibility to track them with the bioluminescence imager, their good growth rate and the fact that they can be applied into BALB/c mice where they originate from and they are syngeneic with this strain. This experimental setup was evaluated before and was successful [127]. All cells were injected intravenously to imitate the process of vascular migration, 4T1-luc cells migrated from the blood right into the lungs, almost without exception while the Jurkat-luc cells invaded a variety of organs.

4.1. Establishment of a murine leukemia model

The aim of this experiment was to determine a suitable mouse model for a leukemia experiment, here we worked with Jurkat-luc cells. Mice should receive cells via i.v. injection, afterwards bioluminescence imaging should be performed to evaluate the distribution of the cells in the body. Our future plan was to treat mice, which received leukemia cells, with our anti-cancer agents in such models. But because of the fact that we used a human leukemia cell line for the first time in one of our in vivo experiments, the choice of a suitable mouse strain had to be taken, that is why we performed this preliminary experiment. For other leukemia models NSG mice were used, but in all of these experiments patient derived leukemia cells have been chosen which are very sensible and have special needs for growing [143] [144]. But, to our knowledge, there exist no published data on what kind of strain is the most suitable for other leukemia cell lines, e.g. Jurkat-luc. So, our aim was to evaluate which strain is optimal. Three associated strains which all hold the Scid immunodeficiency, Scid, Nod-Scid and Nod Scid Gamma (NSG) mice were chosen. The difference between them is that Scid mice hold the Scid deficiency but an intact innate immune system while Nod-Scid have additionally a reduced innate immune system concerning macrophages, dendritic and natural killer cells and the complement system, while NSG mice hold additionally deficits in interleukin signaling. Scid and Nod-Scid mice were imaged six times and NSG mice were imaged nine times during the experiment. In NSG mice, bioluminescence signals were visible from day five after cell inoculation on, the signal increased from day to day. However, in Scid and Nod-Scid mice, it was not possible to detect any bioluminescence signal over the whole experimental period. Which led to the conclusion that probably just NSG mice are suitable for leukemia models, independent from the type of injected leukemia cells. (Figure 30) Although all mice have similar deficits, it seemed that the interferences in interleukin signaling, which just emerge in NSG mice, are decisive for the dissemination of leukemia cells.

4.2. In vivo evaluation of the inhibition of tumor cell dissemination by tetrandrine and soraphen A

Tumor metastases are the end product of a long cascade of biological steps which lead to tumor formation in distinct places far from the original tumor. Metastasis is a major problem in therapy because adjuvant therapy or surgical resection can cure bounded primary tumors, but concerning metastases it is much more difficult to administer a therapy because of its systemic nature and the resistance of disseminated tumor cells to existing therapeutic agents. More than 90 % of all deaths occurring during cancer disease are attributed to metastasis and not to the primary tumors from which these malignant lesions arise [145] [146]. So, it is absolutely necessary to search on anti-cancer agents that embank metastasis. Actually, within our tumor models, we performed tumor dissemination experiments, because the tumor cells did not have to invade actively into the blood circulation, but the new tumors which were formed in different organs can be equated with growths arisen of a metastatic spread of solid tumors. Our aim was to evaluate the efficacy of two natural compounds, Ca²⁺ channel blocker tetrandrine and ACC inhibitor soraphen A, against tumor dissemination within different murine models.

For the evaluation of tetrandrine, originally isolated from *Stephania tetrandra*, different allograft experiments with 4T1-luc cells and BALB/c mice were necessary. So, our mice and the cells were syngeneic. First, we established a 4T1-luc metastasis model where mice were either treated with tetrandrine or vehicle for three times. On day eight after cell injection, bioluminescence imaging with the IVIS® Spectrum was performed. The tetrandrine treated group showed a higher tumor burden in the lungs than the control group. (Figure 32) We actually expected to see the opposite. Tetrandrine was solved in DMSO, solutol and PBS in this setup and we had little problems to get it solved, so the solution regime had to be adjusted.

We changed the experimental setup then, mice received a combination of tetrandrine pre-treated cells and tetrandrine therapy. This time, tetrandrine was solved in sterile filtered HCl according to Sakurai et al. [40]. Some of our animals showed small wounds at the i.p. injection area referable to the HCl used as solvent. Furthermore, the group receiving tetrandrine pre-treated cells in combination with single tetrandrine therapy showed the highest tumor burden in the lungs. (Figure 34) So, we sought for possible explanations. According to Jin et al., even one i.p. tetrandrine application harms the lungs intensely. At a dosage of 150 mg/kg, once applied, tetrandrine caused significant alveolar edema and hemorrhage [35]. So, the lungs of our mice probably got damaged by tetrandrine itself and so more tumor cells were able to form growths there. Treated mice also suffer from a weaker general condition compared to control animals. With regard to the wounds after i.p. injections, HCl might not be a suitable solvent for tetrandrine. In addition, 4T1-luc cells proliferate very fast, with one imaging performance eight days after cell injection, it cannot be guaranteed that the amount of tumor cells in the lungs is based on dissemination

only. This could also be based on a few cells that migrated into the lungs prior to day eight and then proliferated there.

Due to the difficulties of mice treating with tetrandrine, we changed the experimental setup completely. Mice received with tetrandrine pre-treated cells compared to mice which received control cells. We performed bioluminescence imaging with the IVIS® Spectrum two times, on day 5 and day 8 after cell application to provide more information on tumor dissemination. On day five, significant results were reached. (Figure 36) This shows that tetrandrine has an anti-cancer effect. But its relevance for clinical usage when the cells are pre-treated is limited. The better approach surely is to administer a therapy in mice. To realize this, a suitable method of application, a treatment regime and tolerable solvent have to be evaluated in further experiments, lower dose rates of tetrandrine and an improved mixture for its solution are absolutely necessary.

A similar experiment was performed with the natural compound soraphen A, originally isolated from *Sorangium cellulosum*. Rare in vivo data exist concerning the use of this ACC inhibitor in murine cancer models [147]. We wanted to evaluate its effect on tumor dissemination with BALB/c mice syngeneic with 4T1-luc cells. Cells were pre-treated with soraphen A in two concentrations and then compared to control. (Figure 39) Soraphen A was able to reduce the metastasis of murine breast cancer cells in the lungs, which is the main organ they usually invade, in two concentrations. But more in vivo experiments with a treatment regime for the mice themselves have to be performed to prove the anti-cancer effect in mice and to create a transferable conclusion for its use in clinic. We chose this certain setup because a former experiment performed by Dr. Rebekka Kubisch (University of Munich, Germany) where mice received an i.v. injection of 4T1-luc cells and received soraphen A treatment afterwards did not work within such a setup (data not shown). All in all, we performed a preliminary in vivo experiment with soraphen A on tumor dissemination, but based on the status of available data more investigations are deeply necessary.

5. In vivo evaluation of the involvement of Cdk5 in cancer processes

Cdk5 is associated with a variety of neuronal diseases because its presence in the CNS is incisive [112]. In the last years, its role in cancer diseases has been evaluated more and more. Our lab was already able to show that Cdk5 has a major influence on tumor migration and angiogenesis in vitro [117] and in vivo [113] and that an inhibition of endothelial Cdk5 leads to reduction of tumor growth [130]. We showed that targeting Cdk5 is a new therapeutic approach in HCC treatment [111]. So, we wanted to evaluate its potential as a novel target in cancer therapy within our in vivo experiments.

5.1. Efficacy of Cdk5 knock-down in Huh7 cells and endothelial Cdk5 knock-out in mice

In cancer research more and more knock-out or knock-down models are used nowadays, we contributed to that with a Cdk5 knock-down in Huh7 cells. These knock-out cells were injected into mice, which were treated with sorafenib afterwards. The chosen dosage of 10 mg/kg i.p. can be classified as a low to medium one [100]. It could be shown that the Cdk5 knock-down in cells sensitizes HCC tumors to sorafenib treatment *in vivo*. (Figure 41) This leads to the assumption that the inhibition of Cdk5 might be a therapeutical approach to improve the effect of sorafenib in HCC therapy, because single sorafenib treatment leads to an average longer survival of three months for HCC patients treated with sorafenib than for those given placebo [96]. But not all patients are sensible for sorafenib treatment because of resistances [148]. So the combination of sorafenib treatment with Cdk5 inhibition might be a promising therapeutic improvement, but more investigations are necessary. Especially for clinical use, there have to be more experiments concerning a Cdk5 inhibition through a chemotherapeutic that can be systemically administered.

Concerning a project where the influence of endothelial Cdk5 in tumor angiogenesis was evaluated, we performed an *in vivo* experiment with mice carrying an inducible endothelial Cdk5 knock-out (Cdk5^{fl/fl} VECCre+). Mice were generated by using a Cre-lox system, here the endothelial Cdk5 knock-out was inducible through tamoxifen treatment. A general Cdk5 knock-out in mice is not possible because such animals are nonviable. Murine melanoma cells were injected, and when our mice beared a tumor, they were either treated with Cdk inhibitor roscovitine or vehicle, the first ones showed a lower tumor volume in the end of the experiment. (Figure 42) We were able to show that an inducible endothelial Cdk5 knock-out in mice sensitized tumor cells for chemotherapeutic treatment [130]. Due to limitations in animal breeding, our number of Cdk5 knock-out mice in the groups was relatively small (n=3). It would be an improvement to enlarge the experimental groups to lower the deviations between the single tumor volumes.

5.2. Evaluation of the effect of Cdk5 inhibition in murine limiting dilution experiments

Solid tumors consist of heterogeneous populations of cancer cells which have different abilities to proliferate and to form metastasis. Some cancer cells have limited properties to divide, while others, so-called tumor initiating cells have been identified to possibly have the ability to extensively proliferate and form new tumors [149]. Our aim was to evaluate which effect the number of injected tumor cells (4T1-luc and T24) has on tumor development and growth, both in combination with a form

of Cdk5 inhibition. The background of these experiments was to evaluate the tumor initiating potential of CSCs in different cell lines.

We evaluated a xenograft tumor model with human urinary bladder cancer cells (T24) which contained a stable Cdk5 knock-down (T24 Cdk5 shRNA) and compared their start of growing and development with control cells (T24 nt shRNA). As a result, we are not able to make any clear suggestions. T24 nt shRNA tumors as well as T24 Cdk5 shRNA tumors were visible and palpable from the same time points on. (Figure 43) The expectation was that Cdk5 knock-down in tumor cells would influence the time of tumor arising and growth negatively compared to the control cells without Cdk5 knock-down. Further investigations on biochemical levels were renounced because of the misleading results. But a cell amount of 1×10^6 seemed to lay the best foundations for tumor formation. So, it might not depend on how much tumor cells are injected, because 5×10^6 and 2.5×10^6 cells led to a lower tumor volume in general. If such an experiment has to be repeated, the experimental setup has to be totally changed.

The second limiting dilution experiment we performed is based on an allograft tumor model with murine breast cancer cells and BALB/c mice, hence a syngeneic model. Two groups of mice (n=5) always received the same cell amount. One of those groups was treated as a control the other received the Cdk5 inhibitor dinaciclib. Bioluminescence imaging was used to evaluate tumor metastasis within the body. Results exhibited a great variety of information, a suggestion which tumors arise first or reach the higher volume cannot be made. (Figure 45) The value of this experiment cannot be enlarged through bioluminescence images. (Figure 46) We actually expected that tumor volume should be hampered by dinaciclib treatment. An explanation for the controversial results might be that mice with dinaciclib treatment suffered from a worse general condition than the control mice did after the injection and so, their immune system was harmed through dinaciclib treatment so much that tumor cells had a better chance to invade the lungs and proliferate there before dinaciclib was able to attend its function as chemotherapeutic. If such an experiment should be repeated, it might be an improvement to lower the dosage of dinaciclib and to choose a cell line which proliferates slower than 4T1-luc cells.

V. Summary

Cancer diseases are a major burden on human and animal health, their number will even increase in the coming years, according to statistics. The current strategies of therapy do often not suffice to cure patients or to enhance their survival rate at least. Negative therapeutic side effects, resistances and the formation of metastasis are unfortunately huge stumbling blocks in cancer therapy. So, there is a great need for improved or new therapeutics. Therefore, our lab focuses on new cytostatic drugs, originated from natural compounds or their derivatives for anti-cancer treatment. The aim of this thesis was to establish murine tumor models to evaluate the anti-cancer potential of these compounds *in vivo*. We performed different animal experiments to review their effects on hampering tumor development, growth and dissemination. Partly, the focus was laid on cyclin-dependent kinase 5 (Cdk5) as a target for cancer therapy. Many of the current projects in our lab are about the use of such compounds and a variety of *in vitro* data were already collected. This thesis contributes to these projects with the establishment and realisation of corresponding *in vivo* experiments to reach profound knowledge on the efficacy of the experimental drugs.

Natural compounds and their derivatives are a great source for anti-cancer agents and have broad therapeutic effects, furthermore they are often the template for synthetical drugs. So, their use in the fight against cancer is auspicious and indispensable.

For their evaluation, we started with the performance of some dose finding and pharmacokinetic experiments. Afterwards we evaluated the influence of different anti-cancer drugs on tumor growth and tumor dissemination. A variety of different *in vivo* experiments was established and we were able to show within these chosen setups that V-ATPase inhibitor archazolid A is able to hamper the growth of breast cancer tumors, hepatocellular carcinomas and glioblastomas, partly in combination with other drugs. For example, its combination with MDM2 inhibitor nutlin-3a reached synergistic effects against cancer cells, while the usage of cholesterol synthesis inhibitor simvastatin together with archazolid A was not promising. Archazolid A demonstrated in all of our experiments its potential as a cytostatic. But further investigations are needed to evaluate its efficacy in more complex experiments.

The natural compound tetrandrine, a Ca²⁺ channel inhibitor, was shown to reduce tumor metastasis of breast cancer cells in an allograft mouse model while the natural compound sorafenib, an ACC inhibitor, showed promising results in hampering tumor growth of hepatocellular carcinoma cells as well as the dissemination of breast cancer cells, evaluated in xenograft and allograft tumor models.

All natural compounds we investigated showed potential as anti-cancer agents.

Next to these drugs, we also investigated the efficacy of some new synthetic chemotherapeutics.

PDI inhibitor PS89 was chosen to sensitize hepatocellular carcinoma tumor cells for treatment with the established HCC therapeutic sorafenib, but with the chosen

experimental setup we were not able to evaluate its potential, so PS89 should be chosen for further experiments.

Within a xenograft tumor model we were able to demonstrate that LGR 2674, an analogue of Cdk inhibitor roscovitine, hampered the growth of hepatocellular carcinomas. This substance was used in this kind of experiment for the first time, so we used simplified setups and further *in vivo* examinations are to be pursued.

A special mechanism in the fight against cancer is the inhibition of Cdk5, which was already shown to be involved in the development and progression of cancer. According to this, we realised different *in vivo* experiments where we focused on Cdk5 as a target. Hepatocellular carcinoma cells carrying a stable Cdk5 knock-down were compared to control cells, with and without sorafenib treatment and so we were able to demonstrate in a xenograft mouse model that a Cdk5 knock-down in cells sensitizes tumor cells for sorafenib treatment. This might be a good therapeutic innovation concerning existing resistances against sorafenib. In another experiment mice with an inducible endothelial Cdk5 knock-out were used and treated with the Cdk inhibitor roscovitine which led to a sensitizing effect on tumor cells for therapy. All in all, we were able to establish murine tumor models to demonstrate that Cdk5 is a promising target in cancer therapy.

In addition, two murine limiting dilution experiments were performed to evaluate the influence of cancer stem cells on tumor development and growth, in both experiments a Cdk5 inhibition was additionally used. One experiment with human urinary bladder cancer cells containing a Cdk5 knock-down and another experiment where Cdk5 was inhibited through dinaciclib led both to no evaluable results. The experimental setup for such experiments has to be changed.

In conclusion, this thesis deals with the realisation of murine tumor models for the *in vivo* evaluation of new therapeutic approaches in cancer therapy, based on natural compounds and their derivatives. Cdk5 was partly focused as an anti-cancer target. Many of the presented results are promising and display encouraging possibilities for cancer therapy, they are initial points for further *in vivo* investigations.

VI. Zusammenfassung

Murine Tumormodelle für die in vivo Evaluierung von Naturstoffen und ihren Derivaten als neue Krebstherapeutika

Krebserkrankungen stellen eine große Belastung für die menschliche und tierische Gesundheit dar, ihr Auftreten soll Statistiken zufolge in den nächsten Jahren sogar noch ansteigen. Die gängigen Behandlungsstrategien reichen oftmals nicht aus um die Patienten zu heilen oder zumindest ihre Überlebensdauer zu verbessern. Therapeutische Nebenwirkungen, Resistenzen und die Bildung von Metastasen sind leider große Stolpersteine innerhalb der Krebstherapie. Somit besteht ein großer Bedarf für verbesserte oder neue Therapien. Dementsprechend fokussiert sich unser Labor auf neue Zytostatika, die von Naturstoffen oder deren Derivaten abstammen und für die Krebstherapie eingesetzt werden können. Das Ziel dieser Arbeit war es Tumormausmodelle zu etablieren um das Potential dieser Stoffe in vivo zu untersuchen. Wir haben verschiedene Tierexperimente durchgeführt um deren Einfluss auf Tumorentstehung, Wachstum und Dissemination zu untersuchen. Teilweise wurde der Fokus dabei auf die cyclinabhängige Kinase 5 (Cdk5) als Target in der Krebstherapie gelegt. Viele unserer aktuellen Projekte beschäftigen sich mit dem Einsatz solcher Substanzen und verschiedenste in vitro Daten wurden bereits generiert. Diese Arbeit leistet mit der Etablierung und Realisierung von den dazugehörigen tierexperimentellen Versuchen einen Beitrag zu all diesen Projekten, um ein grundlegendes Wissen über die Effizienz der Versuchssubstanzen erlangen zu können.

Naturstoffe und ihre Derivate stellen eine große Quelle für Substanzen dar, die gegen Krebs eingesetzt werden können und weisen breite therapeutische Effekte auf, darüberhinaus dienen sie häufig als Grundlage zur Herstellung synthetischer Medikamente. Dementsprechend ist ihr Einsatz in der Krebstherapie vielversprechend und unabdingbar.

Um diese Stoffe zu untersuchen haben wir damit begonnen einige tierexperimentelle Versuche zur Dosierungsbestimmung und zur Pharmakokinetik durchzuführen, im Anschluss haben wir den Einfluss von verschiedensten Stoffen auf Krebszellen im Hinblick auf Tumorwachstum und Tumordissemination hin überprüft.

Eine Reihe verschiedenster in vivo Experimente wurde etabliert, so konnten wir mit den gewählten Versuchen zeigen, dass der V-ATPase Hemmer Archazolid A das Wachstum von Brustkrebstumoren, hepatozellulären Karzinomen und Glioblastomen verringern kann, teils auch in Kombination mit weiteren Substanzen. Beispielsweise hat eine Kombination mit dem MDM2 Hemmer Nutlin-3a synergistische Effekte gegen die Krebszellen gezeigt, während eine Kombination mit dem Cholesterolsynthesehemmer Simvastatin zu keinen befriedigenden Ergebnissen geführt hat. Archazolid A selbst hat in all unseren Versuchen sein Potential als Zytostatikum unter Beweis gestellt. Es sollte nun in weiteren Experimenten

eingesetzt werden, damit seine Wirksamkeit in komplexeren Versuchen überprüft werden kann.

Es konnte außerdem gezeigt werden, dass der Naturstoff Tetrandrin, ein Calciumkanalhemmer, die Dissemination von Brustkrebszellen reduzieren kann, während der Naturstoff Soraphen A, ein ACC Hemmer, vielversprechende Effekte bei der Hemmung des Tumorwachstums von hepatozellulären Karzinomen und der Dissemination von Brustkrebstumoren in einem xenograften bzw. einem allograften Tumormodell gezeigt hat.

Alle Naturstoffe, die wir untersucht haben, haben ihr Potential für den Einsatz in der Krebstherapie unter Beweis gestellt. Neben diesen Naturstoffen, haben wir aber auch das Potential von einigen neuen synthetischen Chemotherapeutika untersucht.

Der PDI Hemmer PS89 sollte hepatozelluläre Karzinomzellen für die Therapie mit dem etablierten HCC Medikament Sorafenib sensibilisieren, mit dem gewählten Versuchsaufbau war es uns aber nicht möglich die Effekte von PS89 auszuwerten, dementsprechend sollte PS89 in weiteren Experimenten zum Einsatz kommen.

Mit einem xenograften Tumormodell konnten wir zeigen, dass LGR 2674, ein Analog des Cdk Hemmers Roscovitin, das Wachstum von hepatozellulären Karzinomen verringern kann. Diese Substanz wurde zum allerersten Mal in solch einem Versuch eingesetzt, dementsprechend wurden vereinfachte Versuchsbedingungen gewählt, somit sind weitere tierexperimentelle Versuche anzustreben.

Ein spezieller Mechanismus in der Krebstherapie ist die Hemmung der cyclinabhängigen Kinase 5, von der bereits gezeigt wurde, dass sie in Tumorentstehungs- und Fortschreitungsprozesse involviert ist. Dementsprechend haben wir verschiedene in vivo Versuche durchgeführt, in denen der Fokus auf Cdk5 als Target gelegt wurde. Hepatozelluläre Karzinomzellen, die einen stabilen Cdk5 Knock-down trugen wurden mit Kontrollzellen verglichen, entweder mit oder ohne anschließender Sorafenib Behandlung. Wir konnten in einem xenograften Mausmodell zeigen, dass ein Knock-down von Cdk5 die Zellen für die Sorafenib Therapie sensibilisiert, was einen neuen vielversprechenden Ansatzpunkt im Bezug auf bestehende Resistenzen gegen Sorafenib darstellt. In einem weiteren Experiment wurden Mäuse, die einen induzierbaren endothelialen Cdk5 Knock-out trugen mit dem Cdk Hemmer Roscovitin behandelt, was dazu führte, dass die Tumorzellen für die Therapie sensibilisiert wurden.

Zusammengefasst war es uns möglich Tumormausmodelle zu etablieren mit denen wir zeigen konnten, dass Cdk5 ein vielversprechendes Target in der Krebsforschung darstellt.

Zusätzlich haben wir zwei tierexperimentelle Limiting Dilution Versuche durchgeführt um den Einfluss von Krebsstammzellen auf die Tumorentstehung und das Tumorwachstum zu untersuchen, in beiden Experimenten wurde zusätzlich eine Cdk5 Hemmung induziert. Sowohl ein Versuch mit menschlichen Blasenkrebszellen, die einen Cdk5 Knock-down trugen als auch ein Versuch in dem Cdk5 durch Dinaciclib gehemmt wurde, führten zu keinen auswertbaren Ergebnissen. Das

experimentelle Vorgehen für derartige Versuche muss grundlegend verändert werden.

Zusammenfassend handelt diese Arbeit von der Realisierung von murinen Tumormodellen für die *in vivo* Evaluierung neuer therapeutischer Ansätze in der Krebstherapie, basierend auf Naturstoffen und ihren Derivaten. Teilweise wurde der Fokus dabei auf Cdk5 gelegt. Viele der Ergebnisse sind aussichtsreich und stellen vielversprechende Möglichkeiten für die Krebstherapie dar, diese können als Ausgangspunkt für weitere tierexperimentelle Untersuchungen angesehen werden.

VII. References

1. Torre, L.A., et al., *Global cancer statistics, 2012*. CA Cancer J Clin, 2015. **65**(2): p. 87-108.
2. Ferlay, J., et al., *Cancer incidence and mortality worldwide: sources, methods and major patterns in GLOBOCAN 2012*. Int J Cancer, 2015. **136**(5): p. E359-86.
3. Jemal, A., et al., *Global cancer statistics*. CA Cancer J Clin, 2011. **61**(2): p. 69-90.
4. <http://www.who.int/mediacentre/factsheets/fs297/en/>. *Cancer Fact sheet N°297*. 2014.
5. Anand, P., et al., *Cancer is a preventable disease that requires major lifestyle changes*. Pharm Res, 2008. **25**(9): p. 2097-116.
6. <http://www.cancer.gov/about-cancer/what-is-cancer>. *What is cancer?* 2015.
7. Mani, S.A., et al., *The epithelial-mesenchymal transition generates cells with properties of stem cells*. Cell, 2008. **133**(4): p. 704-15.
8. Yoo, M.H. and D.L. Hatfield, *The cancer stem cell theory: is it correct?* Mol Cells, 2008. **26**(5): p. 514-6.
9. Liu, X. and D. Fan, *The epithelial-mesenchymal transition and cancer stem cells: functional and mechanistic links*. Curr Pharm Des, 2015. **21**(10): p. 1279-91.
10. Hanahan, D. and R.A. Weinberg, *The hallmarks of cancer*. Cell, 2000. **100**(1): p. 57-70.
11. Hanahan, D. and R.A. Weinberg, *Hallmarks of cancer: the next generation*. Cell, 2011. **144**(5): p. 646-74.
12. Thamm, D. and S. Dow, *How companion animals contribute to the fight against cancer in humans*. Vet Ital, 2009. **45**(1): p. 111-20.
13. <http://www.livescience.com/32860-why-do-medical-researchers-use-mice.html>.
14. Lahlou, M., *The Success of Natural Products in Drug Discovery*. Pharmacology & Pharmacy, 2013. **4**: p. 17-31.
15. Cragg, G.M. and D.J. Newman, *Natural products: a continuing source of novel drug leads*. Biochim Biophys Acta, 2013. **1830**(6): p. 3670-95.

VII. References

16. Harvey, A.L., *Natural products in drug discovery*. Drug Discov Today, 2008. **13**(19-20): p. 894-901.
17. Butler, M.S., A.A. Robertson, and M.A. Cooper, *Natural product and natural product derived drugs in clinical trials*. Nat Prod Rep, 2014. **31**(11): p. 1612-61.
18. Kingston, D.G., *Modern natural products drug discovery and its relevance to biodiversity conservation*. J Nat Prod, 2011. **74**(3): p. 496-511.
19. Jordan, M.A. and L. Wilson, *Microtubules as a target for anticancer drugs*. Nat Rev Cancer, 2004. **4**(4): p. 253-65.
20. Dennie, T.W. and J.M. Kolesar, *Bendamustine for the treatment of chronic lymphocytic leukemia and rituximab-refractory, indolent B-cell non-Hodgkin lymphoma*. Clin Ther, 2009. **31 Pt 2**: p. 2290-311.
21. Sasse, F., et al., *Archazolids, new cytotoxic macrolactones from Archangium gephyra (Myxobacteria). Production, isolation, physico-chemical and biological properties*. J Antibiot (Tokyo), 2003. **56**(6): p. 520-5.
22. Sasse, F., et al., *Argyrins, immunosuppressive cyclic peptides from myxobacteria. I. Production, isolation, physico-chemical and biological properties*. J Antibiot (Tokyo), 2002. **55**(6): p. 543-51.
23. Sasse, F., et al., *Tubulysins, new cytostatic peptides from myxobacteria acting on microtubuli. Production, isolation, physico-chemical and biological properties*. J Antibiot (Tokyo), 2000. **53**(9): p. 879-85.
24. Sasse, F., et al., *Gephyronic acid, a novel inhibitor of eukaryotic protein synthesis from Archangium gephyra (myxobacteria). Production, isolation, physico-chemical and biological properties, and mechanism of action*. J Antibiot (Tokyo), 1995. **48**(1): p. 21-5.
25. Kubisch, R., et al., *V-ATPase inhibition by archazolid leads to lysosomal dysfunction resulting in impaired cathepsin B activation in vivo*. Int J Cancer, 2014. **134**(10): p. 2478-88.
26. Rath, S., et al., *Regulation of endothelial signaling and migration by v-ATPase*. Angiogenesis, 2014. **17**(3): p. 587-601.
27. Sennoune, S.R., D. Luo, and R. Martinez-Zaguilan, *Plasmalemmal vacuolar-type H⁺-ATPase in cancer biology*. Cell Biochem Biophys, 2004. **40**(2): p. 185-206.
28. Fais, S., et al., *Targeting vacuolar H⁺-ATPases as a new strategy against cancer*. Cancer Res, 2007. **67**(22): p. 10627-30.
29. Perez-Sayans, M., et al., *Role of V-ATPases in solid tumors: importance of the subunit C (Review)*. Int J Oncol, 2009. **34**(6): p. 1513-20.
30. Huss, M., et al., *Archazolid and apicularen: novel specific V-ATPase inhibitors*. BMC Biochem, 2005. **6**: p. 13.

VII. References

31. Wiedmann, R.M., et al., *The V-ATPase-inhibitor archazolid abrogates tumor metastasis via inhibition of endocytic activation of the Rho-GTPase Rac1*. *Cancer Res*, 2012. **72**(22): p. 5976-87.
32. Wu, J.M., et al., *Tetrandrine induces apoptosis and growth suppression of colon cancer cells in mice*. *Cancer Lett*, 2010. **287**(2): p. 187-95.
33. Yoo, S.M., et al., *Inhibition of proliferation and induction of apoptosis by tetrandrine in HepG2 cells*. *J Ethnopharmacol*, 2002. **81**(2): p. 225-9.
34. Lu, J.J., et al., *Alkaloids isolated from natural herbs as the anticancer agents*. *Evid Based Complement Alternat Med*, 2012. **2012**: p. 485042.
35. Jin, H., et al., *Pulmonary toxicity and metabolic activation of tetrandrine in CD-1 mice*. *Chem Res Toxicol*, 2011. **24**(12): p. 2142-52.
36. Zhao, X., et al., *Tetrandrine, a bisbenzylisoquinoline alkaloid from Chinese herb Radix, augmented the hypnotic effect of pentobarbital through serotonergic system*. *Eur J Pharmacol*, 2004. **506**(2): p. 101-5.
37. Kwan, C.Y., et al., *Tetrandrine inhibits Ca²⁺ release-activated Ca²⁺ channels in vascular endothelial cells*. *Life Sci*, 2001. **68**(7): p. 841-7.
38. Kwan, C.Y., H.W. Deng, and Y.Y. Guan, *Tetrandrine is not a selective calcium channel blocker in vascular smooth muscle*. *Zhongguo Yao Li Xue Bao*, 1992. **13**(5): p. 385-90.
39. Calcraft, P.J., et al., *NAADP mobilizes calcium from acidic organelles through two-pore channels*. *Nature*, 2009. **459**(7246): p. 596-600.
40. Sakurai, Y., et al., *Ebola virus. Two-pore channels control Ebola virus host cell entry and are drug targets for disease treatment*. *Science*, 2015. **347**(6225): p. 995-8.
41. Dai, C.L., et al., *Tetrandrine achieved plasma concentrations capable of reversing MDR in vitro and had no apparent effect on doxorubicin pharmacokinetics in mice*. *Cancer Chemother Pharmacol*, 2007. **60**(5): p. 741-50.
42. Gao, J.L., et al., *Tetrandrine Suppresses Cancer Angiogenesis and Metastasis in 4T1 Tumor Bearing Mice*. *Evid Based Complement Alternat Med*, 2013. **2013**: p. 265061.
43. Gerth, K., et al., *The soraphens: a family of novel antifungal compounds from Sorangium cellulosum (Myxobacteria). I. Soraphen A1 alpha: fermentation, isolation, biological properties*. *J Antibiot (Tokyo)*, 1994. **47**(1): p. 23-31.
44. Shen, Y., et al., *A mechanism for the potent inhibition of eukaryotic acetyl-coenzyme A carboxylase by soraphen A, a macrocyclic polyketide natural product*. *Mol Cell*, 2004. **16**(6): p. 881-91.

VII. References

45. Jump, D.B., M. Torres-Gonzalez, and L.K. Olson, *Soraphen A, an inhibitor of acetyl CoA carboxylase activity, interferes with fatty acid elongation*. *Biochem Pharmacol*, 2011. **81**(5): p. 649-60.
46. Raymer, B., et al., *Synthesis and characterization of a BODIPY-labeled derivative of Soraphen A that binds to acetyl-CoA carboxylase*. *Bioorg Med Chem Lett*, 2009. **19**(10): p. 2804-7.
47. Tong, L. and H.J. Harwood, Jr., *Acetyl-coenzyme A carboxylases: versatile targets for drug discovery*. *J Cell Biochem*, 2006. **99**(6): p. 1476-88.
48. Schreurs, M., et al., *Soraphen, an inhibitor of the acetyl-CoA carboxylase system, improves peripheral insulin sensitivity in mice fed a high-fat diet*. *Diabetes Obes Metab*, 2009. **11**(10): p. 987-91.
49. Beckers, A., et al., *Chemical inhibition of acetyl-CoA carboxylase induces growth arrest and cytotoxicity selectively in cancer cells*. *Cancer Res*, 2007. **67**(17): p. 8180-7.
50. Trost, B.M., et al., *Asymmetric total synthesis of soraphen A: a flexible alkyne strategy*. *Angew Chem Int Ed Engl*, 2009. **48**(30): p. 5478-81.
51. McMurry, J., et al., *Organic Chemistry. 5th ed.* 1999: Cole Publishing Company.
52. Mundy, B.P., et al., *Concepts of organic synthesis*. 1980: Marcel Dekker, Inc.
53. Warren, S., et al., *Organic synthesis: The Disconnection Approach*. 1983: John Wiley & Sons.
54. Sunjic, V., et al., *Signposts to chiral drugs*. 2011: Springer.
55. Eirich, J., et al., *A small molecule inhibits protein disulfide isomerase and triggers the chemosensitization of cancer cells*. *Angew Chem Int Ed Engl*, 2014. **53**(47): p. 12960-5.
56. Holohan, C., et al., *Cancer drug resistance: an evolving paradigm*. *Nat Rev Cancer*, 2013. **13**(10): p. 714-26.
57. Wilson, T.R., P.G. Johnston, and D.B. Longley, *Anti-apoptotic mechanisms of drug resistance in cancer*. *Curr Cancer Drug Targets*, 2009. **9**(3): p. 307-19.
58. Gruber, C.W., et al., *Protein disulfide isomerase: the structure of oxidative folding*. *Trends Biochem Sci*, 2006. **31**(8): p. 455-64.
59. Ali Khan, H. and B. Mutus, *Protein disulfide isomerase a multifunctional protein with multiple physiological roles*. *Front Chem*, 2014. **2**: p. 70.
60. Grek, C. and D.M. Townsend, *Protein Disulfide Isomerase Superfamily in Disease and the Regulation of Apoptosis*. *Endoplasmic Reticulum Stress Dis*, 2014. **1**(1): p. 4-17.

VII. References

61. Benham, A.M., *The protein disulfide isomerase family: key players in health and disease*. *Antioxid Redox Signal*, 2012. **16**(8): p. 781-9.
62. Wang, D., et al., *Inhibition of human immunodeficiency virus type 1 transcription by chemical cyclin-dependent kinase inhibitors*. *J Virol*, 2001. **75**(16): p. 7266-79.
63. Cicenias, J., et al., *Roscovitine in cancer and other diseases*. *Ann Transl Med*, 2015. **3**(10): p. 135.
64. Liebl, J., et al., *Anti-angiogenic effects of purine inhibitors of cyclin dependent kinases*. *Angiogenesis*, 2011. **14**(3): p. 281-91.
65. Glab, N., et al., *Olomoucine, an inhibitor of the cdc2/cdk2 kinases activity, blocks plant cells at the G1 to S and G2 to M cell cycle transitions*. *FEBS Lett*, 1994. **353**(2): p. 207-11.
66. Meijer, L., et al., *Biochemical and cellular effects of roscovitine, a potent and selective inhibitor of the cyclin-dependent kinases cdc2, cdk2 and cdk5*. *Eur J Biochem*, 1997. **243**(1-2): p. 527-36.
67. Gherardi, D., et al., *Reversal of collapsing glomerulopathy in mice with the cyclin-dependent kinase inhibitor CYC202*. *J Am Soc Nephrol*, 2004. **15**(5): p. 1212-22.
68. Gromnicka, A., *LGR2674 as a novel angiogenesis inhibitor*, in *Department of Pharmaceutical Biology*. 2015, Ludwig-Maximilians-University Munich.
69. Booher, R.N., et al., *MCL1 and BCL-xL levels in solid tumors are predictive of dinaciclib-induced apoptosis*. *PLoS One*, 2014. **9**(10): p. e108371.
70. Paruch, K., et al., *Discovery of Dinaciclib (SCH 727965): A Potent and Selective Inhibitor of Cyclin-Dependent Kinases*. *ACS Med Chem Lett*, 2010. **1**(5): p. 204-8.
71. Parry, D., et al., *Dinaciclib (SCH 727965), a novel and potent cyclin-dependent kinase inhibitor*. *Mol Cancer Ther*, 2010. **9**(8): p. 2344-53.
72. Gregory, G.P., et al., *CDK9 inhibition by dinaciclib potently suppresses Mcl-1 to induce durable apoptotic responses in aggressive MYC-driven B-cell lymphoma in vivo*. *Leukemia*, 2015. **29**(6): p. 1437-41.
73. Martin, M.P., et al., *Cyclin-dependent kinase inhibitor dinaciclib interacts with the acetyl-lysine recognition site of bromodomains*. *ACS Chem Biol*, 2013. **8**(11): p. 2360-5.
74. Nguyen, T.K. and S. Grant, *Dinaciclib (SCH727965) inhibits the unfolded protein response through a CDK1- and 5-dependent mechanism*. *Mol Cancer Ther*, 2014. **13**(3): p. 662-74.
75. <http://www.medchemexpress.com>.

VII. References

76. Shafer, S.L., et al., *Additivity versus synergy: a theoretical analysis of implications for anesthetic mechanisms*. *Anesth Analg*, 2008. **107**(2): p. 507-24.
77. Wang, B., et al., *MDM2 inhibitor Nutlin-3a suppresses proliferation and promotes apoptosis in osteosarcoma cells*. *Acta Biochim Biophys Sin (Shanghai)*, 2012. **44**(8): p. 685-91.
78. Bandaru, S., et al., *Identification of High Affinity Non-Peptidic Small Molecule Inhibitors of MDM2-p53 Interactions through Structure-Based Virtual Screening Strategies*. *Asian Pac J Cancer Prev*, 2015. **16**(9): p. 3759-65.
79. Vassilev, L.T., et al., *In vivo activation of the p53 pathway by small-molecule antagonists of MDM2*. *Science*, 2004. **303**(5659): p. 844-8.
80. Deben, C., et al., *The MDM2-inhibitor Nutlin-3 synergizes with cisplatin to induce p53 dependent tumor cell apoptosis in non-small cell lung cancer*. *Oncotarget*, 2015.
81. Dickinson, E.R., et al., *The use of ion mobility mass spectrometry to probe modulation of the structure of p53 and of MDM2 by small molecule inhibitors*. *Front Mol Biosci*, 2015. **2**: p. 39.
82. Polanski, R., et al., *Senescence induction in renal carcinoma cells by Nutlin-3: a potential therapeutic strategy based on MDM2 antagonism*. *Cancer Lett*, 2014. **353**(2): p. 211-9.
83. Ohnstad, H.O., et al., *MDM2 antagonist Nutlin-3a potentiates antitumour activity of cytotoxic drugs in sarcoma cell lines*. *BMC Cancer*, 2011. **11**: p. 211:1-11.
84. Zhang, F., et al., *Whole-body physiologically based pharmacokinetic model for nutlin-3a in mice after intravenous and oral administration*. *Drug Metab Dispos*, 2011. **39**(1): p. 15-21.
85. Ji, Z., et al., *Vemurafenib synergizes with nutlin-3 to deplete survivin and suppresses melanoma viability and tumor growth*. *Clin Cancer Res*, 2013. **19**(16): p. 4383-91.
86. Xie, X., W.W. Wong, and Y. Tang, *Improving simvastatin bioconversion in Escherichia coli by deletion of bioH*. *Metab Eng*, 2007. **9**(4): p. 379-86.
87. Erkelens, D.W., et al., *Clinical experience with simvastatin compared with cholestyramine*. *Drugs*, 1988. **36 Suppl 3**: p. 87-92.
88. Goldstein, J.L. and M.S. Brown, *Regulation of the mevalonate pathway*. *Nature*, 1990. **343**(6257): p. 425-30.
89. Stalenhoef, A.F., M.J. Mol, and P.M. Stuyt, *Efficacy and tolerability of simvastatin (MK-733)*. *Am J Med*, 1989. **87**(4a): p. 39s-43s.

VII. References

90. Ma, N. and L. Cui, *Comparative efficacy of pitavastatin and simvastatin in patients with hypercholesterolemia: a meta-analysis of randomized controlled clinical trials*. Drug Des Devel Ther, 2015. **9**: p. 1859-64.
91. Gryn, S.E. and R.A. Hegele, *Ezetimibe plus simvastatin for the treatment of hypercholesterolemia*. Expert Opin Pharmacother, 2015. **16**(8): p. 1255-62.
92. Mauro, V.F. and J.L. MacDonald, *Simvastatin: a review of its pharmacology and clinical use*. Dicap, 1991. **25**(3): p. 257-64.
93. Yan, J.Q., et al., *Lovastatin induces neuroprotection by inhibiting inflammatory cytokines in 6-hydroxydopamine treated microglia cells*. Int J Clin Exp Med, 2015. **8**(6): p. 9030-7.
94. Atil, B., et al., *In vitro and in vivo downregulation of the ATP binding cassette transporter B1 by the HMG-CoA reductase inhibitor simvastatin*. Naunyn Schmiedebergs Arch Pharmacol, 2015.
95. Shen, Y.Y., et al., *Molecular mechanism underlying the anticancer effect of simvastatin on MDA-MB-231 human breast cancer cells*. Mol Med Rep, 2015. **12**(1): p. 623-30.
96. Llovet, J.M., et al., *Sorafenib in advanced hepatocellular carcinoma*. N Engl J Med, 2008. **359**(4): p. 378-90.
97. Strumberg, D., *Preclinical and clinical development of the oral multikinase inhibitor sorafenib in cancer treatment*. Drugs Today (Barc), 2005. **41**(12): p. 773-84.
98. Yang, Y., et al., *The monoclonal antibody CH12 enhances the sorafenib-mediated growth inhibition of hepatocellular carcinoma xenografts expressing epidermal growth factor receptor variant III*. Neoplasia, 2012. **14**(6): p. 509-18.
99. Wilhelm, S., et al., *Discovery and development of sorafenib: a multikinase inhibitor for treating cancer*. Nat Rev Drug Discov, 2006. **5**(10): p. 835-44.
100. Wilhelm, S.M., et al., *Preclinical overview of sorafenib, a multikinase inhibitor that targets both Raf and VEGF and PDGF receptor tyrosine kinase signaling*. Mol Cancer Ther, 2008. **7**(10): p. 3129-40.
101. Rini, B.I., *Sorafenib*. Expert Opin Pharmacother, 2006. **7**(4): p. 453-61.
102. Giovannini, C., et al., *Notch3 inhibition enhances sorafenib cytotoxic efficacy by promoting GSK3b phosphorylation and p21 down-regulation in hepatocellular carcinoma*. Oncotarget, 2013. **4**(10): p. 1618-31.
103. Verslype, C., et al., *The management of hepatocellular carcinoma. Current expert opinion and recommendations derived from the 10th World Congress on Gastrointestinal Cancer, Barcelona, 2008*. Ann Oncol, 2009. **20 Suppl 7**: p. vii1-vii6.

VII. References

104. Sonntag, R., et al., *Pro-apoptotic Sorafenib signaling in murine hepatocytes depends on malignancy and is associated with PUMA expression in vitro and in vivo*. Cell Death Dis, 2014. **5**: p. e1030.
105. Runge, A., et al., *An inducible hepatocellular carcinoma model for preclinical evaluation of antiangiogenic therapy in adult mice*. Cancer Res, 2014. **74**(15): p. 4157-69.
106. Marinelli, S., et al., *Evaluation of the impact of transient interruption of antiangiogenic treatment using ultrasound-based techniques in a murine model of hepatocellular carcinoma*. BMC Cancer, 2014. **14**: p. 403.
107. Fendrich, V., et al., *Sorafenib inhibits tumor growth and improves survival in a transgenic mouse model of pancreatic islet cell tumors*. ScientificWorldJournal, 2012. **2012**: p. 529151.
108. Gray, N., et al., *ATP-site directed inhibitors of cyclin-dependent kinases*. Curr Med Chem, 1999. **6**(9): p. 859-75.
109. Ko, J., et al., *p35 and p39 are essential for cyclin-dependent kinase 5 function during neurodevelopment*. J Neurosci, 2001. **21**(17): p. 6758-71.
110. Kobayashi, H., et al., *Phosphorylation of cyclin-dependent kinase 5 (Cdk5) at Tyr-15 is inhibited by Cdk5 activators and does not contribute to the activation of Cdk5*. J Biol Chem, 2014. **289**(28): p. 19627-36.
111. Ehrlich, S.M., et al., *Targeting cyclin dependent kinase 5 in hepatocellular carcinoma - A novel therapeutic approach*. J Hepatol, 2015. **63**(1): p. 102-13.
112. Dhavan, R. and L.H. Tsai, *A decade of CDK5*. Nat Rev Mol Cell Biol, 2001. **2**(10): p. 749-59.
113. Liebl, J., et al., *Cdk5 controls lymphatic vessel development and function by phosphorylation of Foxc2*. Nat Commun, 2015. **6**: p. 7274.
114. Liebl, J., et al., *Twice switched at birth: cell cycle-independent roles of the "neuron-specific" cyclin-dependent kinase 5 (Cdk5) in non-neuronal cells*. Cell Signal, 2011. **23**(11): p. 1698-707.
115. Mapelli, M. and A. Musacchio, *The structural perspective on CDK5*. Neurosignals, 2003. **12**(4-5): p. 164-72.
116. Rosales, J.L. and K.Y. Lee, *Extraneuronal roles of cyclin-dependent kinase 5*. Bioessays, 2006. **28**(10): p. 1023-34.
117. Liebl, J., et al., *Cyclin-dependent kinase 5 regulates endothelial cell migration and angiogenesis*. J Biol Chem, 2010. **285**(46): p. 35932-43.
118. Liang, Q., et al., *CDK5 is essential for TGF-beta1-induced epithelial-mesenchymal transition and breast cancer progression*. Sci Rep, 2013. **3**: p. 2932.

VII. References

119. Ruggeri, B.A., F. Camp, and S. Miknyoczki, *Animal models of disease: pre-clinical animal models of cancer and their applications and utility in drug discovery*. *Biochem Pharmacol*, 2014. **87**(1): p. 150-61.
120. Sausville, E.A. and A.M. Burger, *Contributions of human tumor xenografts to anticancer drug development*. *Cancer Res*, 2006. **66**(7): p. 3351-4, discussion 3354.
121. Marques, S.M. and J.C. Esteves da Silva, *Firefly bioluminescence: a mechanistic approach of luciferase catalyzed reactions*. *IUBMB Life*, 2009. **61**(1): p. 6-17.
122. Christoph, S., et al., *Bioluminescence imaging of leukemia cell lines in vitro and in mouse xenografts: effects of monoclonal and polyclonal cell populations on intensity and kinetics of photon emission*. *J Hematol Oncol*, 2013. **6**: p. 10.
123. Simeoni, M., et al., *Predictive pharmacokinetic-pharmacodynamic modeling of tumor growth kinetics in xenograft models after administration of anticancer agents*. *Cancer Res*, 2004. **64**(3): p. 1094-101.
124. Schneider, L.S., et al., *Vacuolar-ATPase Inhibition Blocks Iron Metabolism to Mediate Therapeutic Effects in Breast Cancer*. *Cancer Res*, 2015. **75**(14): p. 2863-74.
125. Chang, H.L., et al., *Simvastatin induced HCT116 colorectal cancer cell apoptosis through p38MAPK-p53-survivin signaling cascade*. *Biochim Biophys Acta*, 2013. **1830**(8): p. 4053-64.
126. Wang, Y., et al., *Simvastatin induces caspase-dependent apoptosis and activates P53 in OCM-1 cells*. *Exp Eye Res*, 2013. **113**: p. 128-34.
127. Schreiner, L., *Innovative cancer therapeutics based on polymers or biogenic drugs evaluated in murine models*. 2013.
128. Berod, L., et al., *De novo fatty acid synthesis controls the fate between regulatory T and T helper 17 cells*. *Nat Med*, 2014. **20**(11): p. 1327-33.
129. Sernetz, M., *Pharmakokinetik und Wachstumskinetik*. 2000.
130. Merk, H., et al., *Inhibition of endothelial Cdk5 reduces tumor growth by promoting non-productive angiogenesis*. *Oncotarget*, 2016.
131. *Cancer Research: Chemotherapy and Radium Therapy*. *Br Med J*, 1932. **2**(3746): p. 766-8.
132. Malhotra, V. and M.C. Perry, *Classical chemotherapy: mechanisms, toxicities and the therapeutic window*. *Cancer Biol Ther*, 2003. **2**(4 Suppl 1): p. S2-4.
133. Perez-Sayans, M., et al., *V-ATPase inhibitors and implication in cancer treatment*. *Cancer Treat Rev*, 2009. **35**(8): p. 707-13.

VII. References

134. Dick, M., et al., *The effect of simvastatin treatment on endothelial cell response to shear stress and tumor necrosis factor alpha stimulation*. Biomed Eng Online, 2015. **14**: p. 58.
135. Asai, J., et al., *Topical simvastatin accelerates wound healing in diabetes by enhancing angiogenesis and lymphangiogenesis*. Am J Pathol, 2012. **181**(6): p. 2217-24.
136. Fukui, T., et al., *Therapeutic effect of local administration of low-dose simvastatin-conjugated gelatin hydrogel for fracture healing*. J Bone Miner Res, 2012. **27**(5): p. 1118-31.
137. deSouza, R.M., et al., *Has the survival of patients with glioblastoma changed over the years?* Br J Cancer, 2015.
138. Wen, Q., et al., *Association of Diffusion and Anatomic Imaging Parameters with Survival for Patients with Newly Diagnosed Glioblastoma Participating in Two Different Clinical Trials*. Transl Oncol, 2015. **8**(6): p. 446-55.
139. Villalonga-Planells, R., et al., *Activation of p53 by nutlin-3a induces apoptosis and cellular senescence in human glioblastoma multiforme*. PLoS One, 2011. **6**(4): p. e18588.
140. Wada, Y., et al., *The Efficacy of Continued Sorafenib Treatment after Radiologic Confirmation of Progressive Disease in Patients with Advanced Hepatocellular Carcinoma*. PLoS One, 2016. **11**(1): p. e0146456.
141. Geschwind, J.F., et al., *TACE Treatment in Patients with Sorafenib-treated Unresectable Hepatocellular Carcinoma in Clinical Practice: Final Analysis of GIDEON*. Radiology, 2016: p. 150667.
142. Lim, E., K.D. Modi, and J. Kim, *In vivo bioluminescent imaging of mammary tumors using IVIS spectrum*. J Vis Exp, 2009(26).
143. Terziyska, N., et al., *In vivo imaging enables high resolution preclinical trials on patients' leukemia cells growing in mice*. PLoS One, 2012. **7**(12): p. e52798.
144. Vick, B., et al., *An advanced preclinical mouse model for acute myeloid leukemia using patients' cells of various genetic subgroups and in vivo bioluminescence imaging*. PLoS One, 2015. **10**(3): p. e0120925.
145. Valastyan, S. and R.A. Weinberg, *Tumor metastasis: molecular insights and evolving paradigms*. Cell, 2011. **147**(2): p. 275-92.
146. Gupta, G.P. and J. Massague, *Cancer metastasis: building a framework*. Cell, 2006. **127**(4): p. 679-95.
147. Wang, C., et al., *Acetyl-CoA carboxylase- α as a novel target for cancer therapy*. Front Biosci (Schol Ed), 2010. **2**: p. 515-26.
148. Ogasawara, S., et al., *Post-progression survival in patients with advanced hepatocellular carcinoma resistant to sorafenib*. Invest New Drugs, 2016.

VII. References

149. Al-Hajj, M. and M.F. Clarke, *Self-renewal and solid tumor stem cells*. *Oncogene*, 2004. **23**(43): p. 7274-82.

VIII. Appendix

1. Abbreviations

°C	degree Celsius
ACC	acetyl-CoA-carboxylase
ATP	adenosine triphosphate
BC	biotin carboxylase
BCCP	biotin carboxyl carrier protein
BCS	body condition score
BMEL	Bundesministerium für Ernährung und Landwirtschaft
Ca ²⁺	calcium
Cdk5	cyclin dependent kinase 5
CH ₃	methyl group
CNS	central nervous system
CO ₂	carbon dioxide
CoA	coenzyme A
CLL	chronic lymphocytic leukemia
CSC	cancer stem cell
CT	carboxytransferase
d	day(s)
DMSO	dimethyl sulfoxide
Dr.	doctor (PhD)
DFG	Deutsche Forschungsgemeinschaft
EDTA	ethylenediaminetetraacetate
e.g.	exempli gratia (for example)
EMT	epithelial mesenchymal transition
ER	endoplasmatic reticulum
FCS	fetal calf serum
FELASA	Federation of European laboratory animal science associations

VIII. Appendix

G	Gauge
H	height
h	hour(s)
H ⁺	hydrogen
HCC	hepatocellular carcinoma
HCl	hydrochloric acid
HMG-CoA	3-hydroxy-3-methylglutaryl coenzyme A
HPLC	high performance liquid chromatography
i.p.	intraperitoneal(ly)
i.v.	intravenous(ly)
IVC	individual ventilated cage
IVIS®	in vivo imaging systems
K	potassium
kg	kilogram
KH ₂ PO ₄	kaliumhydrogenphosphate
L	length
LD ₅₀	median lethal dose
LDL	low density lipoprotein
LOEL	lowest observed effect level
luc	luciferase
MDM2	mouse double minutes clone 2
mg	milligram
min	minute(s)
ml	milliliter
n	number(s)
Na ₂ HPO ₄	dinatriumhydrogenphosphate
NAADP	nicotinic acid adenine dinucleotide phosphate
NaCl	sodium chloride
No.	number
NOEL	no observed effect level

VIII. Appendix

n.s.	not significant
NSG	Nod Scid Gamma
nt	non targeting
O ₂	oxygen
PBS	phosphate buffered saline
PDI	protein disulfide isomerase
PEG	polyethylene glycols
PFA	paraformaldehyde
Prof.	Professor
R	rest
RNA	ribonucleic acid
ROI	region of interest
rpm	rounds per minute
s.c.	subcutaneous(ly)
Scid	severe combined immunodeficiency
S.D.	standard deviation
sec	second(s)
S.E.M.	standard error of the mean
shRNA	small hairpin ribonucleic acid
TE	trypsin EDTA solution
TD ₅₀	median toxic dose
TPC	two-pore channel
UPR	unfolded protein response
UV	ultraviolet
V-ATPase	vacuolar-type H ⁺ ATPase
W	width

2. Publications

Published:

L. S. Schneider, K. von Schwarzenberg, T. Lehr, M. Ulrich, R. Kubisch-Dohmen, J. Liebl, D. Trauner, D. Menche, A.M. Vollmar

Vacuolar-ATPase Inhibition Blocks Iron Metabolism to Mediate Therapeutic Effects in Breast Cancer. (2015 Jul 15, *Cancer Research*)

H. Merk, S. Zhang, T. Lehr, C. Müller, M. Ulrich, J. Bibb, R. Adams, F. Bracher, S. Zahler, A.M. Vollmar, J. Liebl

Inhibition of endothelial Cdk5 reduces tumor growth by promoting non-productive angiogenesis. (2016 Jan 08, *Oncotarget*)

In revision:

L.S. Schneider, M. Ulrich, T. Lehr, D. Menche, R. Müller, A.M. Vollmar, K. von Schwarzenberg

MDM2 antagonist nutlin-3a sensitizes tumors to V-ATPase inhibition

In preparation:

K. Stoiber, O. Werz, R. Müller, A. Koeberle, M. Winzi, J. Guck, M. Ulrich, S. Zahler, A.M. Vollmar, S. Braig

Targeting membrane rigidity and membrane associated signaling pathways by the acetyl-CoA carboxylase inhibitor Soraphen A: A novel therapeutic option for cancer treatment

K. Bartel, M. Winzi, M. Ulrich, A. Koeberle, D. Menche, O. Werz, R. Müller, J. Guck, A.M. Vollmar, K. von Schwarzenberg

V-ATPase inhibition increases cancer cell stiffness and blocks membrane related Ras signaling - a new option for HCC therapy

L. S. Schneider, C. Grimm, Y. Chao, A. Watermann, M. Ulrich, D. Mayr, C. Wahl-Schott, M. Biel, A. M. Vollmar

Two-pore channel function is crucial for migration of invasive cancer cells

M. Mandl, S. Zhang, M. Ulrich, E. Schmoeckel, D. Mayr, A.M. Vollmar, J. Liebl
Cdk5 implicated in cancer stem cell death by interfering with detachment-induced cell death via BIM

IX. Acknowledgements

First of all I would like to thank Prof. Angelika Vollmar for giving me the possibility to perform this work in her laboratories under her supervision. Thank you for the professional support over the last years, the trust in experimental and organisational tasks and the commitment to confide the care of all our laboratory animals to me.

I would also like to thank Prof. Eckhard Wolf for being my veterinary supervisor and for accepting this thesis at the veterinary faculty.

Many thanks to Dr. Johanna Liebl for all your help concerning experimental questions and for your professional support during my whole time at AK Vollmar. I could not imagine to have been part of a better team than yours.

I would like to thank Prof. Martin Biel and PD Dr. Stylianos Michalakis for sharing the mouse facility with us and for the professional teamwork.

Thanks to our collaboration partners Dr. Jennifer Herrmann, Dr. Christoph Müller and jun.- Prof. Thorsten Lehr who contributed to this thesis.

Special thanks go to all the people keeping the animal facility running, Mariella Grüner, Pierre Roth, Nadine Zerhoch, Selina Scheungrab, Jessica Blank and Ioannis Nekevaris. It wouldn't have been possible to take care of all our mice and to realise my experiments without your support.

Many thanks go to all my colleagues at AK Vollmar, especially to Dr. Kerstin Kick, Dr. Simon Schuster, Jana Peliskova, Bernadette Grohs, Rita Socher and Eva-Maria Baur. Thank you for your friendship and all your help during the last years.

Very special thanks to Kerstin Loske, my right and my left hand, I would not have been able to do all this without you. Thank you for all your professional support concerning the mice and our experiments, for your help in every circumstance and your friendship, including laughter and tears.

Thanks to Jon, Richie, Dave and Tico, I would not have come this far without you.

Thanks Buli, Toretto, Jackson, Amber, Toni and Rosi for sharing your lives with me.

Many thanks to my family and friends, especially to Dr. Christian Schabmüller and Dharshini Bandara for reading all my English paper work since 5th grade.

Clemens, it is not possible to express in words how grateful I am having you by my side.